# High-Loaded Activated Sludge - Improvement of a Solids Retention Time Controlled System


Per Nobel

Water and Environmental Engineering
Department of Chemical Engineering
Master Thesis 2015

LUNDS UNIVERSITET

# High-Loaded Activated Sludge - Improvement of a Solids Retention Time Controlled System

by

Per Nobel

Master Thesis number: 2015-14

Water and Environmental Engineering
Department of Chemical Engineering
Lund University

August 2015

Supervisor: **PhD Åsa Davidsson**
Co-supervisor: **PhD David Gustavsson**
Examiner: **Professor Jes la Cour Jansen**

Picture on front page: Foaming at an activated sludge line at Sjölunda WWTP. Photo by Per Nobel.

| **Postal address** | **Visiting address** | **Telephone** |
|---|---|---|
| P.O. Box 124 | Getingevägen 60 | +46 46-222 82 85 |
| SE-221 00 Lund, Sweden | | +46 46-222 00 00 |
| **Web address** | | **Telefax** |
| www.vateknik.lth.se | | +46 46-222 45 26 |

# Preface

This thesis finalises my Master of Science degree in Environmental Engineering at Lund University and is the result of my work at Sjölunda Wastewater Treatment Plant (VA SYD) in Malmö, Sweden during the spring semester of 2015. It is especially dedicated to my family, including my partner in life Nikán Zarghani and also Fariba Shojaei and Jan Ekman. Thank you for your love and endless support!

Next, I would specifically like to thank Gabriel Persson, who was engaged in a parallel project for his own MSc degree. The commitment, ideas and findings of Gabriel were essential for the completion of the project presented herein. The author recommends anybody who would like to achieve further insights into the modelling and process optimisation of Sjölunda WWTP to also read the MSc thesis of Gabriel (see list of references).

I would like to give great thanks to my supervisor, David Gustavsson (VA SYD) for offering the opportunity for me to engage in the most interesting of projects, which have improved my engineering abilities and knowledge about wastewater treatment. I would like to thank my supervisor at Lund University, Åsa Davidsson, for her guidance in the project and the thesis as well as for her expert input on methane potential tests. At Lund University, I would also like to give thanks to Gertrud Persson for her assistance in the laboratory and Jes la Cour Jansen for expert input in the area of wastewater treatment technology.

At Sjölunda WWTP, the following persons have all been of great help for the completion of the project: Max, Ylva, Anneli, Ansaam, Asraa, Rawan and Nelson.

Finally, I would also like to thank DHI Water & Environment for supplying the WEST model software and Enrique for his excellent technical support.

Per Nobel

Malmö, August 2015

# Abstract

Although 100 years old, the activated sludge system remains inevitable for modern wastewater treatment. Advancements within the development of mainstream nitrogen removal techniques based on anaerobic ammonium-oxidising bacteria have renewed the interest in traditional, high-loaded activated sludge systems for COD removal only. In order for activated sludge plants to be efficient in terms of energy use, methane production and areal footprint, the retention time for the active organisms, or analogously the solids retention time, needs to be kept low and precisely regulated.

At Sjölunda wastewater treatment plant, Sweden, an automated solids retention time control system at one of the activated sludge lines was recently implemented. Operation of the experimental line with solids retention time set to 1.2 days with the controller was compared to a manually regulated line, operated at a higher solids retention time (≈ 2.0 days). A model for scenario predictions was constructed in the WEST software using the Activated Sludge Model 2d of the International Water Association. It was found that the operation at low solids retention time consistently produced an effluent higher in suspended solids and particulate COD. Through laboratory settling tests, this was found to be due to a higher fraction of non-settleable solids, a mechanism not captured by the model. Low solids retention time also proved to worsen foaming issues. Based on laboratory test and model simulations, neither was the WAS methane potential nor the sludge to substrate yield found to increase at the lower solids retention time. It was found that the main motivation for solids retention time control at the plant is for increased process stabilisation, which may be even more accentuated in the future when the organic load increases and the solids retention time naturally has to decrease. Still, unreliably online sensor readings of the system constitute an obstacle for a precise regulation.

*Keywords: High-loaded activated sludge; Solids retention time control; Activated Sludge Model; Non-settleable solids; Sludge foaming.*

# Sammanfattning

Trots att aktivtslamprocessen är 100 år gammal är den än idag helt central för biologisk rening av avloppsvatten. Framsteg i utvecklingen av ny teknik för kväveavskiljning baserad på anammoxbakterier, med potentialen att förbättra verkens energibalans, har medfört ett förnyat intresse i den traditionella aktivtslamprocessen där huvudsyftet är COD-avskiljning. För samtida aktivtslamsystem gäller att om de ska vara effektiva i termer av energianvändning, biometangasproduktion och landanvändning så måste uppehållstiden för de aktiva mikroorganismerna i systemet, eller slamåldern, hållas kort. Slamåldern måste hela tiden övervakas och regleras med hög precision.

Sjölunda avloppsvattenreningsverk i Malmö är södra Sveriges största kommunala verk och renar vatten från hushåll och industrier motsvarande 300 000 personekvivalenter. Verket är utrustat med en högbelastad aktivtslamanläggning för COD-avskiljning och viss dentrifikation av rejektvatten (förnitrifiering), medan nitrfikation sker i efterföljande biobäddar föjt av anoxiska, denitrifierande bassänger med bärarmaterial (engelska: moving bed biofilm reactor).

Helt nyligen så implementerades en automatiserad slamåldersstyrning på en av de högbelastade aktivtslambassängerna. Utfallet av att köra den automatiskt reglerade linjen vid en slamålder på 1,2 dagar jämfördes mot traditionell körning på referenslinjen, vilket i medeltal gav en slamålder på omkring 2 dagar. Samtidigt modellerades linjerna med hjälp av mjukvaran WEST, baserat på den allmänt vedertagna modellen ”Activated Sludge Model 2d” från International Water Association. Resultaten från två analyskampanjer för karakteriseringen av avloppsvatten till och från det studerade processavsnittet samt av slammet användes för att generera indata till modellen. Genom kalibrering mot observerad utdata var det möjligt att skapa en valid modell.

Baserat på resultaten av flödesproportionella dygnsprov framgick det den lägre slamåldern innebar en konsekvent högre koncentration av suspenderat material och partikulär syreförbrukande substans i utgående vatten. Den troliga förklaringen var att fraktionen icke-sedimenterbara partiklar ökade för slammet. Låg slamålder visade sig också innebära en förhöjd mängd ljust skum i den luftade delen av reaktorn, även om det framstod som att den egentliga bakgrunden till skumproduktionen hade en annan förklaring. Ingen signifikant skillnad i potentialen för metangasproduktion kunde påträffas i överskottsslammen från de två linjerna. Inte heller förhöjdes utbytet slam till inkommande organsikt substrat ($BOD_7$) i någon avsevärd utsträckning. Istället framstod det som att den största möjliga fördelen med det nya kontrollsystemet är en stabilisering av processen. Denna verkan bedöms kunna vara av särskild betydelse i framtiden då slamåldern *måste* förkortas som en följd av en ökad hydrauliskt och organisk belastning på aktivtslamsystemet. Men för att det nuvarande systemet ska kunna innebära fördelar mot den manuella styrstrategin så måste man komma tillrätta med osäkerheten i instrumenten för online-mätningar av systemets koncentrationer av suspenderat material, vilka ligger till grund för styrningen av systemet.

# Symbols and abbreviations

| Symbol | Description | Unit |
|---|---|---|
| a | Sludge growth constant | kg SS/kg $BOD_7$·d |
| A | Empirical factor, aeration model | - |
| $A_{sp}$ | Specific area of diffusers for aeration | $m^2$ |
| b | Specific decay rate of sludge | 1/d |
| $b_H$ | Specific decay rate of heterotrophs | 1/d |
| bCOD | Biodegradable COD | mg COD/L |
| B | Empirical factor, aeration model | - |
| BMP | Biomethane potential | mL $CH_4$/g VS |
| BOD | Biological oxygen demand | mg $BOD_7$/L |
| COD | Chemical oxygen demand | mg COD/L |
| $COD_{filt,1.6}$ | Filtrate COD, 1.6µm pore size filter paper | mg COD/L |
| $COD_{filt,0.1}$ | Filtrate COD, 0.1µm pore size membrane | mg COD/L |
| $COD_S$ | Soluble COD | mg COD/L |
| $COD_X$ | Particulate COD | mg COD/L |
| DO | Dissolved oxygen | mg $O_2$/L |
| $f_{BOD}$ | Correction factor to account for cell decay | - |
| f_*i* | COD fraction of organic matter type *i* | mg COD/mg COD |
| $f_{ns}$ | Fraction of non-settleable solids | - |
| F/M | Food-to-microorganism ratio | g $BOD_7$/g MLSS·d |
| H | Altitude for aerator | m |
| HRT | Hydraulic retention time | d |
| $k_{la}$ | Oxygen transfer coefficient | 1/d |
| $K_P$ | Controller factor of proportionality | - |
| $K_{MP}$ | Specific heterotrophic growth rate on $X_S$ | 1/d |
| L | Mass load of balanced variable | ton/d |
| LF | Loading factor | g $BOD_7$/g MLSS·d |
| M | Mass stored within a system | ton |
| MCRT | Mean cell residence time | d |
| MLSS | Mixed liquor suspended solids | mg/L |
| $N_d$ | Number of diffusers | - |
| OUR | Oxygen uptake rate | mg $O_2$/L |
| $Q_i$ | Flow rate of *i* | $m^3$/d |
| $Q_n$ | Normalised airflow | $Nm^3$/d |

| | | |
|---|---|---|
| $r_h$ | Parameter for settling in the hindered zone | L/mg |
| $r_p$ | Settling parameter characteristic at low X | L/mg |
| $r_v$ | Volumetric rate of reaction | $d^{-1} \cdot m^{-3}$ |
| $Rho_{air}$ | Air density | $g/m^3$ |
| $S_A$ | Fermentation products | mg COD/L |
| $S_F$ | Fermentable, readily biodegradable substrate | mg COD/L |
| $S_I$ | Inert soluble organic material | mg COD/L |
| $S_S$ | Readily biodegradable substrate ($S_A + S_F$) | mg COD/L |
| SRT | Solids retention time | d |
| $SV_{30}$ | Sludge volume after 30 min of column settling | mL/L |
| SVI | Sludge volume index | mL sludge/g SS |
| $t_d$ | Time for depletion of $S_s$ in OUR experiment | h |
| $t_s$ | Time immediately after $S_s$ depletion | h |
| $T_i$ | Controller integral time | d |
| $T_I$ | Controller integral time | h |
| TSS | Total suspended solids | mg/L |
| u | Control signal | - |
| $v_0$ | Maximum theoretical settling velocity | m/h |
| $v_0'$ | Maximum practical settling velocity | m/h |
| $V_i$ | Volume of system *i* | $m^3$ |
| $v_{sj}$ | Settling velocity in SST sludge layer *j* | m/h |
| VFA | Volatile fatty acid | mg COD/L |
| $X_i$ | Suspended solids concentration in SST layer *i* | mg SS/L |
| $X_{AUT}$ | Autotrophic biomass (denitrifying) | mg COD/L |
| $X_H$ | Heterotrophic organisms | mg COD/L |
| $X_{in}$ | SST feed concentration | mg SS/L |
| $X_l$ | Lower SS limit of settling velocity region III | mg SS/L |
| $X_{Lim}$ | Minimal attainable SS in a sludge blanket | mg SS/L |
| $X_{min}$ | Minimal attainable SS through gravity settling | mg SS/L |
| $X_I$ | Inert, particulate organic matter | mg COD/L |
| $X_{PAO}$ | Polyphosphate accumulating microorganisms | mg COD/L |
| $X_{PP}$ | Polyphosphate internal storage products of PAO | mg COD/L |
| $X_U$ | Upper SS limit of settling velocity region III | mg SS/L |
| $X_S$ | Slowly biodegradable substrate | mg COD/L |
| $X_T$ | Threshold suspended solids concentration | mg SS/L |
| $Y_H$ | Biomass yield for heterotrophic growth (aerobic) | mg COD/mg COD |

| | | |
|---|---|---|
| ZSV | Zone settling velocity | m/h |
| $\alpha$ | Vesilind settling model parameter | L/mg |
| $\alpha$SOTE | Oxygen transfer efficiency for new aerators | - |
| $\Delta O_{Ss}$ | $S_s$ associated oxygen uptake (oxidation) | mg $O_2$/L |
| $\eta$ | Substrate removal efficiency | kg $BOD_7$/kg $BOD_7$ |
| $\mu_H$ | Maximum specific growth rate of heterotrophs | 1/d |
| $\tau$ | Balancing period for mass balance | 1/d |

| **Abbreviation** | **Description** |
|---|---|
| Anammox | Anaerobic ammonium oxidation |
| ASM | Activated sludge model |
| AS | Activated sludge |
| BNR | Biological nutrient removal |
| G2:1 | HLAS line 2:1 (automated SRT controlled) |
| G2:2 | HLAS line 2:2 (manually MLSS controlled) |
| HLAS | High-loaded activated sludge |
| ICA | Instrumentation, control & automation |
| IWA | International Water Association |
| ML | Mixed liquor |
| NTF | Nitrifying trickling filter |
| PAO | Polyphosphate accumulating microorganisms |
| SD | Standard deviation |
| SBR | Sequencing batch reactor |
| SST | Secondary settler tank |
| WAS | Waste activated sludge |

# Table Of Contents

# 1 Introduction

Invented about 100 years ago, the activated sludge (AS) process was especially designed for removal of organic matter from wastewaters. This remained the main purpose of the AS process until the 80's and 90's when the need for enhanced nitrogen removal was brought forward, especially as a consequence of eutrophication. Aerobic heterotrophs for COD removal now had to make room for nitrifiers as well. Due to the autotrophic nature of the latter organisms their specific growth rate is lower and the solids retention time (SRT) must therefore be longer than in a high rate AS (Salem *et al*., 2005). The AS process was also adapted for denitrification, which meant that the process became partly anoxic and sometimes also anaerobic with the introduction of polyphosphate accumulating organisms (PAO), performing biological phosphorus removal (Olsson *et al.*, 1998; Henze *et al.,* 2000a).

New wastewater treatment process configurations, in which nitrogen removal are performed separately from the AS-system, have increased the interest in the traditional AS for COD removal only. At Sjölunda WWTP in southern Sweden (Hanner *et al.,* 2003), there are currently pilot-trials for a future introduction of total autotrophic nitrogen removal, i.e. the nitritation-anammox process, in the mainstream (Gustavsson *et al*., 2014). In the anaerobic ammonium oxidation (anammox) process, nitrogen removal is performed by anammox bacteria which utilise nitrite as electron acceptor and ammonium as an electron donor (Strous *et al.*, 1998). Thus, nitrite does not have to be converted to nitrate prior to reduction into nitrogen gas, which implies lower oxygen consumption. In addition, organic carbon is not needed, as for in heterotrophic denitrification, which increases the biogas production potential (Kartal *et al.,* 2010). Presumably more wastewater COD can be removed in the primary settlers and sent directly to the digester for biogas production without deterioration of effluent nitrogen levels. This further improves the plant energy balance (Siegrist *et al*., 2008).

At Sjölunda WWTP, a high-loaded activated sludge (HLAS) is in operation. Nitrification is performed in the preceding trickling filters and denitrification mainly in anoxic moving bed biofilm reactors and partly in the anaerobic zones of the AS system (pre-denitrifying configuration). Receiving wastewater on average from 300,000 population equivalents today, the plant must cope with a higher future load and more stringent effluent quality demands without increasing its environmental footprint in terms of net energy usage and air emissions. One way to deal with a higher organic and hydraulic load is to operate at a lower SRT (Walker, 1971; Ekama, 2010). At the Hyperion WWTP in Los Angeles, the flow through the secondary treatment was increased by 25% by accepting a lower SRT (1.5 d from 3.1 d), without deterioration of effluent quality (Shao *et al.*, 1992).

Shorter SRT also mean that carbon removal is achieved through assimilation and/or adsorption rather than through mineralisation, since hydrolysis of organics will be less complete. This was proved in a pilot study, comparing operation at SRT between 2 and 4 days (Ge *et al.*, 2013). An implication is reduced aerobic oxidation and thus lower aeration cost per unit mass of removed COD. This is also due to the fact that the endogenous respiration decreases. The endogenous respiration is generally interpreted as the part of biomass oxygen consumption not associated with the oxidation of substrate (Hagman & la Cour Jansen, 2007). This oxygen consumption can be explained by process like lysis, maintenance and predation (van Loosdrecht & Henze, 1997). The methane production through anaerobic digestion increases

since the sludge contains relatively more degradable organic matter (Ge *et al.,* 2013). Thus, shortened SRT might improve the plant energy balance.

Through the years, many different control strategies for the regulation of the SRT have been developed. The more recent strategies include online sensor based controllers (Smith *et al.*, 2013). Recently, such a control strategy was implemented at one of the HLAS lines at Sjölunda WWTP. The purpose of the controller, which regulates waste activated sludge (WAS) withdrawal based on suspended solids sensors, is to allow for operation at a fixed, targeted SRT.

# 2 Aim

The aim of the present investigation was to evaluate and compare the new, automated SRT control system at Sjölunda WWTP to a previous control strategy relying on manual regulation of WAS withdrawal. The motivation was that operation at an appropriate SRT was believed to be crucial for ensuring effluent quality but also for avoiding strong foaming in the aerated basin, a working environment issue. Also, the project aimed at finding a control strategy for an improved plant energy balance. A part goal was to construct a calibrated model of the HLAS plant, which could be used for determining an optimal target SRT. In a broader perspective, the project intended to test the applicability of mathematical modelling of a HLAS plant at an SRT < 2.0 d.

More specifically, the project aimed at giving answer to the following questions:

- Which is the target SRT most appropriate for the operation of the HLAS plant at Sjölunda with regard to the following process characteristics:
    i. Effluent quality (COD, suspended solids, biological nutrients)
    ii. Level of sludge foaming in the aerated basin
    iii. Sludge production and methane potential
    iv. Energy efficiency (aeration, sludge pumping and dewatering ability)
- Is it advantageous to implement SRT control at the HLAS lines at Sjölunda WWTP? Is the controller reliable?
- Is it appropriate to use the ASM2d model for modelling a HLAS line operated at low SRT? Can this model be implemented in the WEST modelling software? How well would such a model predict the outcome of operation at different SRT? What are the limitations?

In order to address to the implications of operation at different SRT, the following hypotheses were tested:

- Low SRT implies increased biogas production. However, effluent quality will be poorer at the same time.
- Too low SRT implies foaming issues.
- The SRT affects the sludge settling properties.

# 3 Theoretical background

## 3.1 SRT control strategies

In an AS process, the sludge in the biological reactor is let to settle in a subsequent settler and then recycled to the reactor. The excess sludge, i.e. the sludge production, is withdrawn from the systems and further treated. This way, the hydraulic retention time (HRT) and the mean cell residence time (MCRT) of the active microorganisms are separated. This offers the possibility to retain both slowly and fast growing microorganisms within the process (Henze *et al*., 2000b). The MCRT is often referred to as the sludge age (Hammer & Hammer, 2012) or analogously the solids retention time (SRT) (Kos, 1998). However, one often differs between the total and the aerobic, anoxic and anaerobic SRT. For example, the aerobic SRT is the residence time for which the biomass spend in the aerated part of the AS process (Henze *et al*., 2000b). The aerobic SRT can be defined according to Equation 3.1.

$$SRT_{aerob} = \frac{MLSS \cdot V_{aerob}}{Q_e \cdot SS_e + Q_w \cdot SS_w} \quad (3.1)$$

where:

MLSS = Mixed liquor suspended solids concentration in the aerated basin

$V_{aerob}$ = Volume of the aerated basin

$Q_e$ = Effluent flow rate

$Q_W$ = Waste activated sludge flow rate

$SS_e$ = Effluent suspended solids concentration

$SS_w$ = Waste activated sludge suspended solids concentrations

According to Equation 3.1, the aerobic SRT can be interpreted as the amount of cells present in the aerobic basin (nominator) in relation to mass flow of cells out of the activated sludge system (denominator). One way to control the SRT is to regulate the waste sludge flow rate, $Q_w$. This can be done manually or through an automated controller.

Controlling the level of solids in an activated sludge plant is crucial for efficient operation (Walker, 1976). For biological nutrient removal (BNR) AS plants, SRT is the most fundamental parameter for operation and control (Ekama, 2010). Nitrifiers, for example, are autotrophic and exhibit low specific growth rate. Thus, at low SRT they can potentially be washed out (Ekama, 2010).

For AS plants designed for organic material (i.e. COD) removal only, the SRT can be allowed to be much lower and the reactor volumes are consequently smaller in relation to the loading. Basically, HLAS plant for COD removal can be designed and operated knowing only the biodegradable organic load on the plant and the fractions of non-biodegradable organic material of the influent. The daily demand of oxygen can be derived from the organic load and the

SRT whereas the secondary settler tank (SST) surface area required is given from the peak hydraulic load (Ekama, 2010).

### 3.1.1 Traditional approach to solids control in AS systems

Through the years, the rate of sludge wastage have often been adapted to fit a certain loading factor (LF), or equivalently the food-to-microorganism ratio (F/M) (Ekama 2010; Walker, 1971). It can be calculated as the $BOD_7$-load in relation to the solids concentration of the aerated tank (g $BOD_7$/g MLSS·d). Given the range of the F/M which the AS plant typically operates within, it can be classified as high-rate/high-loaded (F/M> 0.5 g $BOD_7$/g MLSS·d), conventional (F/M = [0.2 - 0.5] g $BOD_7$/g MLSS·d) or extended aeration (F/M = [0.05 - 0.2] g $BOD_7$/g MLSS·d). The chosen mode of operation typically affects settling properties, effluent quality and aeration demands (Hammer & Hammer, 2014).

Regulating the SRT after a certain F/M ratio is laborious, especially if $BOD_7$ is the measured loading parameter (the analysis requires that the wastewater is incubated for seven days). Instead, the by far most common method of solids level control over the years involves keeping the MLSS at some set level by manually regulating the sludge wastage. Usually, this level is based simply on experience of system response. The outcome of this control-strategy might be acceptable if loading rates are fairly constant on a day-to-day basis as well as during the day. However, a sudden increase in organic loading will increase biomass production and MLSS will consequently rise. With MLSS control, this motivates increased sludge wastage in order to balance the unusual high sludge concentration. This is a typical pit-fall since such action will lower the F/M ratio, which can cause unwanted plant behaviour, e.g. deterioration of effluent quality (Ekama 2010; Walker, 1971).

### 3.1.2 Operational benefits of fixing the SRT

Fixing the SRT means that the F/M ratio is more or less fixed, since there is a direct relation between these two variables (Ekama 2010; Walker, 1971). Walker (1971) described this relation mathematically from a few equations and here it is described similarly. An equation for the net increase of sludge (solids) in the AS system may be expressed according to Equation 3.2:

$$\Delta M/\Delta t = a \cdot \Delta F/\Delta t - b \cdot M \tag{3.2}$$

for which:

M = Amount of solids (sludge) in the system (kg SS)

$\Delta M/\Delta t$ = Net increase of solids (sludge) in the system (kg SS/d)

$\Delta F/\Delta t$ = Substrate removal rate (kg $BOD_7$/d)

a = Sludge to substrate growth constant (kg SS/kg $BOD_7$ removed/d)

b = Specific decay rate of the sludge (1/d)

Dividing Equation 3.2 with the total amount of solids in the system leads to Equation 3.3:

$$\frac{\Delta M/\Delta t}{M} = a \cdot \frac{\Delta F/\Delta t}{M} - b \tag{3.3}$$

The left hand side of Equation 3.3 can be understood as the change of solids mass in relation to the amount of solids present in the system. Hence, it is realised that this term is equal to the inverse of SRT for that system. If M is defined as the amount of solids in the mixed-liquor of the aerobic basin, then $\Delta M/\Delta t/M$ equals the aerobic SRT. The term $(\Delta F/\Delta t)/M$, on the right hand side of the equation, equals the amount of removed substrate in relation to the amount of solids present in the system. With the latter definition of M, $(\Delta F/\Delta t)/M$ is analogous to the aerobic food-to-microorganism ratio times the substrate removal efficiency of the system. Thus, Equation 3.3 may be rewritten into:

$$\frac{1}{SRT,aerobic} = a \cdot F/M_{aerobic} \cdot \eta - b \tag{3.4}$$

where:

$\eta$ = substrate removal efficiency of the system (kg $BOD_7$ removed/kg influent $BOD_7$).

$F/M_{aerobic}$ = aerobic food-to-microorganism ratio (kg $BOD_7$/kg $MLSS_{aerobic}$/d)

Assuming the substrate removal rate $\alpha$ to be rather constant means that the SRT remains proportional to the inverse of F/M. Since an increased load implies an increased growth of biomass, the system must withhold more sludge – otherwise the F/M is increased and the SRT decreased. Consequently, the response of a SRT controlled system to a higher organic load is that MLSS is increased.

MLSS also increases with decreased temperature for an SRT controlled system (Walker, 1971). At lower temperatures, the endogenous respiration rate of the sludge, and thus the specific biomass decay rate b, is lower and more sludge is produced in relation to the organic load (Ekama, 2010). In order for the F/M ratio and the SRT to be fixed, MLSS controlled systems are consequently operated at higher MLSS during winter than in the summer. If not, the F/M ratio would decrease and the SRT increase. Since SRT controlled systems automatically adjust to these changes, the SRT can completely substitute the F/M or LF factor as an indicator of plant operation for such systems (Ekama, 2010).

### 3.1.3 Hydraulic control of the SRT

Complete hydraulic control of the SRT can be achieved by removing a fixed volume of the mixed liquor each day, which preferably is let to settle in a separate settler and the wasted. The rest of the mixed liquor is loaded onto other secondary settlers, which returns all of the settled sludge back to the reactor. This design was first proposed by Garret (1958). It is understood that for such a system it most hold that if the volume of mixed liquor for each day is kept constant, the SRT is completely fixed (Equation 3.5). Note that this is under the assumption that a very small proportion the sludge goes out with the effluent.

$$\text{SRT} = \frac{V_{reactor}}{Q_{WML}} \tag{3.5}$$

where $Q_{WML}$ is the flow of wasted mixed liquor per day and $V_{reactor}$ the reactor volume.

### 3.1.4 Fixing the SRT using instrumentation, control and automation (ICA)

A modern approach to SRT control is to automate the rate of sludge wastage, $Q_W$, through a control system based on the measurement of online sensors. Through this approach, less laboratory analysis are required for SRT and F/M determinations which are needed for manually fixing the SRT. In addition, the continuous monitoring and regulation allows for a more stable operation (constant F/M) which may act to reduce for instance Nocardia foaming issues (Smith *et al.*, 2013). This allows for a more aggressive (lower SRT) operation of adsorption style HLAS plants, with less risk of plant upset (Miller *et al.*, 2014).

However, laboratory analysis must still be applied in order to monitor the correctness of the online-sensors, which requires calibration (Rieger *et al.*, 2005). One of the reasons why ICA systems have not been widely applied is due to lack of confidence in the sensors and the automated regulation among the plant operators and engineers. Although suppliers claim contemporary technology to be mature for application in full-scale plants (Smith *et al.*, 2013), the reliability in the online sensors appears to be the biggest obstacle. Miller *et al.* (2014) evaluated the regulation of an SRT control system for an adsorption style HLAS process (the A-stage of an A/B-process, see section 3.3.3 for the definition of an A/B-process). Two optical SS sensors, for effluent and MLSS concentrations, were evaluated. It was found that the effluent SS sensor suffered from low precision, although trueness were in a 95% confidence interval, according to the method of Rieger *et al.* (2005) for the quantification of uncertainties in online sensors. The low precision was believed to be due to variability in effluent composition, possibly due to the presence of colloids. It was not believed to be due to fouling of the optics of the instrument, which was equipped with an ultrasonic cleaning mechanism. The MLSS sensor showed great variability in the readings, although constantly calibrated. It was concluded that the sensor was not applicable for the intended purpose.

## 3.2 Theory and models for the settling of sludge

Hindered settling is the settling process during which particles can be identified as a sludge blanket, in which the mass of particles settle as a unit. In this process, intra-particulate forces hinders particles to settle as individual entities at different velocities. The latter settling process is denoted discrete particle settling (Takács *et al.*, 1991). A well recognised settling model, more recently reviewed by Vanderhasselt & Vanrolleghem (2000), is the Vesilind settling model as described by Equation 3.6:

$$v_s = v_0 e^{-\alpha X} \tag{3.6}$$

where:

$v_s$ = Settling velocity of the suspension (m/h)

$v_0$ = Maximum (theoretical) settling velocity (m/h)

X = Suspended solids concentration (mg/L)

$\alpha$ = Settling model parameter (L/mg)

However, the model of Vesilind is only applicable to hindered settling conditions - Vanderhasselt & Vanrolleghem (2000) proved the model to be insufficient in predicting settling in

the very dense bottom layer of the SST. Here, particles settles through compression settling, in which the sludge blanket is compressed by the weight of particles (Takács *et al.* 1991). In the upper, less dense layers of the SST, flocculent settling is pre-dominant, which means that particles form separate flocc entities rather than a uniform sludge blanket as they settle. Since the Vesilind model has been found to overestimate the settling velocity in this region, Takács *et al*. developed a two term exponential expression for the settling velocity of the suspension. For this settling velocity function, the first term describes the hindered settling based on the Vesilind model whereas the second is a correction term to account for flocculent and discrete particle settling at lower concentrations (Equation 3.7). In the model of Takács *et al*., which divides the SST into 10 vertical layers, the settling velocity function is used for the derivation of the particle mass upward and downward fluxes between the layers, *j,* based on mass balancing.

$$v_{sj} = v_0 e^{-r_h X_j^*} - v_0 e^{-r_p X_j^*} \tag{3.7}$$

$v_{sj}$ = Settling velocity in flux layer *j* (m/h)

$v_0$ = Maximum theoretical settling velocity (m/h)

$r_h$ = Settling parameter characteristic of the hindered settling zone (L/mg)

$r_p$ = Settling parameter characteristic of low solids concentrations (L/mg)

The variable $X_j^*$ is defined as the difference between SS in layer *j* and the minimum attainable SS of the suspension:

$$X_j^* = X_j - X_{min} \tag{3.8}$$

$X_j$ = SS in layer *j*

$X_{min}$ = minimal attainable SS concentration

The minimal attainable SS can be expressed according to Equation 3.9:

$$X_{min} = f_{ns} \cdot X_{in} \tag{3.9}$$

$f_{ns}$ = fraction of non-settleable solids

$X_{in}$ = SST feed concentration (mg SS/L)

In the model of Takáks *et al.* (1991), the default SST feed layer, that is the layer on which the mixed liquor (ML) is loaded to the SST, is layer number 5, that is at the middle of the SST. If the activated sludge unit is perceived as a CSTR, i.e. ideal mixing of solids, the SST feed concentration, $X_{in}$, equals MLSS.

In order to further correct for the overestimation of particle settling velocity, the model of Takács *et al.* (1991) introduces an expression for the maximal practical settling velocity, $v_0$', which limits the settling velocity in the transition region between hindered settling and settling at lower concentrations:

$$0 < v_{sj} \leq v_0' \tag{3.10}$$

Taken together, Equation 3.7 and Equation 3.10 forms a system of equations for the settling velocity in feed layer *i.* The settling velocity as a function of concentration (X) is depicted in Figure 3.1. In region I, no settling occurs as the minimal attainable solids concentration is reached. Region II represents settling at low concentration and III the transition zone between hindered and flocculent/discrete particle settling. Region IV is dominated by hindered settling and compression settling at higher concentrations. $X_I$ denotes the lower SS limit of region III and $X_U$ the upper limit of the same region.

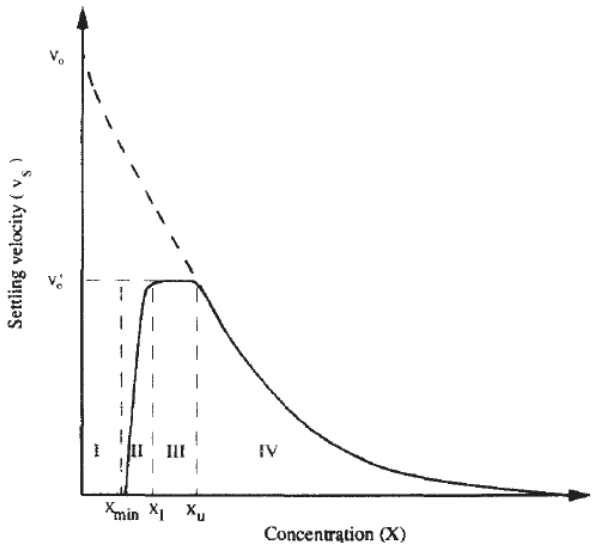


*Figure 3.1. Theoretical model for settling velocity as a function of the concentration of solids (X) in the water column of a SST. Figure from Takács et al. (1991). Published with permission from Elsevier.*

### 3.2.1 The Takács-SVI model extension

Characterising hindered settling in a SST can be done empirically through Zone settling velocity (ZSV) tests (section 4.4.3), as described by e.g. Catunda & van Haandel (1992). However, since these test are tedious, scholars have tried to find methods of quantifying sludge settling properties through the sludge volume index (SVI) instead (Wahlberg & Keinath, 1988; Daigger & Roper, 1985). The SVI (mL/g) index is typically defined according to Equation 3.11:

$$\text{SVI} = \frac{\text{SV}_{30}}{\text{MLSS}} \cdot 1000 \tag{3.11}$$

where $SV_{30}$ (mL/L) is the settled sludge blanket volume, 30 min after the sludge have been introduced to a 1000 mL measuring cylinder, with standardised dimensions for SV determination. By relating ZSV tests to SVI determinations, Daigger & Roper (1985) found an empirical relation between SVI and the hindered settling parameter (α) of the Vesilind settling velocity function (Equation 3.12). Since hindered settling is described through an analogous parameter $r_h$ in the model of Takács *et al.* (1991), the relation can be applied to the latter model aswell. Equation 3.12 describes this relation:

$$r_h = \frac{0.148 + 0.00210 \cdot SVI}{1000} \quad (3.12)$$

The standard SST settling model of the WEST modelling tool uses an extension of the model of Takács *et al.* in which $r_h$ is calculated from a input SVI-index accordning to Equation 3.12. In addition, the extended Takács-SVI model uses two more model input parameters. These are $X_{lim}$, which decides the minimum attainable solids concentration in a sludge blanket, and $X_T$, the threshold suspended particle concentration. $X_T$ decides the maximum attainable solids concentrations for layers above the SST feed layer - if $X_j > X_{Lim}$ for such a sludge layer $j$, downward solids flux from layer $j+1$ to $j$ is not permitted. Table 3.1 lists all the Takács-SVI model input parameters.

Table 3.1. Settling parameters for the extended Takács-SVI settling model

| Parameter | Description | Unit |
|---|---|---|
| $\mathbf{v_0}$ | Maximum theoretical settling velocity | m/d |
| $\mathbf{v_0'}$ | Maximum practical settling velocity | m/d |
| $\mathbf{r_p}$ | Parameter for settling at low concentration | L/mg |
| $\mathbf{f_{ns}}$ | Non-settleable fraction of suspended solids | - |
| **SVI** | Sludge volume index | mg/L |
| $\mathbf{X_{Lim}}$ | Minimum attainable concentration in a sludge blanket | mg/L |
| $\mathbf{X_T}$ | Threshold suspended solids concentration | mg/L |

## 3.3 AS system modelling

### 3.3.1 The ASM models

The ASM series consists of well recognised mathematical models for activated sludge systems at different levels of complexity (Henze *et al.*, 2000a). The model used for this thesis was the ASM2d.

### 3.3.2 Fractionation of COD

A key foundation for the ASM models is the expression of organic matter in terms of COD, which is advantageous partly because it provides a connection between organic substrate, biomass and utilised oxygen. By using a compact matrix notation, all the reactions of the AS units can be expressed in terms of conversion and consumption of oxygen. The matrix notation has become a standard among scholars in biokinetic modelling. Being able to read the matrix notation for the individual reactions is useful for any scholar or engineer who wants to understand any process occurring in the AS units. The model descriptions of Henze *et al.* (2000a) thoroughly describe the reaction matrices for the different ASM models and how to interpret them. However, there are several software platforms, like WEST, MATLAB/Simulink, BioWin etc, in which the model can be implemented which will handle the different reactions (Copp, 2015).

The ASM divides COD into different fractions (Figure 3.2). The most fundamental subdivision is that between biodegradable and non-biodegradable organic matter. The latter is inert to the system, and passes through without any change in its form. Secondly, ASM differs between soluble, $S_i$, and particulate, $X_i$, components $i$. For example, the solvable, non-biodegradable organic matter, $S_I$, will have the same concentration in the influent as in the effluent. The particulate counterpart of the inert organic fraction, $X_I$, will sediment in the sec-

ondary clarifier and eventually be removed from the system (Henze *et al.*, 2000a). Particulate rest material due to the decay of biomass, is also to be considered non-biodegradable and is associated with $X_I$ in the ASM2d model (Henze *et al.*, 2000a).

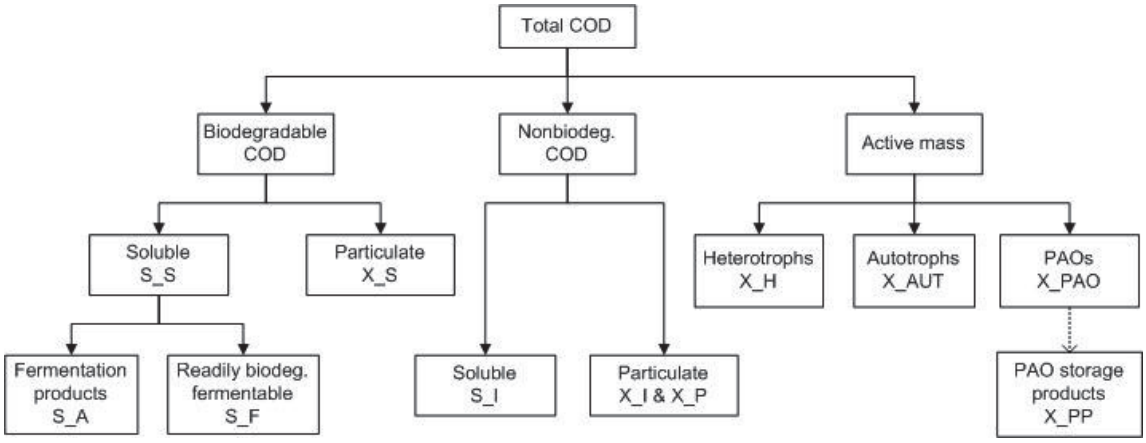


*Figure 3.2. Theoretical fractionation of COD for ASM2d.*

The biodegradable part of the organic matter is also divided into a soluble and a particulate fraction, denoted $S_S$ and $X_S$ respectively. The ASM models recognises the soluble fraction as readily biodegradable organic matter and the particulate fraction as slowly degradable. However, slowly degradable organic matter might in fact be solvable in a real process (Henze *et al.*, 2000a). In the ASM2d model, the readily degradable fraction is further fractionised into fermentation products, $S_A$, and fermentable readily degradable organic material, $S_F$. Fermentation products may be used by PAOs under anaerobic conditions – for modelling purposes they are assumed to be acetate (Henze *et al.*, 2000b).

PAO active biomass is denoted $X_{PAO}$. Heterotrophic and autotrophic biomass is denoted $X_H$ and $X_{AUT}$ respectively. For the modelling of polyphosphate accumulation and organic P removal process, ASM2d also recognises polyphosphate storage products, $X_{PP}$. These are cell internal storage products utilised by the PAOs, but not to be considered as a part of the active mass of the latter (Henze *et al.*, 2000a).

***Motivation for the used notation***

It should be noted that efforts have been made recently to standardise the notation system for wastewater modelling, since different recognised models use significantly different notations. A proposal for such a standardisation is presented by Corominas *et al.* (2010), featuring several of the scholars who have been engaged in the International Water Association (IWA) task group and the development of the models applied during the last decades. A motivation for such a standardisation is that notations applied in the modelling of e.g. AS processes may be used in other WWT processes.

For this thesis, it was decided to use the notation of the ASM2d model as presented by its authors (Henze *et al.*, 2000a). The main reason was that the WEST software, in which the model was implemented, uses the original notation. It is believed that anyone who would like to use the WEST model constructed for this project, while using this thesis as a reference, would gain from having the model components presented analogously in the software as in this text.

### 3.3.3 The implication of SRT on the relative amount of inert COD

Characterisation of the inflow wastewater to the AS process is useful for model output data. For example, the aeration demand can be estimated from the fraction of total biodegradable COD. The filtrated (1.6 µm filter paper) effluent COD corresponds more or less to the inert soluble COD fraction (Choubert *et al*., 2013). However, the different fractions must be defined accordingly to the processes considered.

In a lab-scale experiment, Haider *et al*. (2013) compared the inert fractions of soluble COD in wastewater in the A- and B-stages of a two-stage AS process. In such process, the two AS stages are separated by a SST for the A-stage only, primarily removing organics through adsorption. Settled sludge from the B-stage, typically with a longer SRT, is usually only recirculated back to the B-stage and not to the A-stage (Böhnke & Diering, 1986). It was found that the inert soluble fraction was roughly twice as high in the A-stage (SRT < 1 d) compared to the B-stage (SRT> 10 d), i.e. $S_{I,\ A\text{-}stage}/\ S_{I,\ B\text{-}stage} \approx 2$ (Haider *et al.,* 2013). The authors concluded that short SRT benefits fast growing bacteria which are only partly able to degrade the soluble organic material – in a two-stage process the rest must be degraded in the B-stage. Of course, this also translates to other AS process configurations – a single stage, high-loaded AS with short SRT will leave soluble organic matter for tertiary treatment stages which could have been degraded given a longer SRT.

It shall be pointed out that no difference in $S_{I,\ A\text{-}stage}/\ S_{I,\ B\text{-}stage}$ was recorded when the SRT of the A-stage was varied in between 0.4 and 1.0 days in the experiment of Haider *et al*. (2013). Neither was it possible to determine beyond which SRT in the A-stage for which the $S_{I,\ A\text{-}stage}$ starts to decrease to finally reach $S_{I,\ B\text{-}stage}$.

### 3.3.4 Oxygen uptake rate (OUR): Determination of kinetics and COD fractions

Oxygen uptake rate (OUR) tests have been applied for many years for the characterisation of wastewaters, evaluation of process performance and for determination of parameters for SRT regulation (Hagman & la Cour Jansen, 2007). Since all rate equations and organic fractions in the ASM models of IWA are quantified in terms of oxygen (COD), it is convenient to use OUR for the fractionation model. Usually, it is the soluble fraction of organic matter, $S_s$ (represented by the sum of $S_A$ and $S_F$ in the ASM2d model), that is determined through OUR tests rather than the particulate fraction (Ekama *et al*., 1986; Wentzel *et al*., 1995).

OUR might also be used to determine some kinetic parameters and relations, like the maximum specific growth rate of heterotrophs, $\mu_H$ (Ekama *et al*., 1986) or the half-saturation constant for soluble substrate, $K_S$ (Kappelar & Gujer, 1992). Kinetics can be accessed through the construction of a sub-model, representing the OUR experiment. For the determination of kinetics, simulations are useful in connection to a plant sub-model. Martinello (2013) and Polizzi (2013) constructed such a sub-model based on the Benchmark model no. 1 (BSM1) together with a full model of the HLAS lines at Sjölunda WWTP, all implemented in the MATLAB/Simulink software. The sub-model was to represent the batch experiment, and was modelled as a smaller activated sludge unit in Simulink. By calibrating the OUR response of the experiment to that observed in the sub-model, Martinello and Polizzi were able to estimate the biomass concentration, heterotrophic specific growth rate and half-saturation coefficient for soluble substrate ($K_s$, ASM1 model parameter) of the mixed liquor in the full scale plant.

The first ASM model of IWA did not include heterotrophs in the influent wastewaster to the AS system as a separate organic fraction since its influence had been disregarded in the preceding UCT model of Dold *et al.* (1980). The reason was that South African pipes are generally short and can be considered anaerobic. Hence there will be limited heterotrophic growth in the wastewater on its way to the WWTP. However, for European wastewaters the fraction of $X_H$ of raw wastewaters can be much higher; levels of up to 20% heterotrophs to total influent COD have previously been recorded (Kappelar and Gujer, 1992). Consequently, not considering influent $X_H$ fractions might have significant influence on model predictions of the studied plant (Wentzel *et al.*, 1995).

An easy approach to OUR is the method presented by Hagman & la Cour Jansen (2007), in which the dissolved oxygen (DO) concentration is monitored during cycles of aerated and non-aerated time intervals. If DO is not allowed to get too low, the oxygen uptake rate can be assumed to be constant throughout a cycle. The OUR can then be accessed from the decline in DO (linear) during the non-aerated intervals, and the utilised amount of oxygen as the integral of the respirogram OUR curve. The maximum OUR is observed when all the active microorganisms grow at their maximum specific growth rate (Hagman & la Cour Jansen, 2007).

# 4 Materials & Methods

## 4.1 Overview of the methodical approach

In order to provide input data for the construction of a model of the two HLAS lines to be compared, a two day wastewater characterisation campaign was performed (on the 10th and 11th of February 2015). For the sampling of influent and effluent wastewater, automatic samplers for time-proportional sampling were used (Wastewater vacuum sampler, type: JZ10CBC0, Efconomy, The Netherlands ) (Figure 4.1). The samples represented the average wastewater composition of every two hour interval. The fractions of organic matter of the influent and the effluent over the two days were determined through oxygen uptake rate (OUR) tests and lab-scale filtrations.

The confidence of the SRT control instrument was evaluated through comparison between the recorded sensor measurements (suspended solids) and grab samples for laboratory analysis. The sensors were briefly evaluated in terms of instrument precision, trueness and response time.

The hypothesis about the implications of operation at a lower SRT were tested through a full-scale test campaign (between the 18th of March and the 30th of April) during which one of the HLAS lines was operated at a low target SRT (1.2 d), using instrumental control, and compared to a reference line operated at a higher target SRT (≈ 2.0 d). The G2:2 line was operated using manually control excess sludge withdrawal, according to the traditional fixed MLSS control strategy (see section 3.1.1). The reason for comparing the G2:1 line with the G2:2 line was that they are analogous with respect to zone volumes, sedimentation basins and distribution of fine bubble disc diffuser for aeration (section 4.2). During the test period, settling properties were determined through laboratory sludge volume index (SVI) and zone settling velocity (ZSV) tests. Effluent quality was evaluated through analysis of daily flow proportional samples. Biogas production potential (BMP) of the waste sludge was determined through laboratory experiments by incubating the WAS in small batch reactors, monitored with gas chromatography according to Hansen *et al.*, 2004. Activated sludge foaming in the aerated zones where characterised through ocular observations of the HLAS lines.

The methodology for the modelling of the HLAS lines was based on the guidelines for AS modelling procedure described by Rieger *et al.* (2013). The two lines were set up in the WEST modelling software. The model was based on the ASM2d of the IWA task group (Henze *et al.*, 2000a). It was provided input data based on the results from the characterisation campaign. The model was then used to simulate the process at different SRT set-points for the same data. The most appropriate SRT set-point in terms of sludge yield, effluent quality and aeration energy demand was implemented at one of the lines and briefly evaluated. Finally, the model was validated and recalibrated against the optimised line and the reference line using results from two-hour time proportional samples of a one day measurement campaign, during which the opitmisied control strategy was applied at G2:1 ($SRT_{set}$ = 1.6 d using ICA). Figure 4.2 illustrates an overview of the methodological approach for the project.

*Figure 4.1. Automatic wastewater sampler used for the sampling of influent and effluent wastewater. Both time proportional and daily flow proportional samples were taken during the project period.*

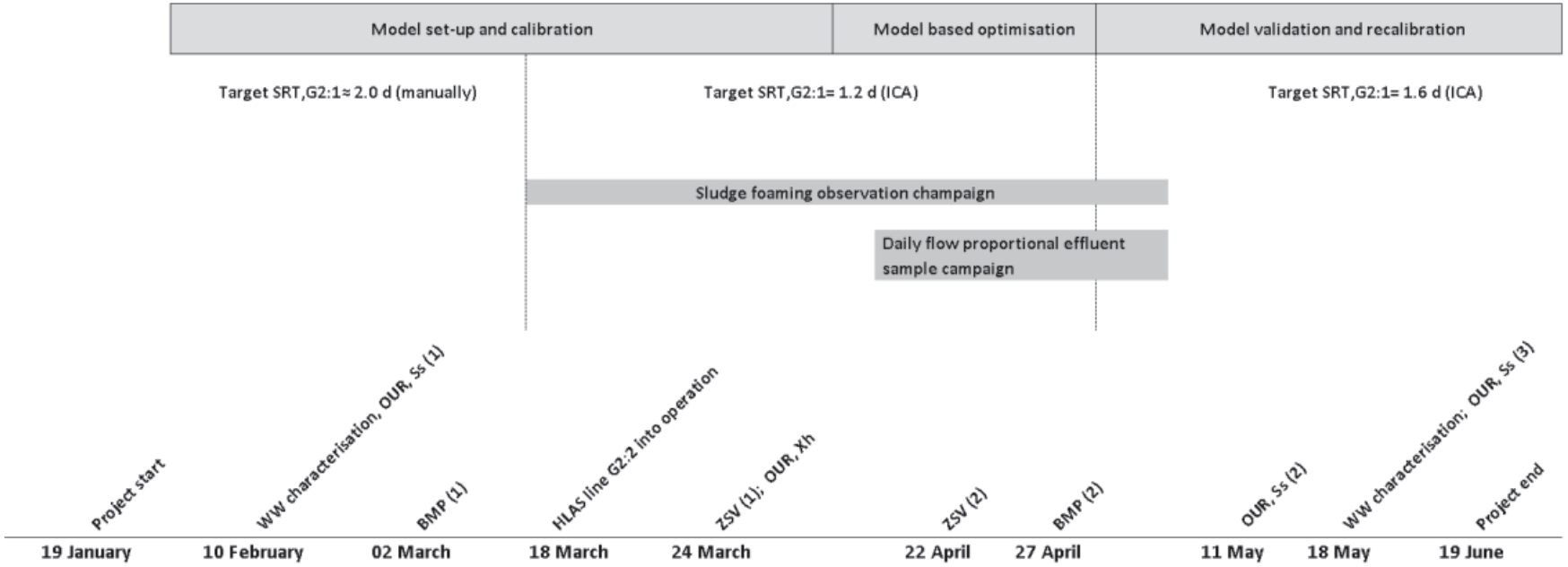


*Figure 4.2. Overview of the methodological approach for the project*

### 4.1.1 Analytical methods and equipment for the characterisation of wastewater

During the wastewater characterisation campaigns and daily flow proportional effluent sample campaign, influent and effluent wastewater as well as the mixed liquor and the WAS were analysed with regard to SS, VSS, COD, VFA and phophours and nitrogenous species.

***Wastewater analysis performed at the laboratory of Sjölunda WWTP***

For the determination of SS and VSS, 1.6 µm pore size glass microfiber filter papers (Art. No:410124, Grade: MGA, Munktell Filter AB, Falun, Sweden) were used (Figure 4.3).The analysis were performed according to Swedish standards (SIS, 1981). These filters were also used for the determination of filtrate COD ($COD_{filt,1,6}$). In addition, two types of 0.1 um cellulose nitrate membranes were used (Cat. No: 7181-004, Size: 47 mm ∅, Whatman Int. Ltd, Maidstone, UK); (Cat. No: 10402014, Size: 50 mm ∅, Whatman™, GE healthcare, Buckinghamshire, UK) for the determination of the true soluble COD fraction ($COD_{filt,0.1}$) as well as for the estimation of TSS (see section 5.7.1 about the distinction of soluble, colloidal and particulate fractions of organic matter). Since the two 0.1 µm membranes were from the same manufacturer and consisted of the same material, they were assumed to have the same properties in terms of separation. No further investigations were made in this regard and the filters were used interchangeably.


*Figure 4.3. The two types of 0.1 µm cellulose membranes and the 1.6 µm glass filter paper used for filtration analysis.*

Standard methods were applied for the determination of total nitrogen (ISO 15923-1:2013 mod SS-EN ISO 11905-1), total phosphorus (ISO 15923-1:2013 mod SS-EN ISO 6878:2005) and phosphate (ISO number unknown), using a spectrophotometer (Gallary Plus, Thermo Scientific).

For the first wastewater campaign ($10^{th}$ and $11^{th}$ of February), COD, $COD_{filt,1.6}$ and $COD_{filt,0.1}$ were analysed using a robot (Dr 5000 Robot, Hach Lange, Germany) together with ampoules (APC 114 and APC 314, Hach Lange, Germany). During the daily flow proportional sample campaign, COD, $COD_{filt,1.6}$ and $COD_{filt,0.1}$ were determined using a spectrophotometer for manual use (Dr 5000, Hach Lange, Germany) and a heating block (LT 200, Hach Lange, Germany) for the heating of ampouls (LCK 414, Hach Lange, Germany). The analyses were performed according to the instructions of the distributor (Hach Lange).

For the determination of $BOD_7$ and $BOD_{7,filt,1.6}$, a biochemical method was applied (SS-EN 1899-1) using a robot (Robot, Skalar Analytical, the Netherlands). The latter robot was also used for the determination of alkalinity ($HCO_3^-$), using a titration method (SS-EN ISO 9963-1).

Ionic nitrogen species were determined manually (without a robot) using ampouls from Hach Lange (Germany): $NH_4^+$-N (LCK303), $NO_2^-$-N (LCK341), $NO_3^-$-N (LCK339). For the wastewater characterisation campaigns, a DR 2800 spectrophotometer (Hach Lange, Germany) was used for the analysis and during the daily flow proportional sample campaign a Dr 5000 spectrophotometer (Hach Lange, Germany). Iron species ($Fe_{tot}$, $Fe^{2+}$, $Fe^{3+}$) were also determined manually using ampouls (LCK320) and analysed with the Dr 5000 spectrophotometer (Hach Lange, Germany).

***Wastewater analysis performed at the laboratory of the department of Water and Environmental Engineering, Lund University***

The analysis of volatile fatty acids (VFA) was performed by a standard method applied at the department of Water and Environmental engineering (Lund University, 2015). Filtrated (1.6 µm filters, as above) influent and effluent wastewater samples at a volume of 0.9 mL were mixed with 0.1 µm phosphoric acid for conservation at 1 mL plastic vials. Within 2-3 days after conservation, the samples were analysed for acetate and propionate using a gas chromatograph (GC 6850, Agilent, Santa Clara, U.S.) equipped with a flame ionisation detector and a HP-FFAP column (CTA19095F-123E).

## 4.2 Plant description: the HLAS lines at Sjölunda WWTP

The flow through the primary and secondary treatment steps at Sjölunda WWTP is divided into two parallel sections prior to being combined and loaded onto nitrifying trickling filters (NTF) (Hanner *et al.*, 2003). The two HLAS lines studied in the presented project, G2:1 and G2:2, are part of the D1 section. This section consists of four primary clarifiers and six preceding, parallel HLAS lines. The HLAS lines are provided with two secondary settling tanks (SST) each. Chemical precipitation with $FeSO_4$ for enhanced phosphorus removal is performed in the primary clarifiers.

The six HLAS lines are divided into three stages (G1; G2; G3). The sub-lines within each stage (two for each stage) are more or less analogous to one another. Sub-lines of different stages within the D1 section are very similar in terms of reactor and secondary settler tank (SST) dimensions. There are however considerable differences in distribution of the fine bubble disc diffusers for aeration between sub-lines of different stages.

The two studied lines for this project, G2:1 and G2:2 (the part of the G2 stage), together receives one third of the flow of the primary effluent of the D1 section during normal operation (when all six lines are operating). Each of the sub-lines is set to receive half of this flow through the separation of a ski board splitter. A flow sensor measures the total influent flow rate to the stage.

Each HLAS line consists of five zones. The first two zones (referred to as zone number 1 and 2) are anoxic, in which there are minor denitrification of nitrate from the return reject water flow that is loaded to the HLAS lines. The other three zones are aerobic, aerated with disc diffusers positioned at the bottom of the reactor tank. The volume of mixed liquor in each

zone for the lines at G2 are [183; 196; 417; 422; 385] $m^3$ for zone number 1 to 5. The total secondary settler surface area, taking both SST in together, is 467 $m^2$ for each sub-line. The SST depth is 3.8 m.

### 4.2.1 The SRT control system at G2:1

The principle of the ICA based SRT control system implemented at the G2:1 line is presented in Figure 4.4. Based on the readings of two flow rate sensors (inflow and waste sludge flow) and three optic SS sensors (ITX-20 SS sensor, Cerlic Controls AB, Segeltorp, Sweden) the set-point rate of sludge wastage (signal r) is calculated in accordance with the set-point SRT decided by the operator (Equation 4.1). Note that Equation 4.1 is a rearrangement of Equation 3.1 (section 3.1), where the effluent flow rate have been expressed as the difference between the influent and waste sludge flow rates. Subscribt *m* denotes a measured signal and subscribt *r* a set-point (reference) value.

$$Q_{was,r} = \frac{\frac{MLSS_m \cdot V_{aerob}}{SRT_r} - Q_{In,m} \cdot SS_{e,m}}{SS_{W,m} - SS_{e,m}} \quad (4.1)$$

The error signal, *e*, is defined as the difference between the controller set-point, r, and the measured rate of sludge wastage:

$$e = r - Q_{W,m} \quad (4.2)$$

The control signal, u, is given from proportional integration in the PI regulator (Equation 4.3). It decides the rate of sludge wastage through regulation of a control valve, as depicted in Figure 4.4.

$$u = K_P(e + 1/T_i \int e(t)dt) \quad (4.3)$$

where $K_P$ is the factor of proportionality and $T_i$ the integral time. There are also max and min values for u:

$u_{min}$ = 1.0 L/s

$u_{max}$ = 5.0 L/s

This is a safety limitation in the event of malfunction of the controller system. In addition, the controller is adapted to regulate the sludge wastage in order for MLSS to be in a specific interval:

$1700 \leq MLSS \leq 3000$ mg SS/L

Finally, there is a limitation for the minimum waste sludge suspended solids concentration, according to:

$SS_{w,\,min}$ = 5000 mg SS/L

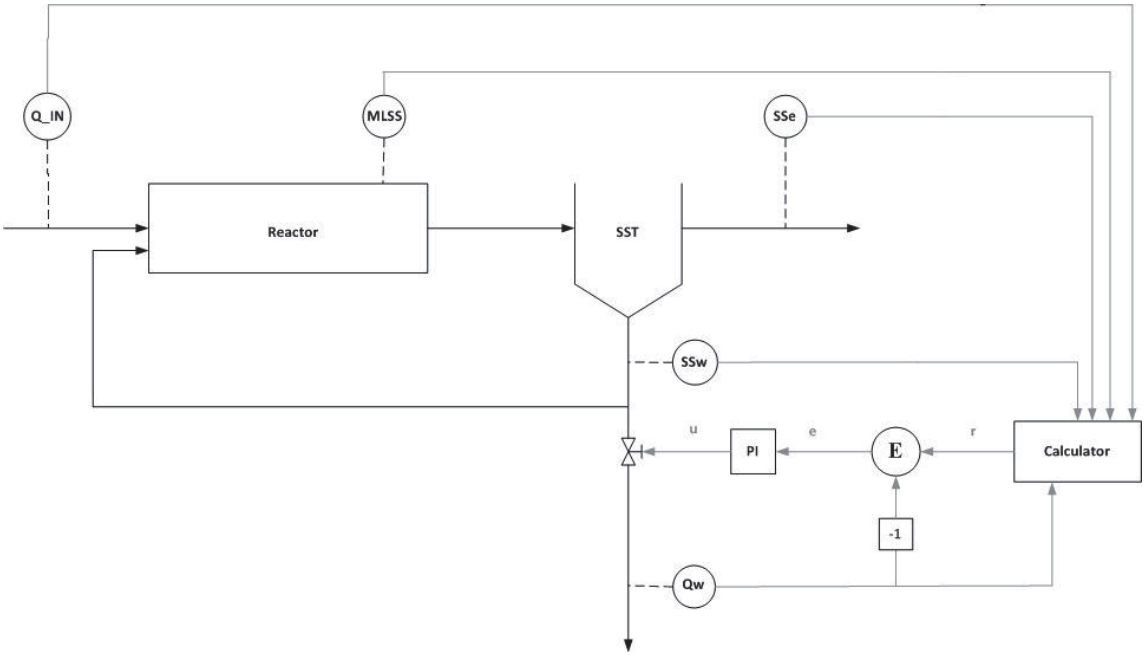


*Figure 4.4. Principle for the ICA based SRT control system applied to the G2:1 line at Sjölunda WWTP.*

The SS sensors and their positioning at the G2:1 line are presented in Figure 4.5. The sensors were equipped with an automatic self-cleaning mechanism for the prevention of fouling. During the project period, they were occasionally cleaned manually. The sensors were also regularly calibrated towards laboratory SS measurements. At the 9$^{th}$ of April, the response time were approximately evaluated by putting the sensors in clean water and then back into the process water again as described by Rieger *et al.* (2005).

*Figure 4.5. Pictures of online sensors for the measurement of suspended solids concentrations in (from left to right) the WAS, the mixed liquor of zone 5 and the SST effluent. 9$^{th}$ of June 2015.*

## 4.3 Influent wastewater characterisation: Oxygen uptake rate (OUR)

### 4.3.1 Fraction of heterotrophic biomass ($X_H$) in the influent

In order to determine the COD fraction of heterotrophic biomass ($X_H$) in the AS plant influent, a microorganism respiration test based on that presented by Wentzel *et al.* (1995) was performed. The experiment was performed on the 24th of March with a grab sample of influent wastewater to the G2:1 line, collected at 08.00.

Two batch reactors, consisting of 500 mL open top glass beakers, where supplied with 450 mL fresh influent wastewater. The reactors were put in a waterbath keeping a constant temperature of 20 °C. Next, 1.35 mL of 12 mg/L allylthiourea (ATU) was added to prevent the activity of nitrifying bacteria, since only heterotrophic oxygen uptake was to be measured. At the same time, 4.5 mL 0.236 g/L $(NH_4)_2SO_4$ and 5.5 mL 0.044 g/L $KH_2PO_4$ where added in order to make sure that there was a sufficient supply of nutrients available, in the form of ammonium and phosphate, to sustain heterotrophic growth at a maximum specific rate.

The reactors were stirred using magnetic stirrers and simultaneously aerated using a compressor. Aeration was performed in cycles. For every 10 min cycle, reactors were aerated for 5 min and then non-aerated for another 5 min. The level of dissolved oxygen (DO) was monitored with an oxymeter and the data was recorded on two data loggers (HQ40d multi, Hach, Germany). After 7 h and 42 min, the experiment was stopped. The reason to stop the experiment at this time was that the exponential growth phase was expected to be over at that time but also practical limitations. From the decline in DO-levels during the non-aerated intervals, the oxygen uptake rate throughout the test could be derived.

The $X_H$-fraction of the influent wastewater can be calculated by deriving a function for the exponential increase in OUR that is observed in the test due to heterotrophic growth. In the initial phase of the experiment, before solvable substrate has been depleted, there is no substrate inhibition. Neither will there be oxygen inhibition due to the supply of air, as long as DO levels are not allowed to drop too much (in the experiment, DO was always above 6 mg $O_2/l$). During these conditions, a simplified expression for biomass growth can be written according to:

$$\frac{dX_{H,inf}}{dt} = (\mu_{H,inf} + K_{MP,inf} - b_{H,inf})X_{H,inf} \quad (4.4)$$

where:

$X_{H,inf}$ = active heterotrophic biomass concentration in the influent (mg COD/*L*)

$\mu_{H,inf}$ = max. specific growth rate of $X_{H,inf}$ on directly and readily degradable substrate

$K_{MP,inf}$ = maximum specific growth rate of $X_{H,inf}$ on slowly degradable substrate

$b_{H,inf}$ = specific decay rate of $X_{H,inf}$

Note that the above specified parameters are for influent heterotrophic biomass ($X_{H,inf}$) and not for the heterotrophs of the activated sludge ($X_H$). There might be significant differences in the composition of the heterotrophic populations between influent wastewater and sludge (Wentzel *et al.*, 1995). Also note that there is no equivalent parameter to maximum specific

growth rate on slowly degradable substrate in the ASM models. The ASM models only considers growth on soluble substrates, which can be made accessible through prior hydrolysis (Henze *et al.*, 2000a).

Through integration, Equation 4.4 can be written as:

$$X_{H,inf\,(t)} = X_{H,inf\,(0)} e^{\mu_{H,inf} + K_{MP,inf} - b_{H,inf})} \tag{4.5}$$

The OUR at time = t from the start of the experiment can be expressed in terms of $X_{H,inf(t)}$ and the net specific growth rate:

$$OUR_{(t)} = \frac{1-Y_{H,inf}}{Y_{H,inf}} (\mu_{H,inf} + K_{MP,inf})\, X_{H,inf\,(t)} \tag{4.6}$$

If $X_{H,inf(t)}$ in Equation 4.6 is substituted with Equation 4.4, the following expression for the natural log of $OUR_{(t)}$ is given:

$$\ln OUR_{(t)} = \ln \left[ \frac{1-Y_{H,inf}}{Y_{H,inf}} (\mu_{H,inf} + K_{MP,inf})\, X_{H,inf(t)} \right] + (\mu_{H,inf} + K_{MP,inf} - b_{H,inf})t \tag{4.7}$$

Since the natural log of an exponential function is a straight line, it is realised that the slope of this line is:

$$\text{slope: } (\mu_{H,inf} + K_{MP,inf} - b_{H,inf}) \tag{4.8}$$

$$\text{y-axis intercept: } \ln \left[ \frac{1-Y_{H,inf}}{Y_{H,inf}} (\mu_{H,inf} + K_{MP,inf})\, X_{H,inf(0)} \right] \tag{4.9}$$

Now, rearranging Equation 4.9, we might express $X_{H,inf(0)}$ according to:

$$X_{H,inf(0)} = \frac{e^{y-intercept}}{\frac{1-Y_{H,inf}}{Y_{H,inf}} (\mu_{H,inf} + K_{MP,inf})} \tag{4.10}$$

Finally, inserting the expression for the slope of the log exponential function (4.8) yields:

$$X_{H,inf(0)} = \frac{e^{y-intercept}}{\frac{1-Y_{H,inf}}{Y_{H,inf}} (slope + b_{H,inf})} \tag{4.11}$$

Knowing the initial COD concentration of the wastewater, the fraction of heterotrophic biomass in the influent in relation to particulate COD can simply be calculated as:

$$f_{X_H} = \frac{X_{H,inf}}{COD_{X,inf}} \tag{4.12}$$

where $COD_X$ is the particulate COD concentration in the influent.

### 4.3.2 Fraction of easily biodegradable substrate ($S_s$) in the influent

Two different types of OUR tests were performed in order to determine the fraction of soluble, easily biodegradable matter ($S_s$). One method used the same experimental design as for the determination of the $X_H$ fraction as presented above; the two fractions can in fact be de-

termined from the same experiment (Wentzel *et al.*, 1995). The other method, also performed as a laboratory batch test, used a mix of influent wastewater and activated sludge from the aerobic basin as reactor medium, and was based on the method of Ekama *et al.* (1986). For the latter experiment, oxygen uptake is mainly associated with that of heterotrophic activity in the sludge whereas the former depends on the OUR of heterotrophs present in the influent wastewater only (section 4.3.1).

***Determination of $S_s$ based on the oxygen uptake of influent heterotrophs***

In order to calculate the amount of $S_S$ in the influent wastewater using the method of Wentzel *et al.* (1995), the initial concentration of heterotrophic biomass, $X_{H,inf(0)}$, must first be calculated (section 4.3.1). Based on $X_{H,inf(0),}$ one is able to derive a function for heterotrophic growth on slowly biodegradable substrate, $X_S$, by studying the OUR immediately after $S_s$ depletion, that is just after the precipitous drop in OUR. An equation for OUR on $X_S$ as a function of time can be expressed according to Equation 4.13:

$$OUR_{X_S(t)} = \frac{1-Y_H}{Y_H} K_{MP} \cdot X_{H,inf\,(0)} e^{(\mu_{H,inf}+K_{MP}-b_H)t} \tag{4.13}$$

When Equation 4.13 is rearranged into Equation 4.14, an expression for a hypothetical maximum specific heterotrophic growth rate, $K_{MP}$, on $X_S$ is:

$$K_{MP} = \frac{OUR_{X_S(t=s)}}{\frac{1-Y_H}{Y_H} X_{H,inf(0)} e^{(\mu_{H,inf}+K_{MP}-b_H)t=s}} \tag{4.14}$$

where t = s is the time immediately after the precipitous OUR drop, that is immediately after $S_S$ depletion. At this point in time, OUR is believed to be associated with growth on $X_S$ and endogenous respiration only (Wentzel *et al.*, 1995). $S_S$ can now be calculated analytically according to Equation 4.15:

$$S_S = \frac{1}{1-Y_H} \int_{t=0}^{t=d} OUR_{tot} - OUR_{X_S} \tag{4.15}$$

where t = d is the time observed for the precipitous OUR drop, that is exactly at $S_S$ depletion (note that t = d < t = s). $S_S$ can also be accessed graphically from the respirogram as the difference between total OUR and a hypothetically derived OUR curve on $X_S$. Finally, the fraction of easily biodegradable substrate to total soluble COD ($COD_S$) can be calculated as:

$$f\_S_S = S_S/COD_S \tag{4.16}$$

Two trials where made using the method of Wentzel *et al.* (1995) for $S_S$ determination during the second wastewater characterisation campaign of the HLAS lines at G2 (18$^{th}$ of May, 2015) for time proportional influent water samples collected between 14.00 - 16.00 and 22.00 - 24.00. In addition, duplicate batch tests where made one the 11$^{th}$ of May since Persson (2015) was performing a characterisation campaign for model validation of the HLAS lines at G1 by that time. Influent water for the latter experiment was collected between 04.00 - 06.00. All these trials where run for a longer period of time, ≈ 14 h, than the experiment for the determination of $X_H$, performed on 26$^{th}$ of February (section 4.3.1). The reason was that it was desirable to identify a plateau, representing growth on $X_S$ only with simultaneous hydrolysis, in order to be able to precisely decide the actual OUR immediately after $S_S$ depletion. The

determination of the OUR at t = s was believed to be important for the derivation of a more correct hypothetical function for growth on $X_S$.

The same nutrient solution and ATU were added as for experiment of the 24th of February, at the same amounts and at the same time in the experiment.

***Determination of $S_S$ based on oxygen uptake of heterotrophs from activated sludge***
First, 50 mL of activated sludge from the aerobic basin from the studied HLAS line in question, was continuously aerated in a 500 mL glass beaker. The beaker was standing in a water bath, keeping a constant temperature of 20°C and the reactor medium stirred by a magnetic stirrer. Different duration of the initial aeration phase was elaborated on, ranging from 30 min to about 1 hour. The reason for the initial aeration was for organic substrate absorbed onto the activated sludge to be oxidised quickly. After the initial aeration phase, aeration was performed in cycles (in the same way as for the other batch tests, section 4.3.1) for about 1-2 hours. This was done in order to be able to verify that OUR was associated with endogenous respiration only, i.e. no uptake due to the degradation of adsorbed organic matter. At this time, ATU and the standard nutrient solutions were added, in the same amounts as for the influent heterotrophic based experiment (section 4.3.1).

Having pre-aerated the sludge, 400 mL of influent wastewater was added to the beaker, after which the OUR was continuously monitored through aeration cycles. The aeration cycles were run for 2 - 7 hours after the addition of wastewater (the tests performed during the second wastewater characterisation campaign were run for a longer period of time compared to those of the first campaign). Note that the influent wastewater was pre-aerated a couple of minutes in order to be saturated with dissolved air. This was to avoid disturbances in the OUR readings. Since the sludge had been pre-aerated, the OUR response could be associated with oxidation of influent organic substrate only.

The amount of $S_S$ in the influent samples was calculated as the oxygen uptake registered in the respirogram associated with oxidation of $S_s$ times the ratio between utilized and consumed oxygen for the oxidation process (Equation 4.17). The factor $1/(1-Y_H)$ represents the quantity of oxygen that is used for driving the synthesis reaction for biomass growth on $S_S$, that is the amount of $O_2$ that is actually consumed. The rest of oxygen taken up will result in biomass which in turn is COD (Ekama *et al.,* 1986).

$$S_S = \frac{1}{1-Y_H} \Delta O_{S_s} \cdot V_{ww}/(V_{ww} + V_{ML}) \quad (4.17)$$

$$\Delta O_{S_S} = OUR_{S_S} \cdot t_d \quad (4.18)$$

where:
$Y_H$ = Yield coefficient for aerobic heterotrophic growth (mg COD/mg COD)
$\Delta O_{Ss}$ = Oxygen uptake associated with oxidation of $S_s$ (mg $O_2$/L)
$OUR_{Ss}$ = Oxygen uptake rate associated with oxidation of $S_s$ (mg $O_2$/L/h)
$t_d$ = time for depletion of $S_s$ after the start of the experiment.
$V_{ww}$ = volume of influent wastewater added to reactor (mL)
$V_{ML}$ = volume of activated sludge (mixed liquor) added to the reactor (mL)

### 4.3.3 COD mass balances for OUR tests: Reliability of the respirometric method

In order to determine the validity of the results derived from the OUR tests, the difference in COD in the batch reactor before and after the experiment was compared to the OUR recorded in the respirogram. The level of COD recovery can be quantified according to Equation 4.19, as done by Wentzel *et al*. (1995):

$$COD_{recovery} = \frac{COD_{t=T} + \int_{t=0}^{t=T} OUR\ dt}{COD_{t=0}} \qquad \text{(Equation 4.19)}$$

where t = 0 is the time for the start of the experiment and t = T is the time for withdrawal of reactor medium for COD analysis. For practical reasons, t = T was not the time for the end of the experiment for those trials running for a longer period of time (> 9 h). Instead, 50 mL of reactor medium was withdrawn a couple of hours after the estimated time for $S_S$ depletion, several hours before the end of the experiment. In addition, the laboratory COD analysis on withdrawn reactor medium samples was not performed directly. For some of the tests, the samples were kept refrigerated overnight in completely filled and sealed 50 mL plastic flasks. No conservation agent was added to these samples to stop the activity of microorganisms.

## 4.4 Full-scale tests: Implications of low SRT on plant performance

In order to test the implications of lower SRT on plant performance, one of the HLAS lines (G2:1) was set to run at an SRT = 1.2 d using the newly implemented ICA system for SRT control. This change was implemented on 18th of March, 2015. Prior to that, this line had been operated with the traditional MLSS control strategy, giving an approximate SRT of 2.0 d with some variations throughout the day. On the 30th of April, the set-point SRT was increased to 1.6 days to test the implications of the optimised control strategy retrieved from model simulations.

For comparison, the parallel line (G2:2) remained operated with manual MLSS control, SRT ≈ 2.0. Both lines were operated with the same aeration strategy: DO set-points = [0.3; 0.8; 1.7] mg $O_2$/L for zone 3, 4 and 5 respectively.

### 4.4.1 Effluent quality: Daily flow proportional sample campaign

To test the implications of low SRT on effluent quality in full-scale, a daily flow proportional sample campaign was carried out between the 14th of April and the 4th of May, 2015. Primarily, the suspended solids concentration in the influent and the effluent was monitored for the two lines in order to determine differences in solids removal efficiency. Once a week, a larger analysis was carried out in which COD, nitrogen and phosphorus concentrations were determined as well.

### 4.4.2 Sludge foaming: Characteristics and quantity

In order to quantify the difference in sludge foaming between low and high SRT, the sludge foam level was checked several days a week from 12th of March until the 4th of May, 2015, for the two compared parallel lines. The height of the sludge foam blanket was calculated as the difference between the smallest distance of the foam blanket to the basin edge and the water surface level to the basin edge. Since the water surface was sometimes completely covered with foam, a mean water surface level was used for the calculation, which was determined through regular measurements when the surface was not covered. Sometimes, the degree of surface coverage was rather scarce with the foam consisting mainly of dispersed chunks close

to the basin borders. At these occasions, the foam height was determined from the minimum distance to the basin edge from the highest level of the foam chunks. The degree of foam coverage was approximated through ocular observation at each occasion.

In addition, the foam brightness was determined for each occasion. At a few occasions prior to the observation campaign, very dark, almost black, foam was observed. This level of darkness was given a darkness factor of 5. At other occasions, a very bright almost completely white foam had been observed. This foam was given a darkness factor of 1. During the observation campaign, the darkness factor was determined as 1, 2, 3, 4 or 5 depending on how bright was the sludge in comparison to these two extremes.

### 4.4.3 Sludge settling properties: Zone settling velocity tests (ZSV)

In order to derive the maximum theoretical and practical settling velocities ($v_0$ and $v_0$'), the minimum concentration in the sludge blanket ($X_{Lim}$) as well as the sludge volume index (SVI) for the activated sludge of the two studied HLAS lines, zone settling velocity (ZSV) tests was performed at two occasions. At the first occasion, on the 24$^{th}$ of March, tests were performed with ML from the aerobic basin (zone 5) of G2:1 only. By that time, the line was still operated through the traditional MLSS control strategy, using manual regulation of the WAS flow (SRT ≈ 2.0 d). In order to test the implications of SRT on settling properties of the sludge, the second trial was made on the 22$^{th}$ of April, by the time which G2:1 was operated through the ICA control strategy (SRT ≈ 1.2 d) and G2:2 traditionally (SRT ≈ 2.0 d), using ML from both lines.

The ZSV tests were performed in line with the method presented by Catunda & Haandel (1992). Measuring cylinders, with standardised dimensions for $SV_{30}$ tests (volume = 1000 mL) were filled with ML. Then, the change in sludge blanket level was observed for every minute during a period of 10 min. Unlike for the method of Catunda & Haandel (1992), the suspension was not automatically stirred since the necessary equipment was not available. After 30 min, the final sludge blanket level was noted, which gave $SV_{30}$. In addition, MLSS was determined as the mean of triplicate analysis using 1.6 µm filter papers (SIS, 1981). From these results, corresponding SVI calculations were made as well (see section 3.2.1 for the definition of SVI).

The maximum settling velocity, $v_s$, was calculated as the maximum observed ZSV during the 10 minutes long experiment. In order to access the maximum zone settling velocity at different concentrations, representing the different layers of the SST in the Takács-SVI model (section 3.2.1), the ML was diluted with tap water into seven different concentrations. The different dilution consisted of 40; 50; 60; 70; 80; 90; and 100% ML, all for which the maximum ZSV where determined. Additional dilutions, in the range of 15-30% ML where also done in order to find the minimum attainable concentration of the sludge blanket, $X_{Lim}$. The principle for the dilution tests is described from Figure 4.6.

*Figure 4.6. Principle for ZSV tests. Mixed liquor was mixed with tap water and let to settle in 1000 mL measuring cylinders. The picture shows four such cylinders shortly after the tests. The difference in dilution is indicated from the sludge volume at the bottom of the cylinders.*

### 4.4.4 Sludge methane potential (BMP) tests

In order to quantify any difference in methane production potential for the WAS of the two compared HLAS lines operated at different SRT, secondary settler underflow sludge was collected from the two lines during the full-scale test period and then tested with a not standardised method for methane potential determination of organic waste by Hansen *et al.* (2004). The sludge was collected on the 27$^{th}$ of April, about six weeks after the implementation of automated SRT control on the G2:1 HLAS line ($SRT_{setpoint}$ = 1.2 d). The sludge was transported about 20 km by car to the Department of Chemical Engineering, Lund University, directly after sampling, where it was left to settle by gravity in 2.5 L plastic cans for about 2 hours. The sludge was thickened somewhat by pouring of the supernatant, roughly 1/3 of the total volume, of the settled sludge samples. The concentration of total solids (TS) and volatile solids (VS) was determined for the settled sludge according to Swedish standards (SIS, 1981).

The results of the VS analysis was used in order to determine the amount of waste sludge to be added to each of the 2 L glass flasks, serving as anaerobic bioreactors for methane production (Hansen *et al.*, 2004). As an inoculum, digested sludge from one of the anaerobic digesters at Sjölunda, WWTP (named J6) was used. To each of the reactors, 380 g of inoculum was added. Having determined the VS of the inoculum, the amount of WAS needed to be added to each reactor was calculated in order to achieve a total volatile solids content of 8.4 g VS per reactor. These proportions gave the recommended substrate to inoculum volatile solids ratio of 0.67 g/g and a total VS content of almost 10 g/reactor (Hansen *et al.*, 2004; Lund University, 2012a). The reactor medium with the somewhat thicker sludge from the G2:2 line was diluted with tap water in order for the total reactor volume to become exactly 700 mL for both types of sludge substrates. This volume of batch solution allowed for a considerable gas headspace.

Triplicate reactors were set for each of the sludge substrates, meaning there were three glass flasks for each of the two evaluated sludge samples, containing the same amounts of sludge, inoculum and water. It should be mentioned that triplicate reactor series were set for an additional two HLAS lines with the same inoculum, since Persson (2015) was evaluating the implication of dissolved oxygen levels for biogas production at the time.

In addition, cellulose was used as a reference substrate in order to evaluate the quality of the inoculum and the reproducibility of results (i.e. the uncertainty of measurement). For these reactors, 3.37 g of a mixed cellulose powder, consisting of 50% Avicel PH 101 (Fluka Sigma-Aldrich) and 50% microcrystalline cellulose powder (Biomedicals Bier & Berntsen) was added together with 380 g of inoculum for a triplicate series of reactors in order to achieve a total VS content of 8.4 g/reactor. Water was added in order to achieve a total reactor volume of 700 mL. In order to be able to monitor the methane production from the inoculum itself, three reactors were set with only 380 g of inoculum and water (reactor volume = 700 mL).

Before being sealed with a thick rubber septum, the reactors were flushed with pure nitrogen gas in order to ensure anaerobic conditions. The flasks were then incubated at 37 $^{o}$C. In connection to the very start of the experiment, new TS and VS analysis were performed for the sludge substrates as well as for the inoculum. In addition, COD, $COD_{filt,1.6um}$, $NH_4$-N and pH analysis were performed.

***Reference BMP test***

Prior to the main BMP test for the comparison of different SRT operation, an initial reference test was performed, mainly in order to test the method. This test used WAS collected from G1:2 and G2:1 at the 2$^{nd}$ of March. These two lines were operated similarly at the time. The target SRT at both lines was 2.0 days, using the manual control strategy. Set-point DO levels equalled [0.3; 0.8; 1.7] for G2:1 and [0.3; 0.8; 2.0] for G2:2. A mixture of inoculums from the digesters named J5 and J6 were used. The test was performed equivalently to the main test described above, but reactors were incubated for a longer period of time (37 days).

*Figure 4.7. Glass flask reactor for methane production, equipped with a pressure tight rubber septum secured with a metallic lock. The depicted reactor contains a mixture of inoculum, tap water and WAS.*

***Gas chromatography***

The methane production in the reactors throughout the experiment was monitored through gas chromatography. Through the rubber septum of the glass reactors, 0.2 mL of gas were withdrawn from the flasks through the rubber septum using a pressure tight syringe. The gas sample was injected to a Varian 3800 Gas Chromatograph equipped with a thermal conductivity detector (TCD) and 2.0 m (length), 1/8" (diameter), 2.0 mm (film) HAYESEP mesh column in order to find the methane content of the flask (expressed as the area under the gas response curve in the chromatograph). Triplicate measurements were performed for each flask at a time. Also, triplicate measurements were performed on a flask with 100% methane gas. By relating the methane content recorded in the reactors with that of the reference methane flask and multiplying with the available headspace, the volume of methane in the flasks could be determined. The recorded volumes was transformed into gas volume at standard conditions (1 atm, 20 $^{o}$C) by relating to the pressure and temperature in the room at the time of measurements (Hansen et al, 2004; Lund University, 2012a).

Since the reactors produced a considerable amount of methane gas during the experiment (up to 1800 NmL $CH_4$/reactor), it was necessary to equalise the over pressure by releasing some of the gas in the flasks in order to avoid leakage and for the glass flasks not to burst. Gas was released by inserting a needle in the rubber septum immediately after the chromatography reading. For flasks containing sludge as substrate, gas was released 3 and 7 days after the initialization of the experiment. Flasks with cellulose substrate were also equalised twice (7 and 11 days after the start) and flasks with inoculum and water only were not emptied at all.

The experiment was run for 23 days and ended on the 21$^{th}$ of May. At termination of the experiment, TS and VS analysis were performed for all of the reactors as well as COD analysis. $NH_4$-N and pH analysis were performed for one reactor per series of triplicates for the different substrate types.

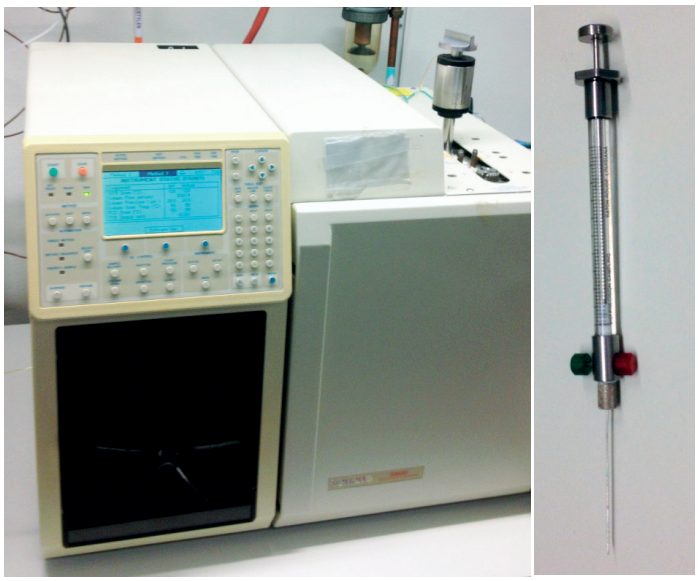

*Figure 4.8. The gas chromatograph (left) used for methane analysis and the pressure tight syringe (right) for gas injections.*

## 4.5 Modelling the HLAS plant

### 4.5.1 Model set-up in WEST

For the initial model the HLAS line G2:1, the only line at which an ICA based SRT control system is implemented, was set up in the WEST software (DHI, 2014). The five different zones, two non-aerated and three aerated, were modelled as five separated but connected AS units. The volumes of the zones were set in accordance with those of the zones in the real line (section 4.2).

The model also included the SST. An extension for the model of Takács (1991) relating hindered settling to the SVI were used for the dynamics of the SST (section 3.2.1) which is standard for the modelling of secondary settling in WEST. For the model, one SST was to represent the two SST for the full-scale plant. The model SST was given the same height as that of the two real SST and a surface area corresponding to the sum of the surface area of the two real SST (section 4.2).

The magnitude of the settler sludge underflow was regulated through an input data block based on the return sludge pumping in the real plant. The WAS flow was also regulated through an input data block.

***Implementation of the ICA based SRT controller at the G2:1 HLAS line in WEST***

The ICA system for SRT control at the G2:1 line was implemented in WEST. As for the real ICA system, the aerobic SRT of the system was calculated from online sensors for flows, suspended solids concentrations and from the volume of the aerobic part of the reactor (Equation 3.1). For the calculation, a calculator block was used. The algorithm for the SRT calculation is pre-implemented in WEST and is performed automatically when connecting the appropriate sensor blocks to the calculator block. In order for the calculator block to calculate the correct SRT, it must receive a measured signal for the effluent flow rate, preferably from a sensor block (Equation 3.1). For the real ICA system at G2:1, the effluent flow rate is calculated as the difference between the influent flow rate and the WAS flow (section 4.2.1)

A PI controller was introduced for the possibility of controlling the SRT through the regulation of the WAS flow. However, for the calibration of the initial model the WAS flow was regulated using data input block based on real data as described above, and not through the ICA system which was not in operation during the first wastewater characterisation campaign (on the $10^{th}$ and $11^{th}$ of February). The modelled ICA system was however used for simulations for the optimisation of the SRT control strategy (section 4.5.3). In addition, the SRT calculator was used to provide the aeration model with a measured SRT signal since the aeration model takes the SRT dependency of oxygen transfer efficiency in to account (see below). The calculated SRT signal was treated in a data treatment block. This standard block of the WEST software smoothens the signal to allow for fewer oscillations in SRT and to break algebraic loops (DHI, 2014).

***Implementation of an aeration model at the G2:1 HLAS line in WEST***

Persson (2015) constructed a calibrated model for the aeration of the aerobic zones of the G2:1 HLAS line at Sjölunda WWTP, based on the data set for the wastewater characterisation campaign of the $10^{th}$ and $11^{th}$ of 2015. This model was based on the Irvine Carbon footprint aeration model of the WEST software (DHI, 2014), which is based on the theory of Boyle (1989). In addition, WEST model is also taking into consideration the relation between SRT

and oxygen transfer efficiency as described by Rosso & Stenstrom (2005) and Rosso *et al.* (2005). The relation between SRT and oxygen transfer efficiency may be described from Equations 4.20 - 4.22 (DHI, 2014):

$$\alpha SOTE = A \cdot log\chi - B \quad (4.20)$$

where:

αSOTE = Oxygen transfer efficiency for new aerators (-)

A = Empirical factor (-)

B = Empirical factor (-)

χ is calculated as:

$$\chi = SRT/Q_n \quad (4.21)$$

where $Q_n$ is the normalised airflow ($Nm^3/d$). The normalised airflow is deduced as:

$$Q_n = \frac{Q_{air}}{A_{sp} \cdot N_d \cdot Depth} \quad (4.22)$$

in which:

$Q_{air}$ = Air flow rate at standard conditions ($m^3/d$)

$A_{sp}$ = Specific area of the diffusers ($m^2$)

$N_d$ = Number of diffusers (-)

Depth = Depth of the fine bubble aerator (m)

In order to model the SRT dependency of the oxygen transfer efficiency, the measure signal for SRT calculated by the calculator block, was sent to the aerators which calculated the αSOTE according to the Equations 4.20 - 4.22.

As for the aeration model of Persson (2015), the airflows to the different zones were provided from aerator blocks, one for each of the aerated zones. The magnitudes of the airflows were regulated by PI-regulators, based on the difference of set-point and meassured DO levels for the different zones. There was one PI-regulator for each aerator. For the initial model, set-point DO levels were set in accordance to those for the characterisation campaign of the 10th and 11th of February. The distribution of fine bubble disc diffusers for aeration were given the same values as for the real HLAS line.

Table *4.1* gives the parameter values for the PI-regulators. Table 4.2 and Table 4.3 gives the values for the non-zone specific and zone specific parameter values for the Irvine carbon footprint aeration model of WEST (DHI, 2014) that was modified. The initial parameter values were set equally to those which Persson (2015) found through calibration of the aeration model, using input data from the characterisation of the G2:1 HLAS line at the 10th and 11th of February.

*Table 4.1. Parameter values for the aerator PI-regulators for the initial model.*

| Parameter | Description | Unit | Zone3 | Zone4 | Zone5 |
|---|---|---|---|---|---|
| $\mathbf{K_p}$ | Factor of proportionality | - | 70 | 70 | 100 |
| $\mathbf{T_i}$ | Integral time | $10^{-4}$ d | 1.0 | 1.0 | 1.0 |
| $\mathbf{u_0}$ | No error action | $Nm^3/d$ | 16000 | 13000 | 8000 |
| $\mathbf{u_{Max}}$ | Max control action | $Nm^3/d$ | 58752 | 44160 | 30720 |
| $\mathbf{u_{Min}}$ | Min control action | $Nm^3/d$ | 7344 | 5520 | 3840 |
| $\mathbf{y_s}$ | Set-point DO | mg $O_2$/L | 0.3 | 0.8 | 2.0 |

*Table 4.2. Non-zone specific manipulated aerator parameter values for the initial model.*

| Parameter | Description | Unit | Value |
|---|---|---|---|
| **H** | Altitude for aerator | m | 0 |
| $\mathbf{Rho_{air}}$ | Air density | $g/m^3$ | 1272 |
| $\mathbf{T_{air}}$ | Temperature of the air | $^oC$ | 3 |
| $\mathbf{T_{water}}$ | Temperature of the water | $^oC$ | 14 |
| $\mathbf{A_{sp}}$ | Specific area of the diffusers | $m^2$ | 0.038* |
| **Depth** | Depth of the fine bubble aerator | m | 3.8 |

*For the calibration, optimisation and validation procedures, the specific area of the diffusers was first set to 0.025 $m^2$ due to a misunderstanding regarding the diffusers in place at the real plant. This figure consequently had to be changed and the simulations re-runned. However, changing the configuration had very little effect on the outcome of simulations.

*Table 4.3. Zone specific manipulated aerator parameter values for the initial model.*

| Parameter | Description | Unit | Zone3 | Zone4 | Zone5 |
|---|---|---|---|---|---|
| **A** | Empirical factor | - | 6.6 | 5 | 7 |
| **B** | Empirical factor | - | 2.6 | 4.5 | 6.2 |
| $\mathbf{N_d}$ | Number of diffusers | - | 428* | 378* | 248* |

* For the calibration, optimisation and validation procedures, the number of diffusers where set to 612, 460 and 320 for zone 3-5 due to a misunderstanding regarding the diffuser configuration of the real plant. These figures consequently had to be changed and the simulations re-runned. However, changing the configuration had very little effect on the outcome of simulations.

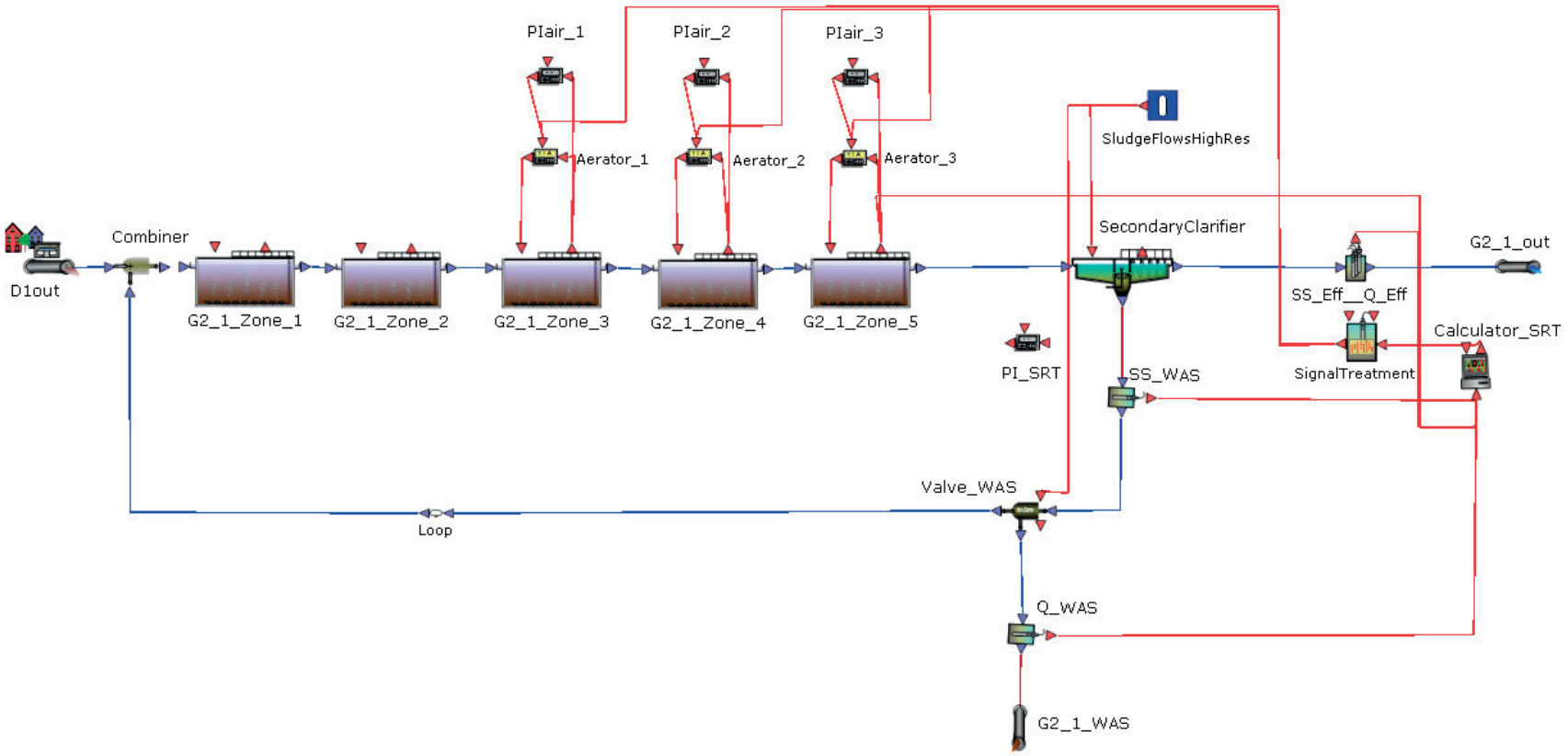


*Figure 4.9. Initial model set up in the WEST graphical interface.*

### 4.5.2 Model input data

The model was provided input data based on the results of laboratory analysis and experiments for the two-day wastewater characterisation campaign ($10^{th}$ and $11^{th}$ of February 2015). In the WEST software, the actual model input used for the simulation is determined through a fractionation scheme, which translates real input data into ASM components. The standard fractionation scheme for the ASM2d model only includes input components for influent water flow ($H_2O$) as well as concentrations for total influent COD (COD), total suspended solids (TSS), total Kjeldahl nitrogen (TKN) and total phosphorus (TP). In order to make the actual ASM2d model components less dependent on fixed fractions, the standard fractionation scheme was modified to include more individual input components. Table 4.4 lists all the input components used and Table 4.5 the ASM2d model components.

*Table 4.4. Model input data components defined for the model.*

| Data input component | Description | Unit |
|---|---|---|
| Water | Influent wastewater flow | $m^3/d$ |
| COD | Total COD | mg COD/L |
| $COD_{filt}$ | Filtrated COD ($COD_{filt,1.6}$) | mg COD/L |
| Acetate | Acetate | mg COD/L |
| SS | Suspended solids | mg COD/L |
| TKN | Total Kjeldahl nitrogen | mg N/L |
| $NH_4$-N | Ammonium nitrogen | mg N/L |
| $NO_2$-N | Nitrite nitrogen | mg N/L |
| $NO_3$-N | Nitrate nitrogen | mg N/L |
| $PO_4$-P | Phosphate | mg P/L |
| Alkalinity | Bicarbonate alkalinity | mg $HCO_3^-$/L |

*Table 4.5. All model components of the ASM2dModTemp model of WEST (DHI, 2014;Henze et al., 2000a). $S_i$ denotes soluble model components i and $X_i$ particulate components i.*

| Model component | Description | Unit |
|---|---|---|
| $S_A$ | Fermentation products (acetate) | mg COD/L |
| $S_{Alk}$ | Bicarbonate alkalinity | mg $HCO^{3-}$/L |
| $S_F$ | Readily biodegradable substrate | mg COD/L |
| $S_I$ | Soluble inert org. matter | mg COD/L |
| $S_{N2}$ | Nitrogen gas | mg N/L |
| $S_{NH}$ | Ammonium nitrogen | mg N/L |
| $S_{NO}$ | Nitrate and nitrate nitrogen | mg N/L |
| $S_O$ | Dissolved oxygen | mg $O_2$/L |
| $S_{PO}$ | Phosphate | mg P/L |
| | | |
| $X_{AUT}$ | Autotrophic (nitrifying) biomass | mg COD/L |
| $X_I$ | Particulate inert org. matter | mg COD/L |
| $X_S$ | Slowly biodegradable substrate | mg COD/L |
| $X_H$ | Heterotrophic biomass | mg COD/L |
| $X_{PAO}$ | Polyphosphate accumulating organisms | mg COD/L |
| $X_{PP}$ | Stored polyphosphate of PAO | mg P/L |
| $X_{PHA}$ | Organic storage products of PAO | mg COD/L |
| $X_{MeOH}$ | Ferric-hydroxide, $Fe(OH)_3$ | mg $Fe(OH)_3$/L |
| $X_{MeP}$ | Ferric-phosphate, $FePO_4$ | mg $FePO_4$/L |
| $X_{TSS}$ | Total suspended solids | g TSS/L |

A component for filtered influent COD was added in order to differentiate between input particulate and soluble COD, since this ratio between the two might vary considerably over the day (Choubert *et al*., 2013). This component was named $COD_{filt}$, based on the COD content of analytical COD of filtrated influent samples using 1.6 µm filter papers (see section 5.7 about defining soluble COD from filtrations with 1.6 µm filters).

Another COD component introduced was the Acetate component, defined as the sum of analytic acetate and propionate recorded from the VFA analysis. The reason why propionate was included is that it is also a volatile fatty acid, directly biodegradable by the microorganisms. The ASM2d assumes all fermentation products, which are directly biodegradable, to be acetate for the modelling purpose (Henze *et al*., 2000a), which is partly a generalisation. Hence, the acetate input component was coupled to the ASM2d model component $S_A$ (see also the theoretical fractionation scheme for COD, Figure 3.2).

***Nitrogen and phosphorus input***

Unlike the standard fractionation scheme, input data was also provided for the ionic nitrogen forms, $NH_4^+$-N, $NO_2^-$-N and $NO_3^-$-N. These were then coupled directly to their nitrogenous ASM2d model counterparts: analytical $NH_4^+$-N to $S_{NH4}$ and the sum of analytical nitrite and nitrate to $S_{NO}$. The ASM models do not distinguish between influent nitrite and nitrate (Henze *et al.*, 2000a). The input of ionic nitrogen made the TKN input component redundant since the magnitude of non-ionic nitrogen input, the organic nitrogen, is decided from fixed nitrogen fractions of the different influent COD components (Henze *et al.*, 2000a). It was decided to keep the TKN input component and couple it to a dummy variable (Org. nitrogen). This component had no effect on the real model. TKN was defined as analytical total nitrogen subtracted by analytical nitrite and nitrate.

An input component for analytical phosphate was introduced and coupled directly to its model counterpart ($S_{PO}$). This made the TP input component redundant for the same reason as for the TKN component – the model COD components hold information about organic phosphorus through fractionation. The TP input component was in fact removed. In addition, an input component was provided for alkalinity and coupled to the model component $S_{Alk}$.

***Fractionation scheme***

Figure 4.10 depicts the fractionation scheme used for the model simulations. This scheme also depicts the central terms used for the fractionation of the different soluble ($S_i$) and particulate ($X_i$) COD components *i*: $f\_S_i$ and $f\_X_i$. For example, the model input component for inert soluble COD, $S_I$, was determined as the difference between analytical soluble COD and readily fermentable COD ($S_F$) plus directly biodegradable soluble COD ($S_A$), using fixed fractions for the $S_F$ component ($f\_S_F$). The particulate inert organic matter model component, $X_I$, was determined from fixed fractions of particulate slowly biodegradable substrate, $X_S$, and influent heterotrophic biomass ($X_H$) COD, as depicted from Figure 4.10. The fraction $f\_S_F$ was based on influent wastewater OUR experiments during the wastewater characterisation campaign as was the fraction of influent heterotrophic biomass (see section 5.2). The fraction of particulate slowly biodegradable substrate, $f\_X_S$, was determined from model calibration. Section 5.7 presents the determined fractions for the COD components based on the results of laboratory experiments and calibration of the initial model.

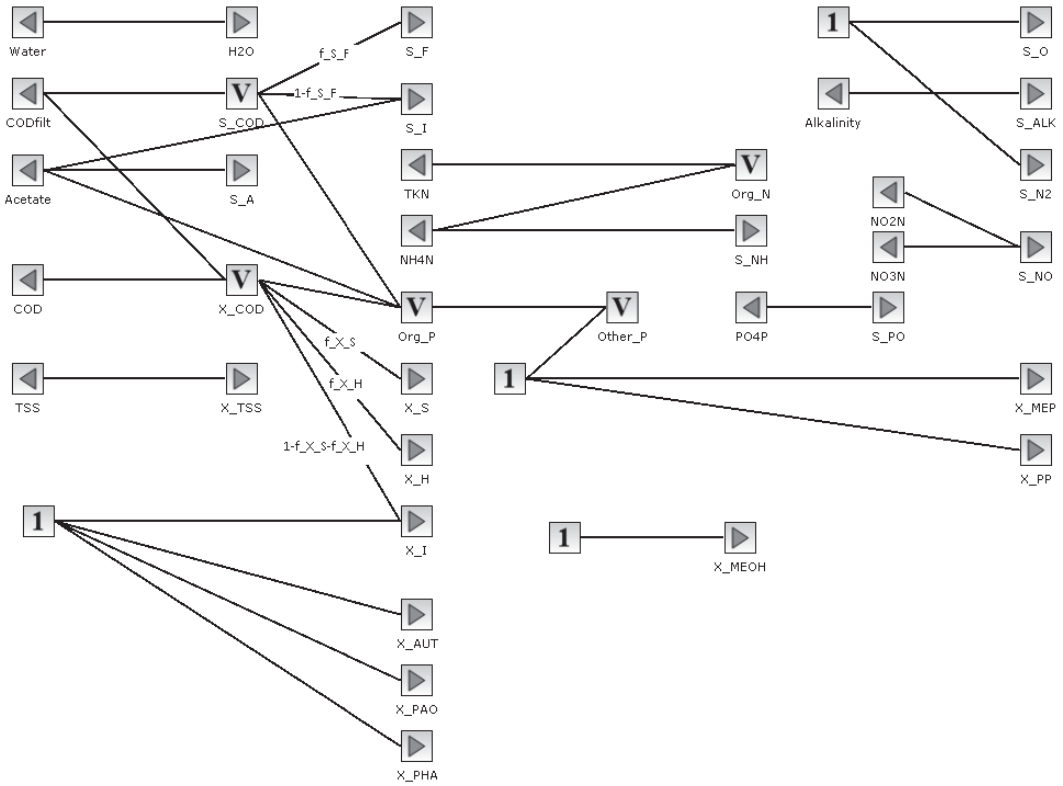


*Figure 4.10. Fractionation scheme for translating analytical input data to the ASM2d model input components. Components with arrows to the left indicate data input components and those with arrows to the rightASM2d model components. f_$S_i$ and f_$X_i$ denotes fixed fractions for soluble and particulate model components i. The dummy components, with the number 1, are coupled to fixed value input components. Variable components, with the letter V, are intermediate components for the coupling of data input to model input components through the different fractions f of the fractionation scheme (DHI, 2014).*

### 4.5.3 Model based process optimisation

***Scenario analysis***

A scenario analysis was performed in which the outcome of steady state simulations at different set-point SRT was analysed. For these simulations, the modelled ICA based SRT controller (section 4.5.1) was used for the regulation of the WAS flow rate. The values for the PI control parameters were set according to Table 4.6. The minimum control action, uMin, was set to 1 L/s (86.4 $m^3$/d), in accordance with the real controller (section 4.2.1). The maximum control action, $u_{Max}$, was set considerably higher (1500 $m^3$/d) than for the real controller (5 L/s = 432 $m^3$/d) in order to be able to simulate really low SRT (down to 0.5 d). The factor of proportionality, $K_p$, and the integral time, $T_i$, were set in order to achieve a fixed SRT without considerable oscillations.

The input data provided was kept the same as for the initial calibrated model. The magnitude of the SST underflow was also kept the same based on input data, only the WAS outtake was

regulated through the SRT controller. Temperatures were also kept the same, as were the parameters for the aeration model. All settling parameters were kept the same as for the initial calibrated model except for the fraction of non-settleable solids, $f_{ns}$. This fraction was manipulated for each simulated set-point SRT based on the fraction of particulate slowly biodegradable substrate, $f\_X_{s,}$ in the reactor for the simulations. Section 5.8 describes how $f_{ns}$ was expressed as a function of $f\_X_s$ based on the results on simulation and full-scale observations.

The outcome of the simulations was used for the prediction of effluent quality and aeration needs as well as for the magnitude of yield, methane potential and dewatering ability of the waste sludge.

*Table 4.6. Model control parameters for the PI regulator for ICA based SRT control*

| Parameter | Description | Unit | Value |
|---|---|---|---|
| **$K_p$** | Factor of proportionality | - | -50 |
| **$T_i$** | Integral time | d | 0.015 |
| **u0** | No error action | $m^3/d$ | 169 |
| **uMax** | Max control action | $m^3/d$ | 1500 |
| **uMin** | Min control action | $m^3/d$ | 86.4 |
| **$y_s$** | Set-point SRT | d | [0.5 - 2.4] |

***Methane potential***

In order to get an idea of the relative change in methane production potential of the sludge, the change in distribution between different model COD fractions were studied at the different simulated set-point SRT. Biodegradability was quantified as biodegradable COD to total sludge COD by dividing the magnitude of the biodegradable COD model components to all the COD model component, according to Equation 4.23:

$$\text{Sludge biodegradability} = \frac{S_A+S_F+X_S+X_H}{S_A+S_F+S_I+X_S+X_H+X_I} \quad (4.23)$$

Note that $X_{Aut,}$ $X_{PAO}$ and $X_{PHA}$ are also biodegradable COD model components. The concentration of the latter two were infinitely small in the modelled reactor, since the model by default assumes no PAO activity, i.e. no biological phosphorus removal. This was assumed to be in line with the situation at the full-scale plant. Although some autotrophic nitrifying bacteria, $X_{Aut}$, was assumed to be present in the influent water and thus also in the reactor (section 5.7.3), the modelled concentration was found to be about 0.2% of that of the heterotrophic biomass, and their presence will thus not affect the sludge biodegradability.

### 4.5.4 Model calibration

The initial model, as presented above, was calibrated against data from experiments and online sensors collected during the two day characterisation campaign of the G2:1 line, performed on the 10th and 11th of February, 2015. The model was calibrated with regard to the concentrations of COD, suspended solids, nitrogenous and phosphorus species in the effluent, the ML (of zone 5) and the WAS.

### 4.5.5 Model validation

The calibrated model was validated towards real data from the one day wastewater characterization campaign of the 18th of March. Since this campaign involved both of the HLAS sub-

lines at G2, the G2:2 line was also modelled in WEST and validated towards the characterisation data. Since the two lines are analogous, the model for the G2:2 lines were kept identical to that of the G2:1 line. The WAS flow was set in accordance with real input data from the characterisation, as was done for the calibration of the initial model. Hence, the collected data was not used for modelling the ICA control system itself. An intention of the validation was also to evaluate the outcome of the proposed ICA based SRT control strategy (SRT = 1.6 d) against traditional operation (SRT ≈ 2.0 d) with MLSS control, and consequently the real lines were set to operate accordingly for the latter characterisation campaign.

# 5 Results and Discussion

## 5.1 Operation at G2:1 and G2:2 during the project period

### 5.1.1 Loadings at G2:1 and G2:2

The organic loading on G2 was fairly constant throughout the project period. However, peak levels were observed in May. Between the 26th of March and the 4th of May, return sludge from the new activated sludge stage, named G4, was loaded on the primary clarifiers of the G1, G2 and G3 activated sludge stages. However, it is hard to distinguish any increased organic loading (Figure 5.1) or influent concentration (Figure 5.2) in terms of $BOD_7$ or COD at the two lines for this period.

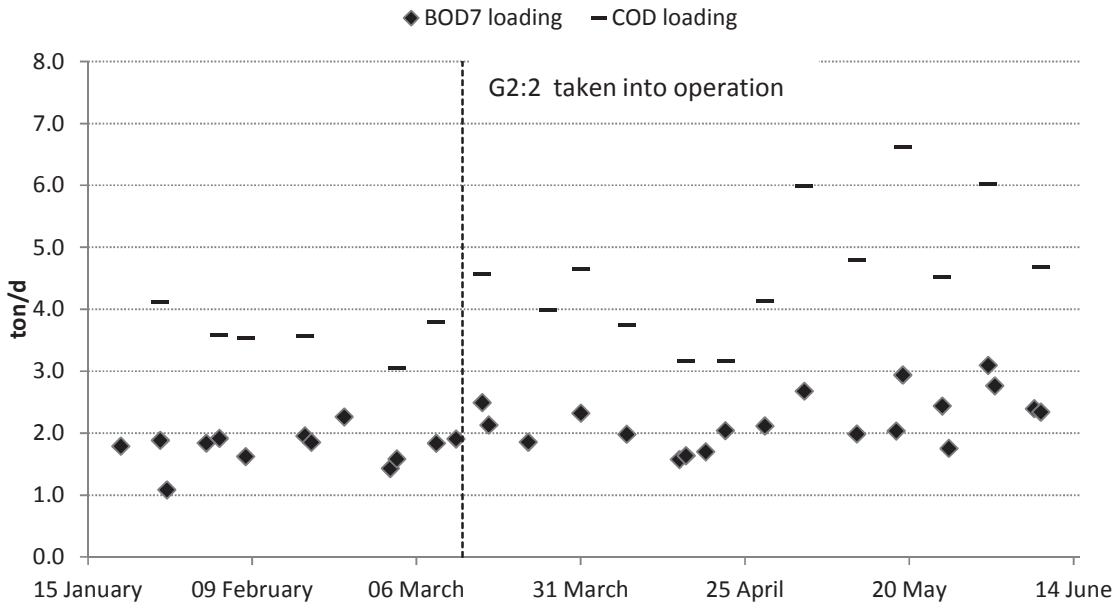


*Figure 5.1. $BOD_7$ and COD loading for each of the two HLAS sub-lines at G2 during the project period, receiving approximately the same amount of influent water. G2:2 was taken into operation at the 18th of March and prior to that the given loading rates are for G2:1 only.*

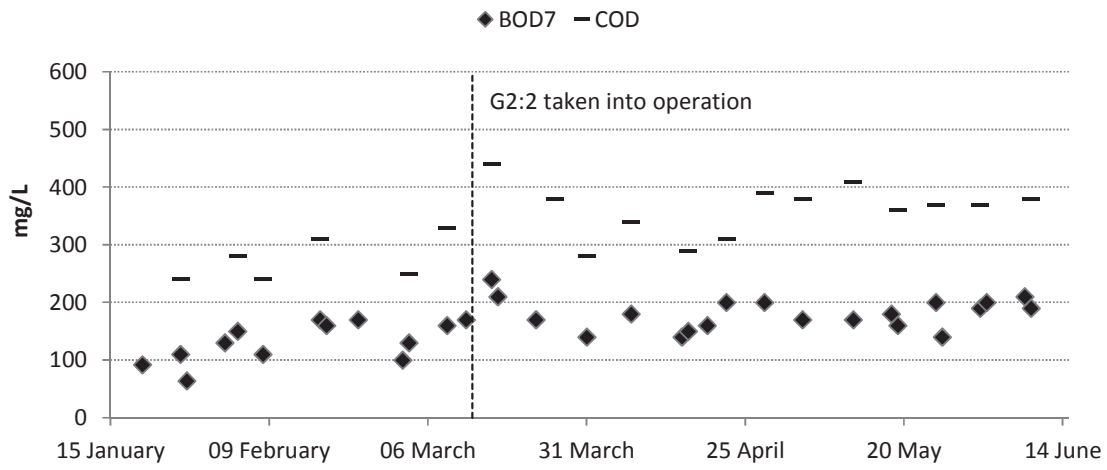


*Figure 5.2. Influent $BOD_7$ and COD concentrations for the two HLAS sub-lines at G2 during the project period. G2:2 was taken into operation at the 18th of March and prior to that the given concentrations are for G2:1 only.*

### 5.1.2 Performance of the SRT controller

As seen from Figure 5.3, the ICA based controller did not precisely fix the SRT to the set-point value of 1.2 days during the evaluation period between the 18th of March and the 30th of April. Variations in SRT during the day decreased somewhat as compared to manual operation prior to the 18th of March. The graph depicts 6 hour averages for sensor based SRT calculations. The SRT calculations, for which the 6 hour averages were calculated from, were made from 5 min average flow rate and SS sensor measurements. Sensor effluent measurements at G2:1 were used for the calculation for both lines, since there was no effluent SS sensor in place at G2:2. The magnitude of effluent SS has limited implications for the SRT calculation since comparably few solids leaves the system with the effluent (Equation 3.1)

The SRT calculations based on laboratory SS analyses were made using 5 min average sensor flow rate measurements and grab samples of ML and WAS. The latter were collected at different days between 07.00 and 07.20. Since laboratory SS measurements of the effluents for the two lines were performed less frequently, 5 min average sensor SS measurements at G2:1 were used for the calculation at both lines also for the laboratory based calculations.

Since the SS of WAS may change considerably over a day, the SRT calculation based on laboratory measurements is not necessary representative for the actual SRT of the plant during a day but only at the precise time for the grab sample. However, this is the way in which the SRT is normally approximated at the plant for the manually controlled lines. A perhaps more preferable way of fixing the SRT manually would be to study the F/M ratio instead, since fixing the F/M is more or less analogous to fixing the SRT (3.1.2). However, the laboratory based SRT calculation may be useful as a check to see if the sensors are calibrated and the regulatory system is working properly. Figure 5.3 illustrates quite some deviations between laboratory and sensor based SRT calculations.

G2:2 was not taken into operation until the 18th of March. Measurements for the SS sensor of WAS at G2:2 were not recorded to the data system prior to the 14th of April, which is why no sensor based SRT calculations are performed prior to that. Initially, there was a lot of problems with the sensors at G2:2, as seen from the difference between laboratory and sensor based SRT calculations prior to the 30th of April.

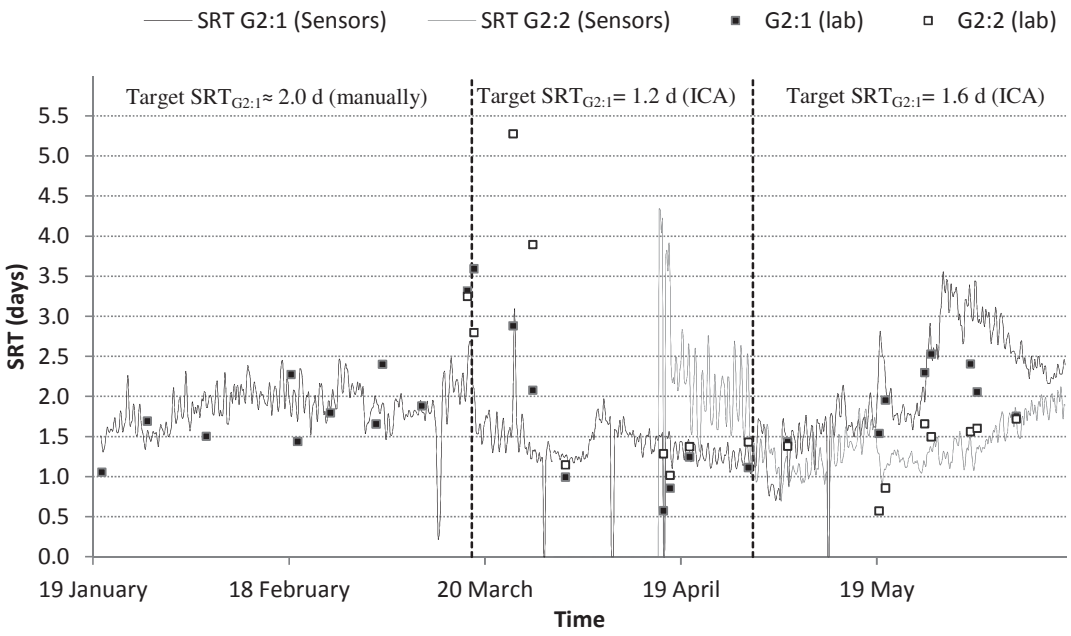


*Figure 5.3. Observed SRT at the two studied HLAS lines during the project period, based on laboratory SS measurements and online sensor readings. Depicted sensor SRT is based on 6 hours averages of SRT calculations, which in turn are based on 5 min average sensor records.*

Shortly after the second wastewater characterisation campaign of the 18th of May, there appeared to be some upset with the ICA controller at G2:1. The controller refused to operate the line at the set-point SRT (1.6 days). Instead, the observed SRT was much higher (Figure 5.3). It was found that there was a discrepancy in the implementation of the allowable range of MLSS which the controller was supposed to operate the plant within (section 4.2.1). For MLSS> 3000 mg/L, the controller had been set to interpret the sensor signal as MLSS = 3000 mg/L and for MLSS < 1700 mg/L as MLSS = 1700 mg/L. Thus, when the loading increased by the middle of May (Figure 5.1), MLSS consequently increased above 3000 mg/L due to the increased amount of substrate available for the heterotrophic organisms to feed on. Instead of increasing the waste sludge flow in order to decrease MLSS, as was the original purpose of the MLSS range limit (section 4.2.1), the controller SRT miscalculated the measured SRT and thus operated the plant at an SRT much higher than according to the set-point value.

***Sensor evaluation***

When subjected to step concentration changes by putting the sensors in tap water (on the 9th of April) and then back into the wastewater again, the sensor response time appeared to be short (≈ 1 min). However, both MLSS sensors and effluent sensors appeared to be insensitive to moderate concentration changes during shorter time periods. This was evident when com-

paring the variation in MLSS and effluent SS of laboratory measurements with sensors values during the characterisations campaigns (see section 5.7.1, Figure 5.27 and section 5.9, Figure 5.41). Between the 17th of March to the 10th of June, sensors were evaluated and calibrated more frequently (calibrations on the 9th and 29th of April, 5th and 26th of May and on the 6th of June). It was hard to fairly evaluate the WAS sensors. The SS of the SST underflow sludge may change quickly as return sludge pumps are turned on and off. Thus, grab samples of WAS may not be representative to the solution measured by the sensor, especially since the timing between the sensor record and the point of sample may not be correct.

Figure 5.4 and Figure 5.5 shows the correspondence between sensor and laboratory MLSS measurements (for Zone 5) between the 17th of March and the 10th of June. These were easier to justly evaluate than the WAS SS sensors since there were less variation in MLSS than WAS over shorter time periods. A less satisfying correlation is seen for the MLSS sensor at G2:2 (Figure 5.5).

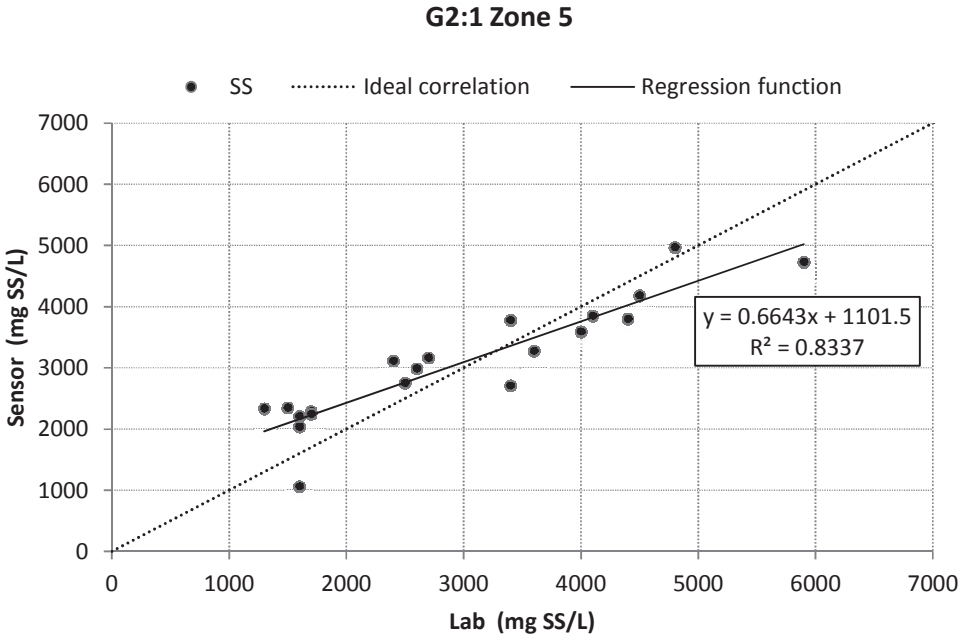


*Figure 5.4. MLSS sensor measurements (5 min averages) at G2:1 plotted against laboratory MLSS measurements for grab samples collected between the 17th of March and the 10th of June.*

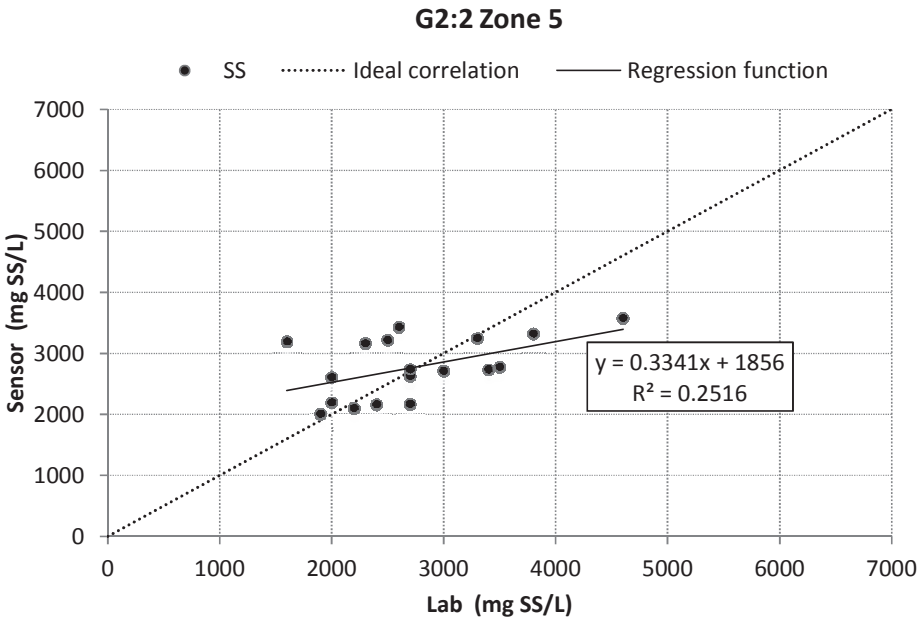


*Figure 5.5. MLSS sensor measurements (5 min averages) at G2:1 plotted against laboratory MLSS measurements for grab samples collected between the 17th of March and the 10th of June.*

It was found that there was poor mixing at the point of measurement for WAS SS (Figure 5.6a), and also at the point of WAS outtake (Figure 5.6b). There appeared to be flocculation near the sludge surface, which suggested sedimentation. Possibly, the sensor SS measurements may not have corresponded to the actual WAS SS. This may have contributed to false controller SRT calculation and thus operation at an SRT not equivalent to the set-point value.

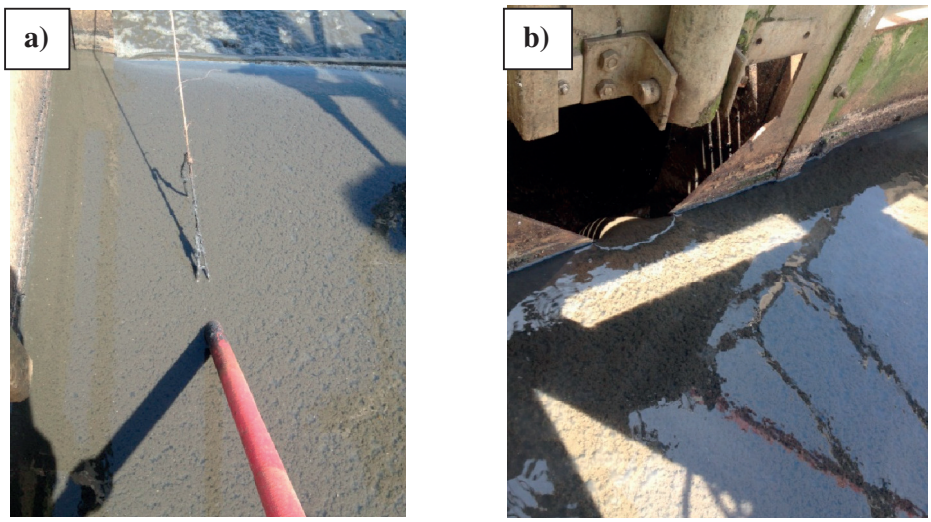


*Figure 5.6. a) Point of sensor measurement of WAS SS. b) Flocculation of solids near the sludge surface at the point for WAS outtake. It is thus likely that measured WAS SS does not correspond to actual WAS SS. 1st of June 2015.*

## 5.2 Results of OUR tests

### 5.2.1 Fraction of heterotrophic biomass ($X_H$) in the influent

Figure 5.7a shows the experimental results of the OUR test performed on the 24th of March, for the determination of influent $X_H$. HLAS influent water for the experiment was collected as a grab sample at 08.00. The figure clearly illustrates the exponential heterotrophic growth. As expected, a precipitous drop in OUR was observed, in this case at t = 7.38 h after the initialisation of the experiment. From Figure 5.7c, it is clear that DO never dropped below 6 mg/L. OUR can thus be assumed to have been fairly constant throughout each of the aeration cycles.

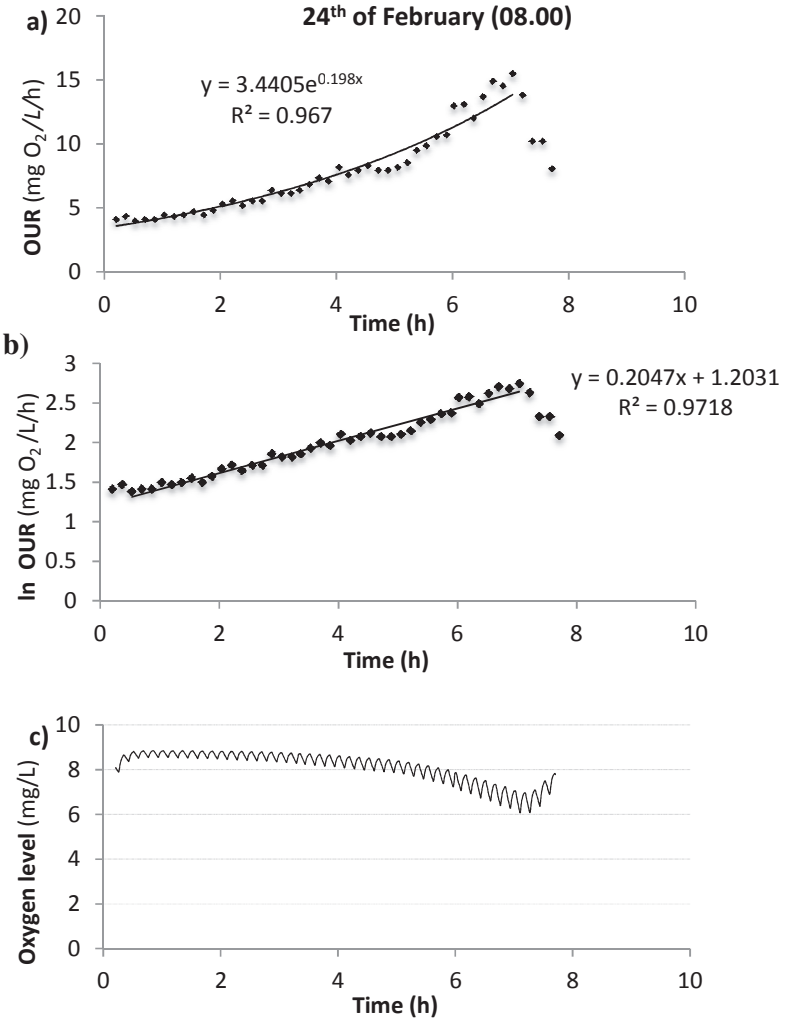


*Figure 5.7. a) OUR for batch reactor 2, t hours after starting aeration cycles. The drawn line represents the exponential curve fit up to the precipitous drop in OUR (at depletion of readily degradable substrate, $t_{dep}$ = 7.20 h). b) Natural log for OUR curve. y-axis intercept = 1.20 mg $O_2$/L/h. c) Monitored oxygen level throughout test. DO drops as heterotrophic growth and OUR increases exponentially.*

From the slope and intercept of the natural log of the exponential phase of the fitted OUR curve (Figure 5.7b), the initial $X_H$-concentration of the influent wastewater was calculated according to Equation 4.12, section 4.3.1.

$$X_H = 29 \text{ mg COD/L}$$

The COD concentration of the wastewater before the experiment was determined to:

$COD_{tot}$ = 355 mg/L

$COD_{filt,1.6}$ = 220 mg/L

The particulate COD fraction, $COD_X$, prior to the experiment was calculated as:

$$COD_X = COD_{tot} - 0.80 \cdot COD_{filt,1.6} = 179 \text{ mg COD/L}$$

since it was found in other filtration experiments with 1.6 and 0.1 µm filters that 1.6 µm filters only removes about 80% of the particulate influent COD. The particulate fraction $X_H$ was therefore determined as:

$$f_{X_H} = \frac{X_H}{COD_X} = \frac{28.81}{179} = 16\%$$

This figure is very close to the default value for ASM2d, $f\_X_{H,default}$ = 17%. Lysberg and Neth found a somewhat higher figure at the Gryaab WWTP in Gothenburg, Sweden. Based on several tests using the method of Wentzel *et al.* (1995), they found an average $f\_X_H$ = 22%.

However, the results could not be reproduced by the other batch of the two duplicates. Figure 5.2 illustrated the respirogram of Batch 1. As seen, it was harder to define the exponential growth pattern for this batch. Therefore, it was decided to calculate $f\_X_H$ based on the results of Batch 2 only and not as a mean for the two of them. However, it is clear that there are close similarities in the growth pattern between Batch 1 and 2.

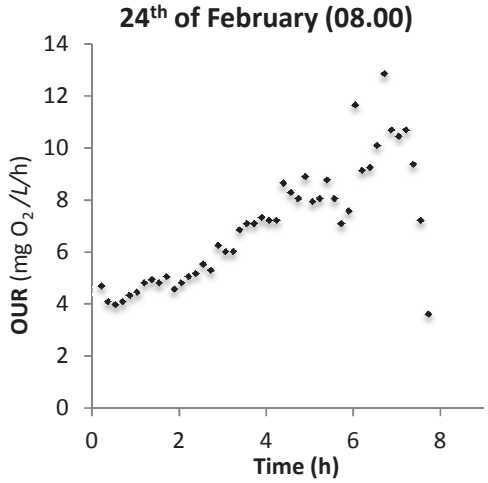


*Figure 5.8. OUR for Batch reactor 1, t hours after starting aeration cycles. Since the exponential growth phase was hard to define for this trial, the results were discarded.*

### 5.2.2 Fraction of easily biodegradable substrate ($S_S$) in the influent

***Determination of $S_s$ based on the oxygen uptake of $X_H$ in the influent***

*Figure 5.9* illustrates the results from two OUR batch tests relying on influent $X_H$ respirometric activity (method of Wentzel *et al.* (1995)). For the test of 11th of May (*Figure 5.9*a), an obvious plateau is observed after the depletion of readily biodegradable substrate ($S_S$), which similarly to the experiment of the 24th of February occurs at around t = 7.2 h after the start of the experiment. Hence, it was possible to derive a growth function for the theoretical growth on $X_S$ only. Through subtraction by total OUR, the influent $S_S$ concentration was calculated as 70 mg COD/L. The fraction of readily biodegradable substrate to soluble COD, f_$S_S$, was then calculated by comparing to the analytical soluble COD concentration ($COD_S$):

$$f\_S_S = \frac{S_{S,OUR}}{COD_S} = \frac{S_{S,OUR}}{0.80 \cdot COD_{filt,1.6}} = 0.47$$

for $COD_{filt,1.6}$ = 177 mg COD/L. The reason for calculating $COD_S$ as $0.80 \cdot COD_{filt,1.6}$ was that 0.80 was the average ratio between COD levels of samples filtered with 0.1 µm membranes and 1.6 µm filter papers at the characterisation at the 10th and 11th of February. $COD_{filt,0.1}$ was assumed to indicate the truly soluble COD fraction (section 5.7.1). For the test in particular, $COD_{filt,0.1}$ was not measured analytically.

Since f_$S_S$ was found to be rather small, so was f_$S_F$:

$$S_F = S_S - VFA = 14 \text{ mg COD/L}$$

$$f_{S_F} = \frac{S_F}{COD_S} = 0.10$$

for a VFA concentration of 53 mg COD/L. Note that VFA was assumed to be $S_A$ (section 4.5.2).

Since f_$S_S$ was rather small, the inert soluble COD concentration was found to be higher than expected (in comparsion to effluent soluble COD levels, as measured analytically).

$$S_I = COD_S - S_S = 72 \text{ mg COD/L}$$

$$f\_S_I = 0.51$$

It shall be noted that f_$X_H$ was determined as 0.17 for the trial of 11th of May, which was very similar to the results of the trial of 24th of February, f_$X_H$ = 0.16 (section 5.2.1). As for the experiment of the 24th of February, the test was performed with duplicate reactors, using the same influent water sample. At the 11th of May, differences in OUR response between the duplicate reactors were really small and thus gave very similar results in terms of derived soluble COD fractions.

The two influent $X_H$ based OUR tests of the 18th of May showed a very different OUR response than for that of the 11th of May. *Figure 5.9*c shows the respirogram for one of those tests, for an influent time proportional sample collected between 14.00 - 16.00. The other test (collected between 22.00 - 24.00) showed similar results. From the respirogram, it is hard to distinguish the heterotrophic growth pattern. In addition, the initial activity appears to be

much higher (OUR response at t ≈ 0), which is likely to be due to a higher initial $X_H$ concentration. The consequence of that is an early depletion of $S_S$ (at t = 4.0 h), as indicated by the graph. Unfortunately, since the growth pattern could not be derived, the f_$X_H$ could not be calculated. An alternative, easier approach was applied to roughly derive the theoretical growth on $X_S$, assuming a constant $X_S$ associated OUR in the interval of t = [0 - 4.0] h. OUR on $X_S$ in this interval was assumed to be approximately the same as that observed at the preceding plateau, representing hydrolysis and oxidation of $X_S$. This way, $S_S$ could still be calculated by subtraction of total OUR in the interval t = [0 - 4.0] h. Despite the obvious difference in OUR response for the tests of the 11th and the 18th of May, the soluble COD fractions were quite similar (Table 5.1).

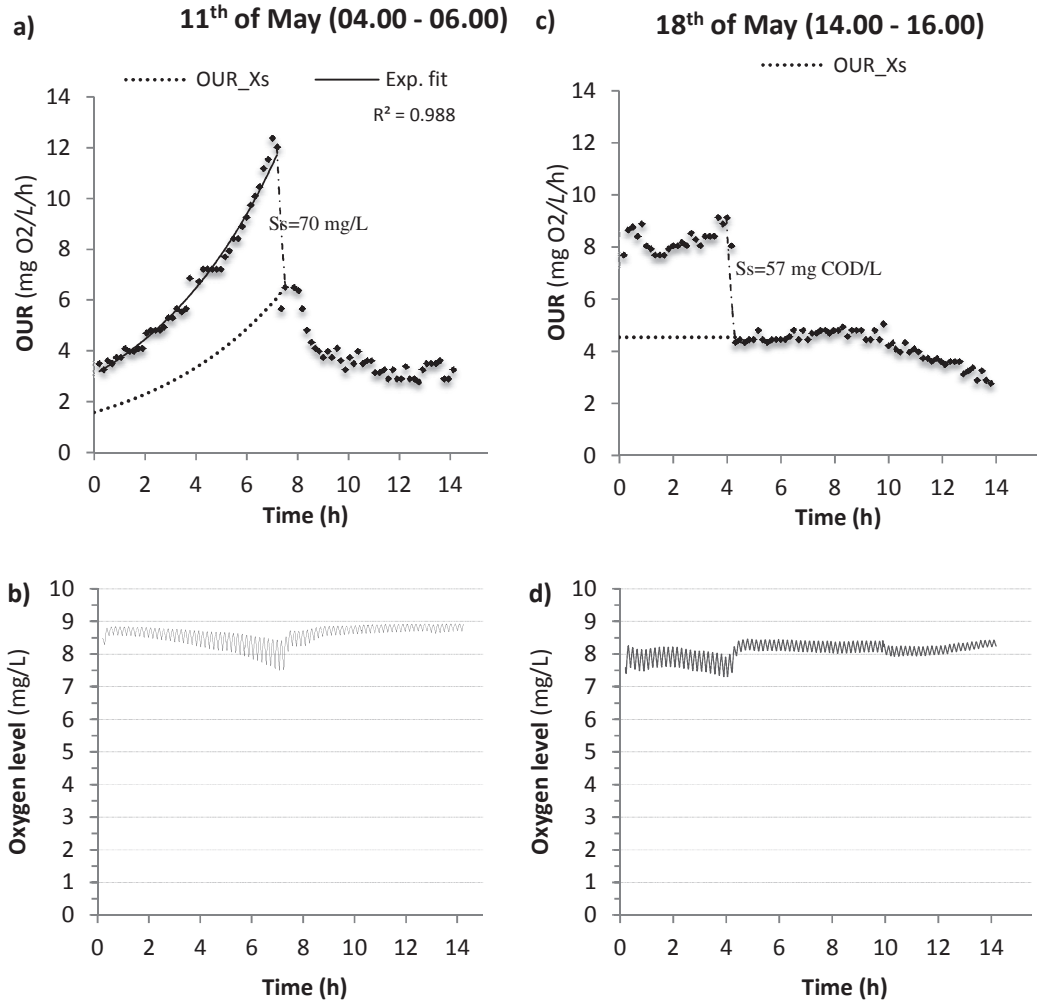


*Figure 5.9. Results of respirometric tests for the determination of $S_s$ in influent wastewater, using the method of Wentzel et al. (1995). Graph a) illustrates OUR for the trial of 11th of May and b) the corresponding DO in the batch reactor throughout the test. Graph c) and d) presents the results for one of the tests of the 18th of May.*

***Determination of $S_s$ based on the oxygen uptake of $X_H$ in the activated sludge***

The outcome of OUR tests relying on the $O_2$ uptake of activated sludge heterotrophs (method of Ekama *et al., 1986)* was similar to that for tests based on the OUR response of $X_H$ in the influent. Figure 5.10 illustrates one of the three analysed tests of the 11th of February, for an influent time proportional sample collected between 08.00 - 10.00. Interestingly, the heterotrophic utilisation of organic matter, corresponding to the area under the first hump, t = [0 - 0.9] h (30 mg COD/L), corresponded to the outcome of the VFA-analysis (VFA = 31.5 mg COD/L). Thus, it was hypothesised that the uptake in this region corresponded to oxidation of $S_A$, the ASM2d model parameter for VFA (section 4.5.2). In turn, $S_F$ was derived from difference in the respirogram, by extrapolating a curve for what was assumed to be simultaneous hydrolysis and oxidation of $X_S$. An linear decline in $X_S$ associated OUR was observed in the respirogram, as indicated by the graph.

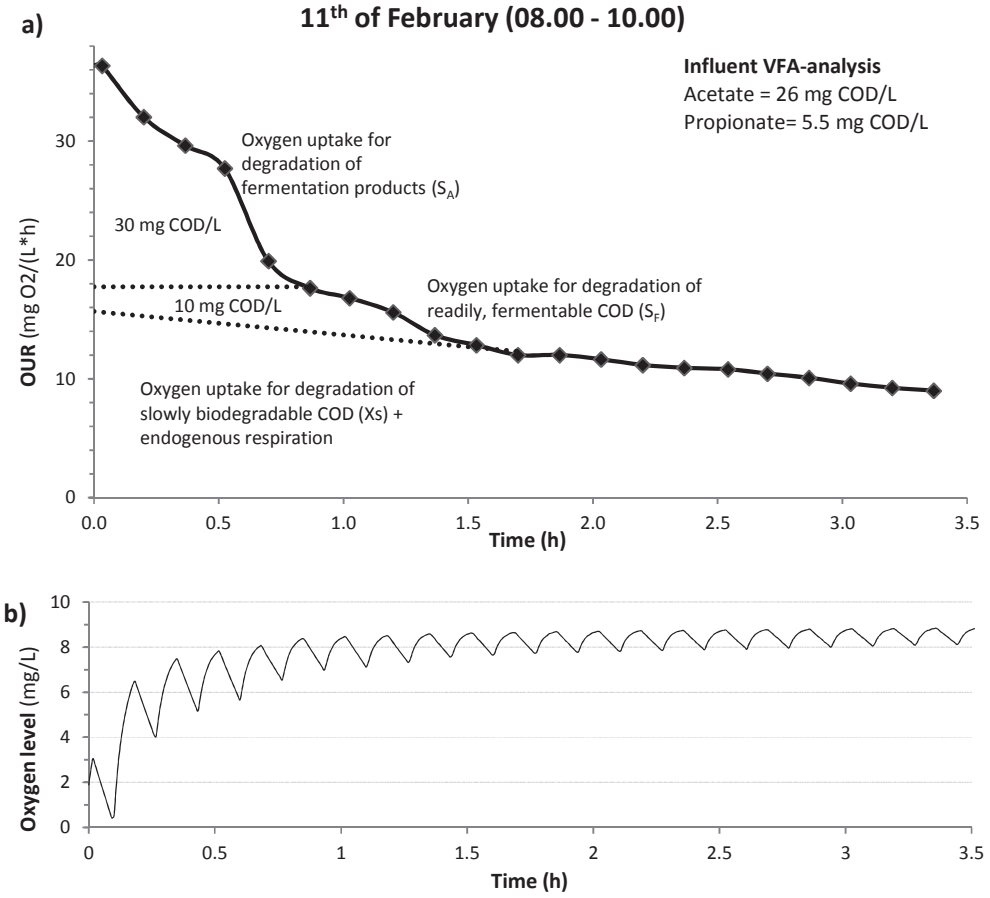


*Figure 5.10 Results of a respirometric test for the determination of $S_s$ in influent wastewater, using the aerobic batch test method of Ekama* et al. *(1986). Graph a) illustrates OUR for the trial of 11th of May and b) the corresponding DO in the batch reactor throughout the test.*

A similar respirometric response was observed with the same method for an influent wastewater sample of the 11th of May (22.00 - 24.00). However, for this test it was not possible to distinguish between $S_A$ and $S_F$ associated $O_2$ uptake from the respirogram. Since the trial of the 11th of May was run for longer than that of 11th of February, it was possible to verify the lin-

ear decline in OUR on $X_S$ after $S_S$ depletion (at t = 1.7 h) with a higher degree of certainty. This respirogram very clearly illustrates the division on growth on readily and slowly biodegradable organic matter.

For the test of 18th of May (Figure 5.11b), the $S_s$ associated $O_2$ uptake was surprisingly small ($S_s$ = 4.1 mg COD/L). A connection was made to the low analytical VFA concentration for the influent sample (16 mg COD/L), although the fact that $VFA_{analytical} > S_{S,OUR}$ seemed unreasonable. A possible explanation to the low $S_S$ concentration can be due to an increased amount of $X_H$ in the influent, as was suspected from the results of the influent $X_H$ based OUR tests for the same date (Figure 5.9c). Consequently, the influent heterotrophs may have consumed the majority of the $S_s$ in the influent water prior to entering the AS plant. Alternatively, $S_S$ was consumed in the sample flasks prior to the start of the experiment, which was initiated 5 hours after sampling. The automatic sampler kept a temperature of 4 $^oC$ and levels of DO is assumed to have been low in the sample flasks. A wastewater sample is expected to be rather stable over a 24 hour period in terms of COD composition, i.e. the fractions should not change. A prerequisite is that the temperature is kept low and rather constant (Choubert et al., 2013). However, the influent sample had to be heated to 20 $^oC$ and quickly aerated prior to the addition to the beaker with activated sludge in order to avoid registering disturbances in the respirogram for the OUR response. If the $X_H$ concentration was higher than normally, it is possible that a considerable amount of $S_S$ was consumed in this pre experimental phase. That could also explain why $VFA_{analytical} > S_{S,OUR}$ for this trial.

A possible explanation for an elevated influent $X_H$ concentration could be the rainfalls that preceded the day of the campaign. The "first-flush" phenomena of the rain events may have contributed to the transportation of $X_H$ from biofilms in the sewer pipes to the WWTP influent.

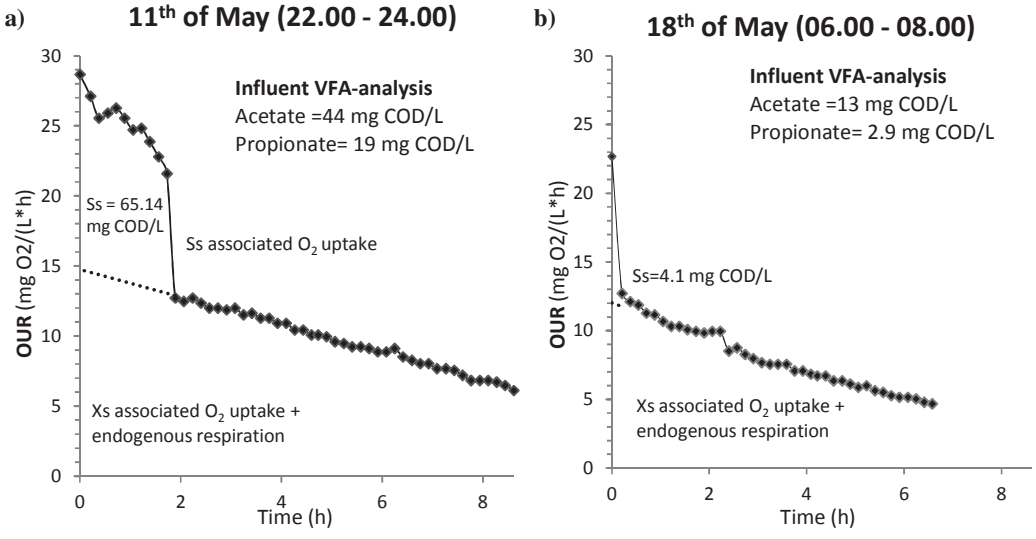


*Figure 5.11. Results of two respirometric test for the determination of $S_s$ in influent wastewater, using the aerobic batch test method of Ekama et al. (1986). Graph a) illustrates OUR for a trial of 11th of May and b) the results for a trial on the 18th of May.*

Table 5.1 summarises the results of all the analysed OUR tests performed for the determination of the soluble COD fractions. As seen, COD balances were satisfying within the range of [95 - 105]% for two of the trials. For practical reasons, it was hard to do COD balances for the activated sludge $X_H$ based OUR tests (it was problematic to take representative samples of the reactor medium without disturbing the experiment). For the OUR test of 24th of February, the COD balance was also satisfying, $COD_{recovery}$ = 100%.

*Table 5.1. Analytical sample data as well as experimental OUR results for all the performed respirometric tests for $S_s$ determination. Results are for OUR tests based on the activity of influent $X_H$ (method of Wentzel et al., 1995) and activated sludge $X_H$ (Ekama et al., 1986).*

| **Experiment** | **Influent sample** | | **Influent sample data** | | | | **Experimental results** | | | |
|---|---|---|---|---|---|---|---|---|---|---|
| **Active heterotrophs** | **Date** | **Time** | **COD (mg/L)** | **$COD_{filt,1.6}$ (mg/L)** | **$COD_{filt,0.1}$ (mg/L)** | **VFA (mg/L)** | **$f\_S_A$ (mg/L)** | **$f\_S_F$ (-)** | **$f\_S_I$ (-)** | **$COD_{Recovery}$ (%)** |
| **Influent** | **5/11** | 04 - 06 | 306 | 177 | - | 53 | 0.37 | 0.10 | 0.53 | 85 |
| **Influent** | **5/18** | 14 - 16 | 317 | 137 | 121 | 42 | 0.35 | 0.13 | 0.52 | 103 |
| **Influent** | **5/18** | 22 - 24 | 452 | 195 | 163 | 64 | 0.39 | 0.16 | 0.45 | 100 |
| **Sludge** | **2/11** | 08 - 10 | 350 | 170 | - | 32 | 0.24 | 0.06 | 0.70 | - |
| **Sludge** | **2/11** | 12 - 14 | 350 | 150 | - | 27 | 0.23 | 0.10 | 0.67 | - |
| **Sludge** | **2/11** | 20 - 22 | 440 | 170 | - | 38 | 0.28 | 0.05 | 0.67 | - |
| **Sludge** | **5/11** | 22 - 24 | 422 | 190 | - | 63 | 0.41 | 0.02 | 0.57 | - |
| **Sludge** | **5/18** | 06 - 08 | 298 | 116 | 82 | 16 | 0.20 | < 0! | 0.80 | - |
| **Average** | **-** | - | **367** | **163** | **122** | **42** | **0.31** | **0.09** | **0.61** | **96** |
| **SD** | - | - | **62** | **27** | **41** | **17** | **0.08** | **0.05** | **0.12** | **9.6** |

## 5.3 Results of daily flow proportional effluent samples

The two investigated HLAS lines showed rather stable operation during the flow proportional effluent sample campaign. This is partly explained by the fact that the loading in terms of suspended solids was rather constant throughout the campaign – at least for the analysed days (COD loadings were also recorded, but not as frequently). All samples were for dry-weather flow except for the last day, 4th of May, for which there was rain. As seen from Figure 5.12, the SS concentration and loading was higher for that day.

From Figure 5.12, it is seen that the effluent SS concentration for the automatically SRT controlled line, was higher than for the manually controlled line, G2:2 (SRT ≈ 2.0 d) throughout the whole campaign. The difference was especially notable for the 4th of May, for which the influent SS concentration and loading were higher. The average SS removal efficiency was 74.5% (SD = 2.8% for the G2:1 line and 78.8% (SD = 2.3%) for the G2:2 line during the test campaign.

Note that the set-point SRT at G2:1 was changed from 1.2 d to 1.6 d at the 30th of April. G2:2 was operated at a target SRT ≈ 2.0 d throughout the whole daily flow proportional effluent sample campaign using manual regulation of the WAS flow.

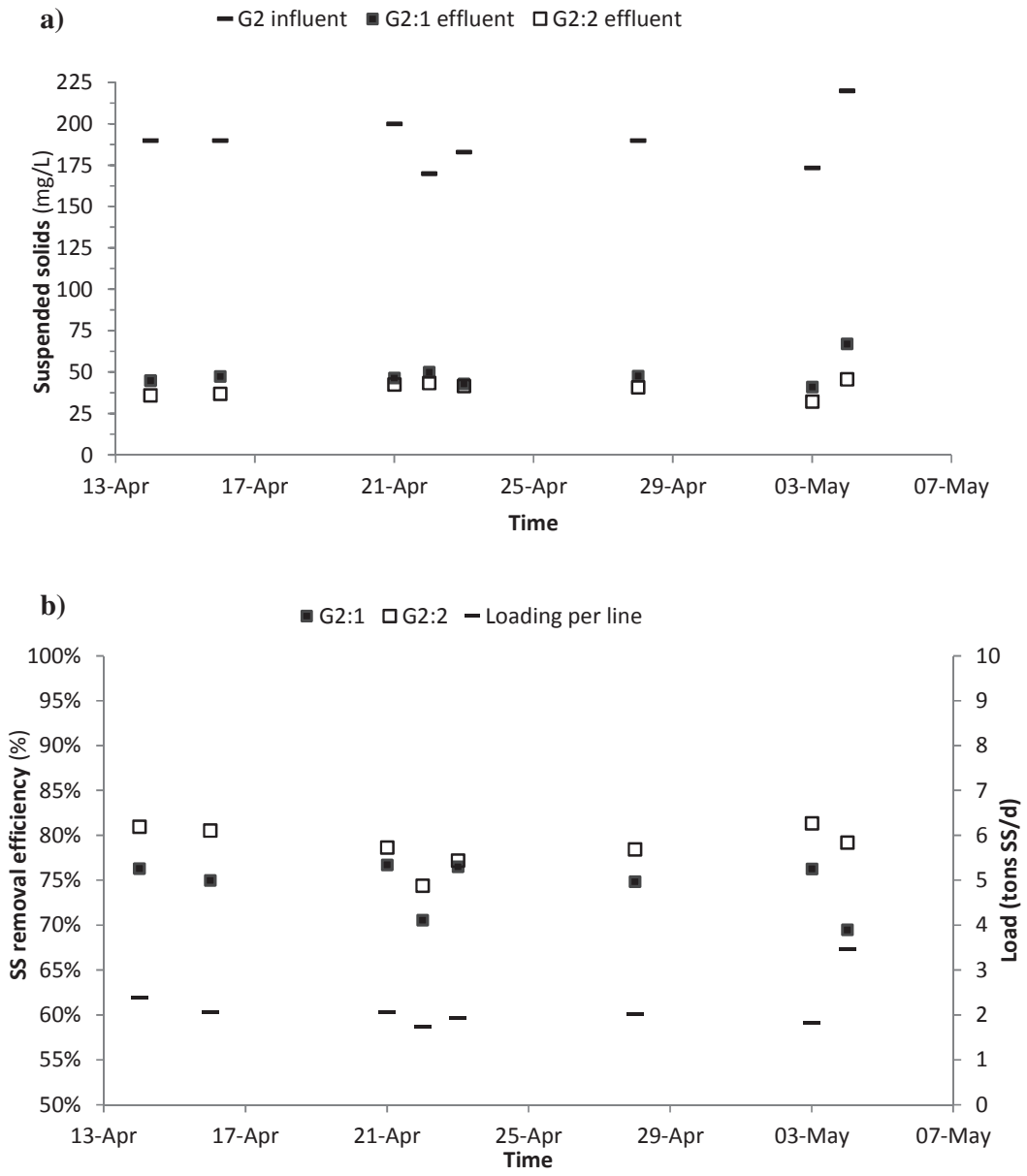


*Figure 5.12.* ***a)*** *Influent and effluent daily flow proportional SS concentrations for the two investigated HLAS lines.* ***b)*** *Corresponding SS removal efficiencies and SS loading.*

There was a similar difference in total effluent COD between the two lines as depicted in Figure 5.13. This means that the effluent SS:COD ratio was similar for the two lines (on average 0.50 mg SS/mg COD for G2:1, SD = 0.062 and 0.48 for G2:2, SD = 0.033). The SS:COD ratio for the influent wastewater was 0.57 mg SS/mg COD (SD = 0.069). The SS:COD ratio was somewhat higher on 4$^{th}$ of May, during which the loading was higher: 0.57 and 0.52 mg SS/mg COD for the effluents of G2:1 and G2:2 respectively and 0.57 for the influent. This ratio can be used for quantifying COD from SS analysis, which can be measured through the online sensors. The ASM models uses a TSS:COD ratio in order to predict sludge SS concentrations and to calculate the loading of solids on the SST, using a standard ratio of TSS:COD

= 0.75 g/g, which is larger than for the influent samples analysed. However, model TSS> $SS_{analytical}$ and therefore $SS_{analytical}$:COD ≠ TSS:COD (see also section 5.7.1).

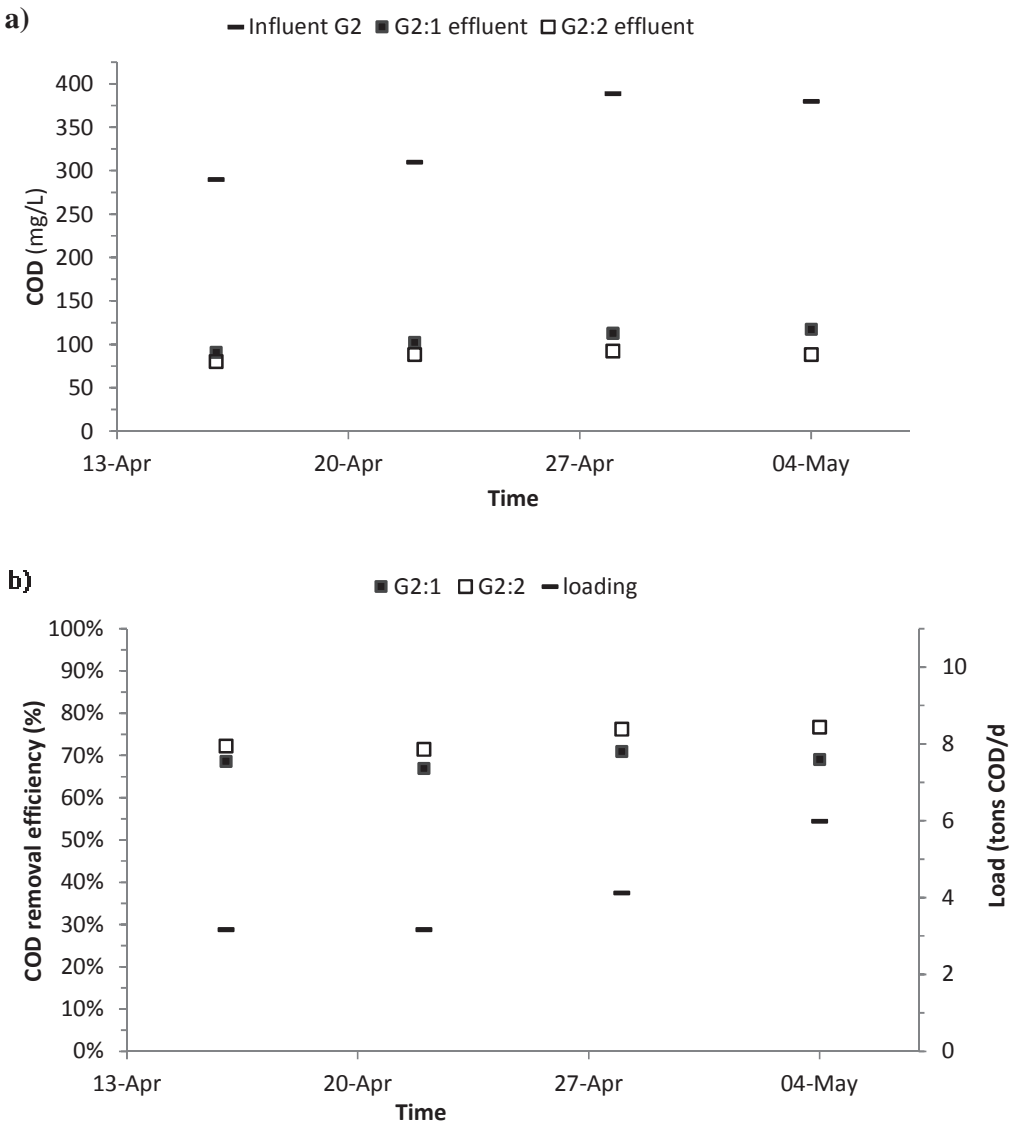


*Figure 5.13.* ***a)*** *Influent and effluent total COD levels for the two studied HLAS lines.* ***b)*** *Corresponding COD removal efficiencies and loading.*

Although the organic particle removal efficiency for the SRT controlled line was clearly worse than for the MLSS controlled line operated at a longer SRT, no clear difference was found for the removal of dissolved and colloidal organic matter (< 1.6 µm in size). From Figure 5.14 it is seen that filtrated (1.6 µm) effluent COD concentrations are similar for the two lines and not consequently lower for the G2:2 HLAS line.

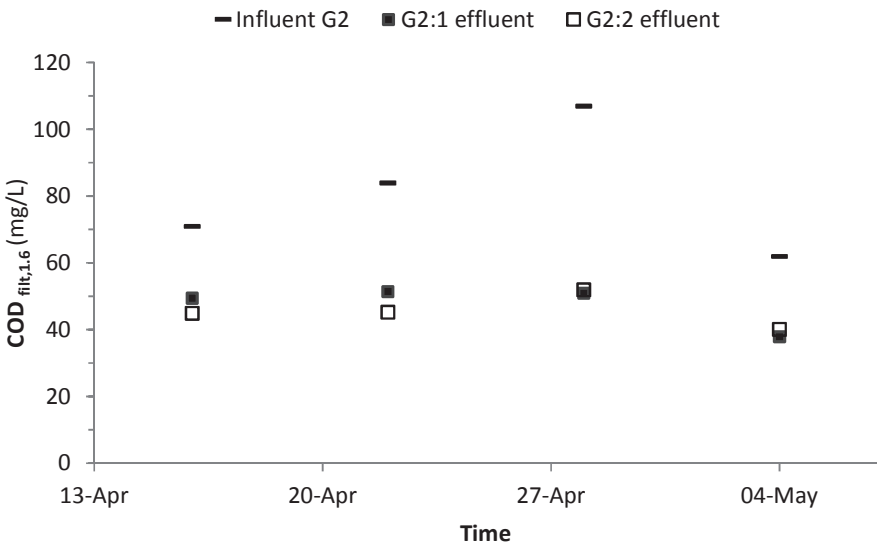


*Figure 5.14. COD concentrations for filtrated (1.6 µm) influent and effluent. Daily flow proportional samples for the two studied HLAS lines.*

Figure 5.15 shows the influent and effluent ratios between 0.1 and1.6 µm filtrates. Since the ratio between $COD_{filt,0.1}$ and $COD_{filt,1.6}$ is far less than 1, there must be significant particulate and colloidal COD content in the size range of [0.1 - 1.6] µm. It is seen that the ratio is lower for influent than for effluent water. From the few daily flow proportional samples analysed, no clear difference in the effluent was observed for the two lines in this regard. The average ratio was 0.84 mg COD/mg COD (SD = 0.091) and 0.85 mg COD/mg COD (SD = 0.015) for the effluents of G2:1 and G2:2 respectively. For the influent, the average ratio was 0.70 (SD = 0.014). As seen from the graph, this ratio is somewhat lower at 4$^{th}$ of May, which experienced a higher COD loading (wet-weather flow).

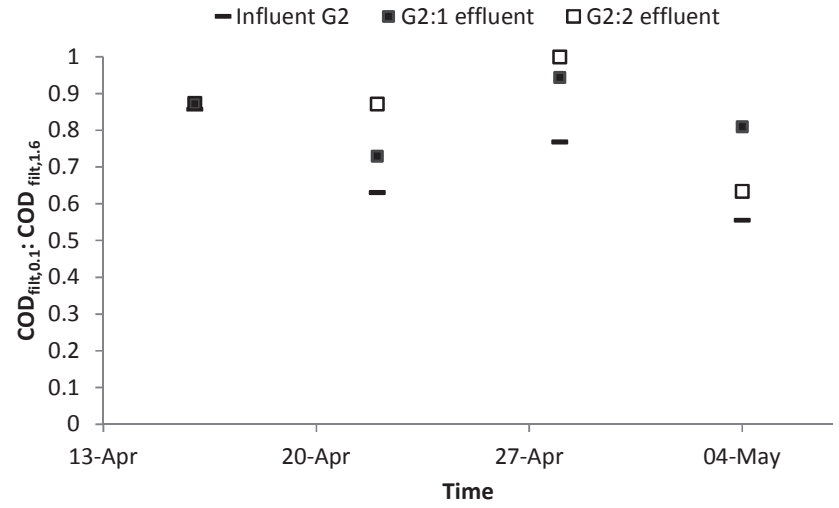


*Figure 5.15. Ratios between COD concentrations for 0.1 and 1.6 µm influent and effluent filtrates for the studied lines.*

From the analysis of effluent filtrates, it appears as though degradation of particulate COD (particles > 1.6 µm) is less complete at a lower SRT (1.2 d). However, degradation of soluble, colloidal and very small particulate (< 1.6 µm) COD do not appear to be significantly SRT dependent in the range of SRT = [1.2 - 2.0] days. The most probable reason to this fact is that particulate COD in general is more slowly biodegradable than soluble COD, which is due to the hydrolysis process which must precede degradation and uptake of the former fraction (Henze *et al.*, 2000a; Wentzel *et al.*, 1995).

### 5.3.1 COD:Nitrogen ratios

The COD to nitrogen concentration ratios of the HLAS effluent is of significant importance for the future implementation of a mainstream Anammox plant (Polizzi, 2013; Miller *et al.*, 2014) but also for the present configuration with preceding nitrification in trickling filters (Andersson *et al.*, 1994; Hanner *et al.,* 2003). Therefore, COD to total nitrogen and COD to ammonium nitrogen ratios were studied for the different daily flow proportional effluent samples. Naturally, the COD:N-tot ratio was higher for the effluent of the G2:1 line operated at a lower SRT, since the total COD level was higher whereas the ammonium level was more or less the same as for the reference line, G2:2 (Figure 5.16). No significant difference in the ratio between filtrated effluent COD and ammonium ($COD_{filt,1.6}$:$NH_4$-N) was found, which can be explained from the fact that the difference in total effluent COD levels between the two lines was mainly due to a higher particulate COD content for G2:1.

The average COD:N-tot ratios were 3.5 mg COD/mg N (SD = 0.65) and 2.7 mg COD/mg N (SD = 0.12) for the G2:1 and G2:2 effluents respectively. These figures should be compared to previous recorded plant data. Between the 1st of January 2002 and the 10th of December 2004, COD, $COD_{filt,1.6}$ and N-tot measurements were regularly taken for daily flow proportional samples of the mixed effluent from the AS lines of G1, G2 and G3. Between these dates, the average COD:N-tot ratio was 3.11 mg COD/mg N (Figure 5.17), which is lower than for the G2:1 effluent but higher than for the G2:2 line during test campaign of this project. The average $COD_{filt,1.6}$:N-tot ratio was 2.54 mg COD/mg N for the mixed G1-G3 effluent between the 1st of January 2002 and the 10th of December 2004.

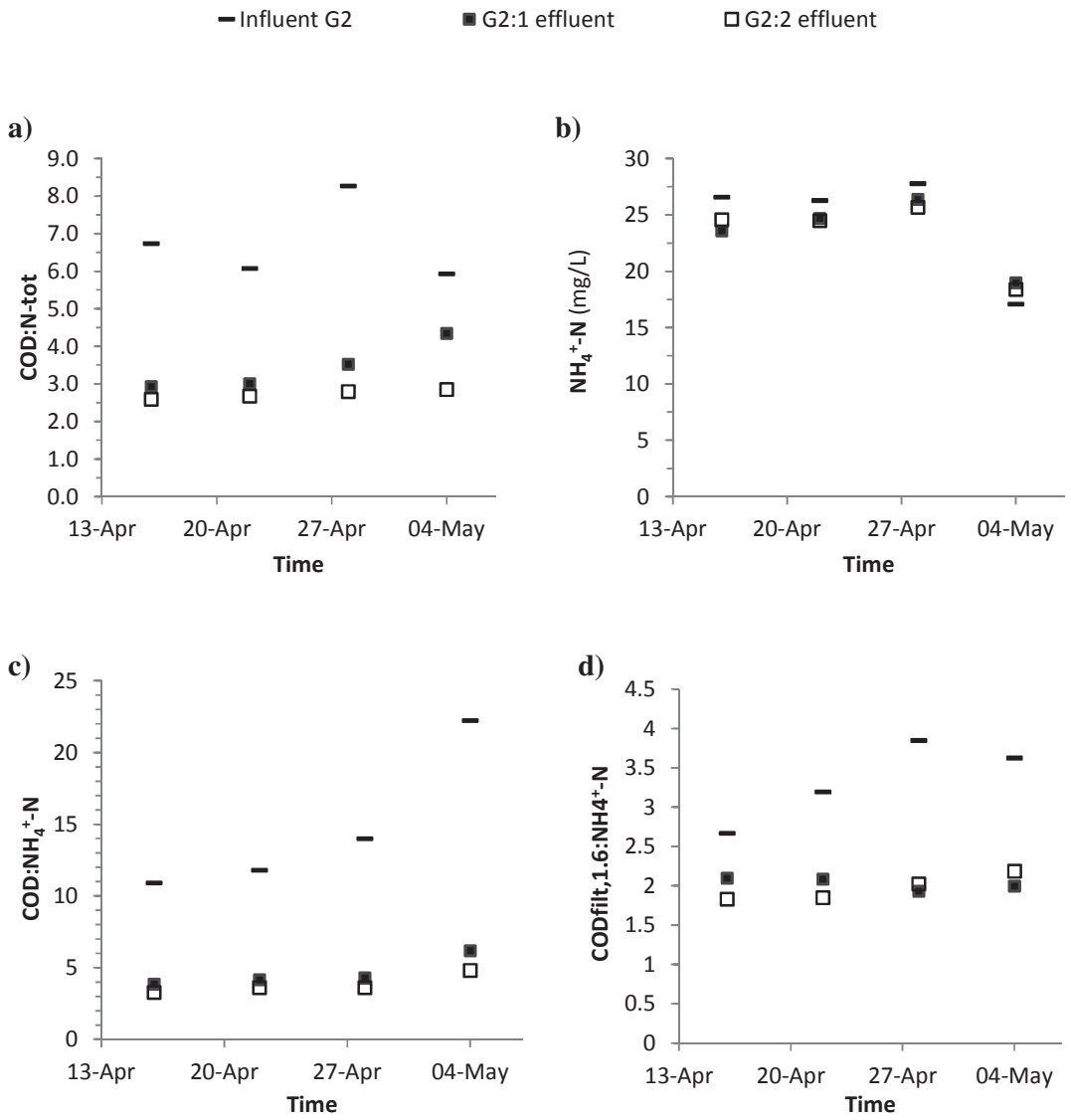


*Figure 5.16.* ***a)*** *COD to total nitrogen ratios for daily flow proportional influent and effluent samples.* ***b)*** *Influent and effluent ammonium concentrations.* ***c)*** *COD to ammonium nitrogen ratios* ***d)*** *Corresponding ratios for filtrated (1.6 µm) influent and effluent samples.*

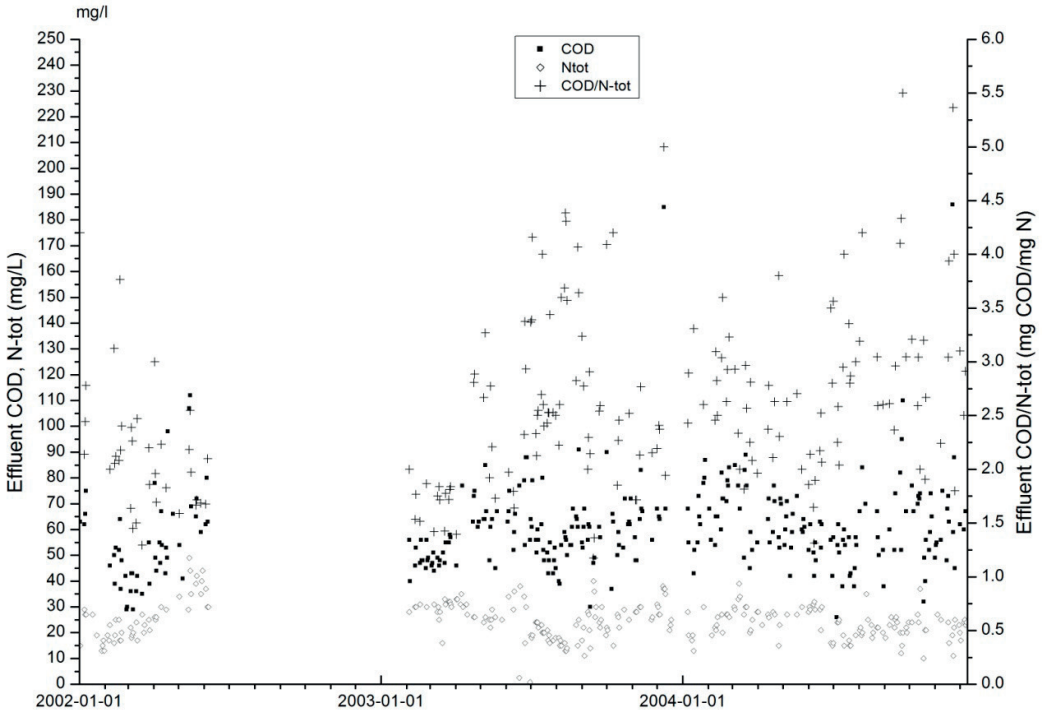


*Figure 5.17. COD and total nitrogen concentration as well as COD:N-tot ratio for the combined G1-G3 HLAS effluents at Sjölunda between 1st of January 2002 and the 10th of December 2004.*

## 5.4 Results of BMP tests

Figure 5.18a illustrates the mean accumulated methane production in the triplicate batch reactors, containing WAS from the two studied lines as substrate. The production in batch reactors with cellulose as a reference substrate and also reactors with only the inoculum are also depicted. It is clear that production is very similar for the two lines throughout the test, although the target SRT were different at the time the substrate WAS samples were collected (target $SRT_{G2:1}$ = 1.2 d; target $SRT_{G2:2}$ ≈ 2.0 d). If there is a difference in BMP between the two WAS samples, it is too small to be quantified with the applied method (Hansen, 2004).

Figure 5.18b depicts net production for the different substrates, which is total production subtracted with the average production of triplicate reactors with inoculum only (no substrate). From this graph it appears as methane production drops between the measurements between day 8 and 10 for the experiment. This is unlikely to be the real case – instead these records can be explained by the fact that the flask with 100% methane for reference measurements might hold an overpressure of methane at the time for gas chromatography tests. This can also explain the decline in net production between day 15 and 22 for all of the evaluated substrates, although it can also be due to minor methane leakage in the reactor flasks. Most likely, the WAS substrates were consumed somewhere in between these days – from which methane

production is to be associated with production from the organic substrate found in the inoculum.

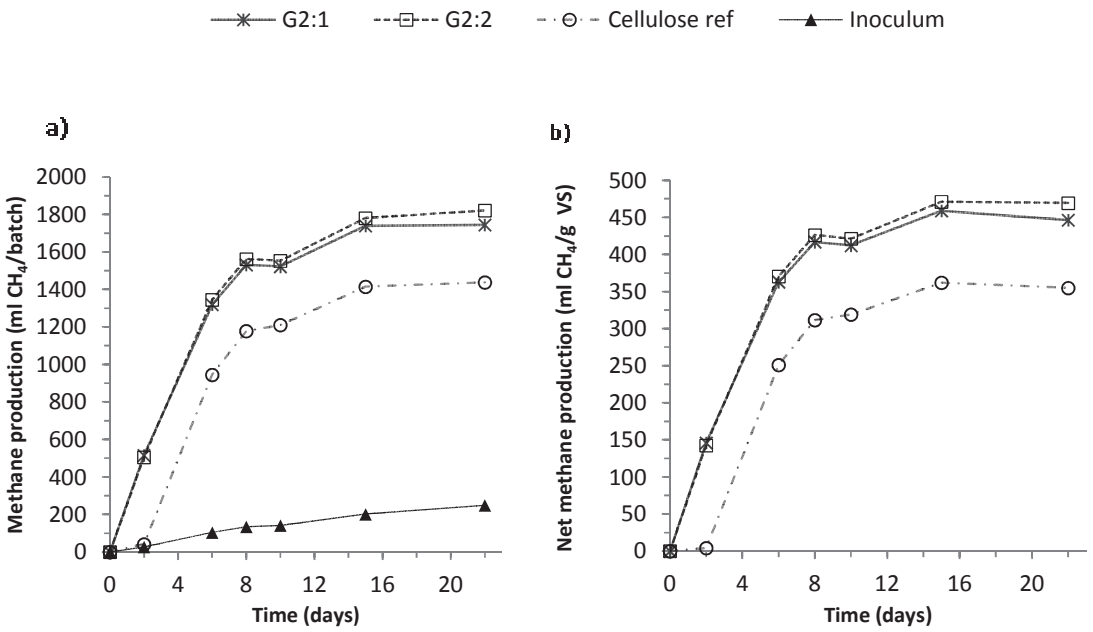


*Figure 5.18.* ***a)*** *Accumulated methane production in batch reactors for WAS from the two studied HLAS lines as well as for the cellulose reference reactors and reactors containing only inoculum.* ***b)*** *Corresponding net accumulated methane production per gram of substrate (average inoculum methane production subtracted). All the depicted results are for the mean production of triplicate batch reactors for each type of evaluated substrate, as well as for the reactors with inoculum only.*

From Figure 5.19, it is evident that the variations in methane production between individual batch reactors within the series of triplicates for each of the evaluated substrates were small. Actually, the variation was larger between the reference batch reactors with cellulose as substrate than for batch reactors containing WAS from the two evaluated HLAS lines. The variation between triplicate reactors with only inoculum was also very small as indicated by the graph. In addition, WAS for the reference BMP test showed similar methane potentials (Appendix, section 9.1)

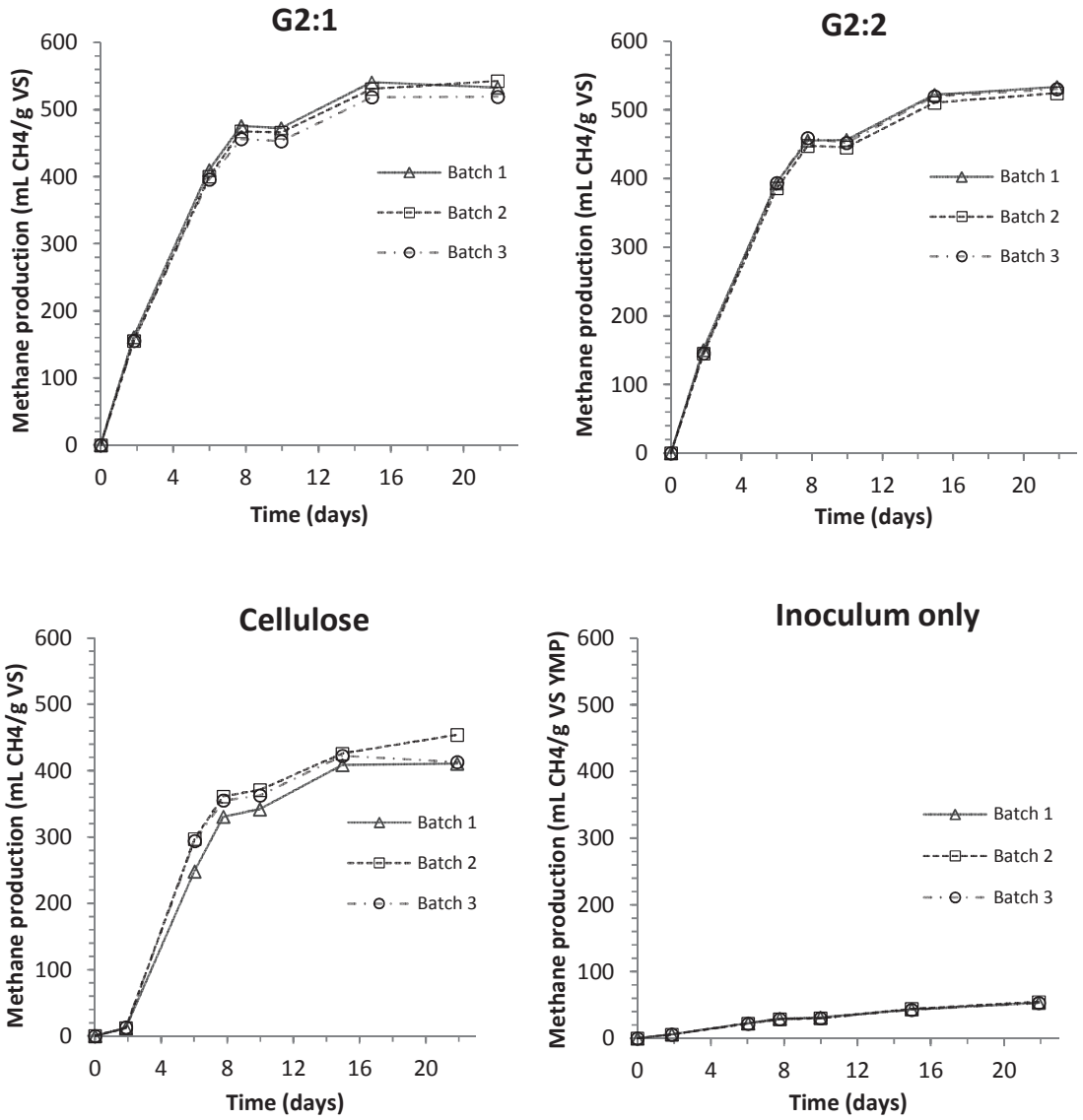


*Figure 5.19. Accumulated methane production per gram of substrate in individual triplicate batch reactors for each of the tested type of substrates, as well as for inoculum only.*

From the above results, there is no indication that operation at an SRT = 1.2 days gives a higher WAS methane production per gram of volatile solids of sludge than operation at an SRT ≈ 2.0 days. If the small deviations within triplicate batches are to be taken in to account, there is no clear difference in methane potential between the WAS from the two lines (Figure 5.20). However, there are considerable uncertainties regarding the actual SRT at which the two lines were operated at for the time of WAS sampling (Figure 5.3, section 5.1.2). It is possible that the difference in actual SRT between the two lines was smaller than intended from target values.

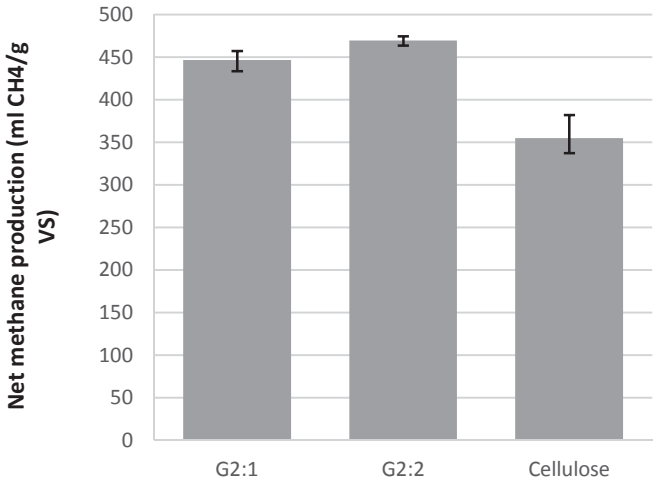


*Figure 5.20. The bars depict the net accumulated methane production, as mean production in triplicate batch reactors at the end of the experiment. Error bars gives maximum and minimum accumulated methane production within triplicate reactors.*

## 5.5 Results of sludge foaming observations

Figure 5.21a depicts the sludge foam blanket height for the two studied lines during the investigated period (12th of March to 24th of April). There seem to be a relation between the two lines in terms of foam height at the different occasions. However, the foam height is consistently somewhat higher at the G2:1 line. For the 19th of March, the foam level is in line with the basin edge for the G2:1 line. However, the foam blanket rarely covered the complete basin (Figure 5.21). Instead, foam generally consisted of dispersed chunks, which became larger near the basin borders. Consequently, the foam height was defined as the maximum height of these chunks (se section 4.4.2).

Although the foam generally did not fully reach the basin edge in height, foam was still able to escape the basin. Generally, bright foam (low darkness factor) appeared lighter and easily travelled out of the basin as small chunks. Figure 5.21c depicts the darkness factor of the foam at the different points of observation. The dark foam had a more dense and sludgy characteristic than the brighter foam. Dark foam seldom appeared as chunks but instead as a blanket, covering more or less the entire aerobic basin. This was the type of foam observed in the beginning of the observation campaign (19th, 23rd, 25th of March). Although not reaching the basin edge at the time of observations, it was evident that there had been a sludge foam overflow prior to that since there was dry dark organic matter spread around the basins. Generally, somewhat brighter and less dense foaming was recorded on the G2:1 line, although there appeared to be a relation between the foam brightness between the lines. It is perhaps not evident what type of foam, which has the most negative effect on the staff working environment. The bright, flighty foam is less sludgy but has a greater tendency to get outside the basin, especially on a windy day. Figure 5.22 exemplifies what the foam looked liked.

Note that the set-point SRT at G2:1 was changed from 1.2 d to 1.6 d at the 30th of April. G2:2 was operated at a target SRT ≈ 2.0 d throughout the whole sludge foaming observation campaign using manual regulation of the WAS flow.

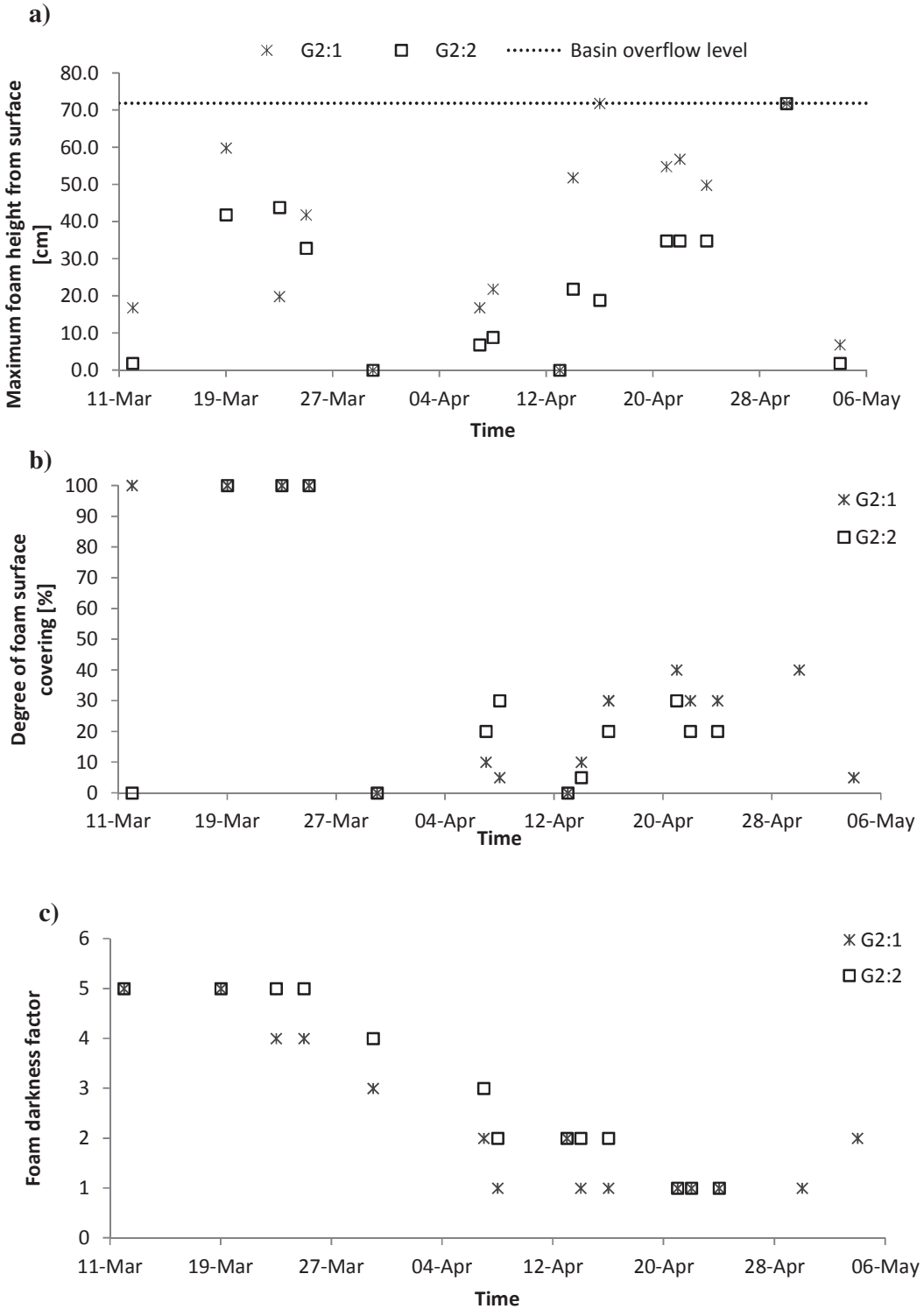


*Figure 5.21.* ***a)*** *Height of sludge foam blanket in the two investigated HLAS lines. For the instances of less than 100% foam surface covering, foam height is given as the maximum height of foam chunks.* ***b)*** *Sludge foam blanket surface covering for the two investigated HLAS lines.* ***c)*** *Sludge foam darkness factor (the author's definition).*

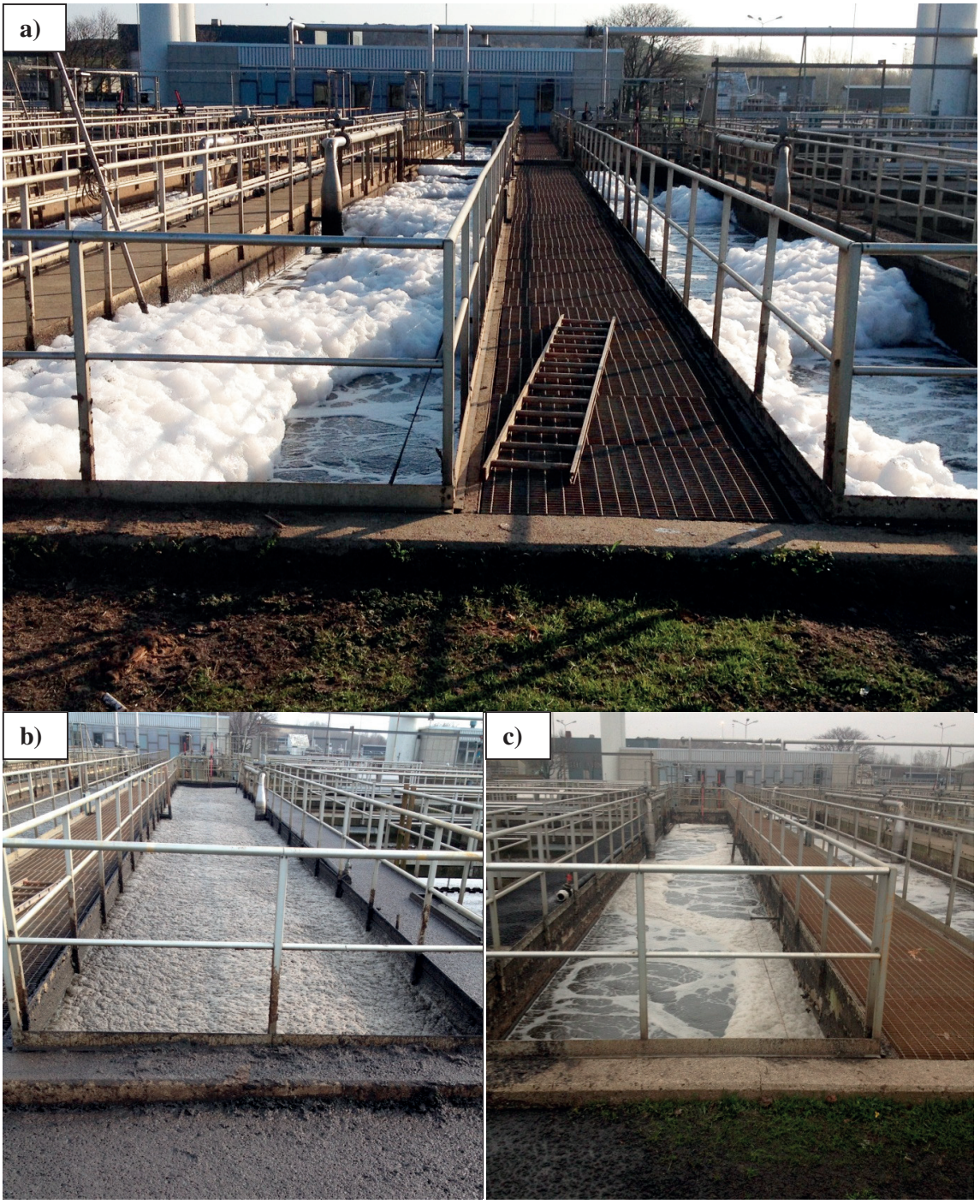


*Figure 5.22. Observed foaming at the studied HLAS lines during the observation campaign.* ***a)*** *G2:1 on the 22nd of April. High level, bright foam (darkness factor = 1), partly dispersed as chunks over the entire aerobic basin* ***b)*** *G2:1 on the 25th of March. Dark, sludgy foam (darkness factor = 5), covering the entire basin. Residues from foam overflow are seen at the edge of the basin.* ***c)*** *G2:2 on the 7th of April. Brown sludge (darkness factor = 3), with a small degree of surface coverage (≈ 20%).*

## 5.6 Results of settling tests (ZSV)

Fitting the recorded settling velocities from the ZSV tests to the Takács-SVI model was unsuccessful for the experiment of the 24th of March as depicted in Figure 5.23a. Settling velocity decreased much faster with increased concentration than for the fitted model curve. The major reason for that was that the hindered settling parameter $r_h$ was set as a function of SVI (section 3.2). Since SVI was a measured and not a calibrated parameter, it was not changed for the model fitting. It was however possible to derive the maximum practical settling velocity, $v_0$' = 104 m/h, from three of the ML dilutions (40, 50 and 60% sludge to tap water) elaborated on. The practical settling velocity is seen in the graph as the horizontal line at X = [1012 - 1515] mg SS/L. It was however possible to reasonably fit the data series to the Vesilind model, which only accounts for hindered settling (section 3.2.1). As seen from Figure 5.23b, this model fits all the data points except for the two representing the two highest ML dilutions (40 and 50% sludge), which are found in the concentration range for the maximum practical settling velocity at 104 m/h. Apparently, the region X = [1012 - 1515] mg SS/L represents a transition region between hindered and flocculent/discrete particle settling at which the Vesilind model is not applicable (Takács *et al.*, 1991).

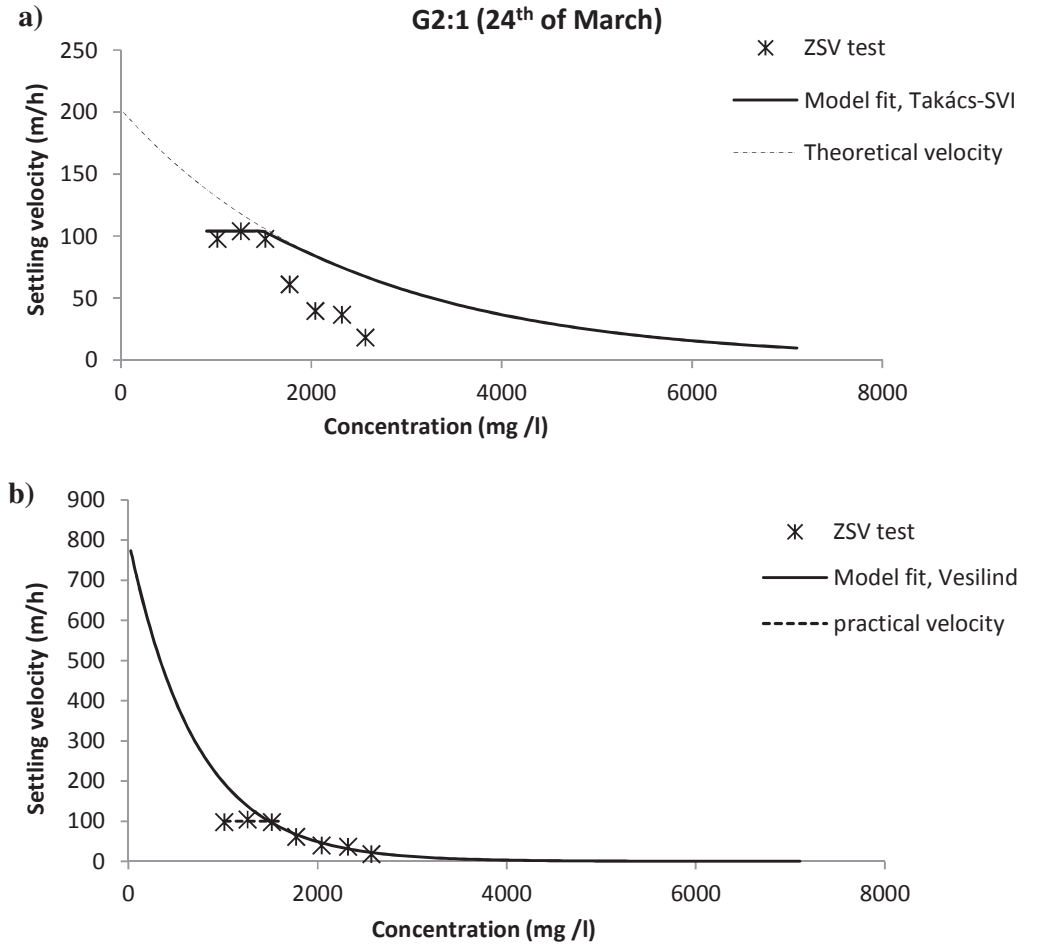


*Figure 5.23. Experimental ZSV data fitted to **a)** the Takács-SVI settling model and **b)** the Vesilind settling model. The experiment was performed on the 24th of March with ML from G2:1.*

The Vesilind model fit results in a maximum theoretical settling velocity ($v_0$ = 800 m/h) that is very high in comparison to that of the WEST default value ($v_{0,default}$ = 474 m/h). Especially as the recorded sludge volume index (SVI = 133 m/h), was high compared to default ($SVI_{default}$ = 100 m/h), which should imply a lower settling velocity in the hindered and flocculent settling regions according to the SVI to $r_h$ relation found by Daigger & Ropper (1985). It was also high in comparsion to calibrated parameter values used by previous modellers of the HLAS at Sjölunda (Martinello, 2013; Klingstedt, 2015), also using SST models based on that of Takács *et al.* (1991).The ZSV data sets for the experiments of the 22nd of April were considerably more fittable to the Takács-SVI model, as indicated by the fitted curves presented in Figure 5.25.

However, the rather low MLSS in the basin at this occaction resulted in a narrow range of ML dilutions to elaborate on. Naturally, it was not possible to gather experimental information on the sludge settling behaviour for concentrations above the MLSS. Moreover, the settling velocity below the minimal concentration of the sludge blanket, $X_{Lim,}$ could not be quantified. The concentration at which the blanket was observed to resolve was at about 700 mg SS/L, corresponding to Mixed Liquor dilutions of about 30% ML to water. This corresponded reasonably well to the WEST default figure for $X_{Lim}$ (900 mg SS/L). Due to the difficulty of quantifying the ZSV in this region, no efforts were made to determine the settling parameter for low concentrations, $r_{p.}$

Figure 5.24 depicts what a mixed liquor sample from the G2:2 line collected on the 22th of April looked like 7 minutes after dilution: 87.5% tap water to 12.5% mixed liquor. The surface layer indicates the presence of non-settleable material. This material acctually accumumulated on the surface shortly after dilution and mixing. This material was found to travel in an upwards direction instead of settling.


*Figure 5.24. Illustration of mixed liquor from the G2:2 line, sampled on the 22th of April, diluted with tap water (87.5% water to 12.5% mixed liquor). The surface illustrates the presence of non-settleable organic matter, travelling in an upwards direction in the beaker.*

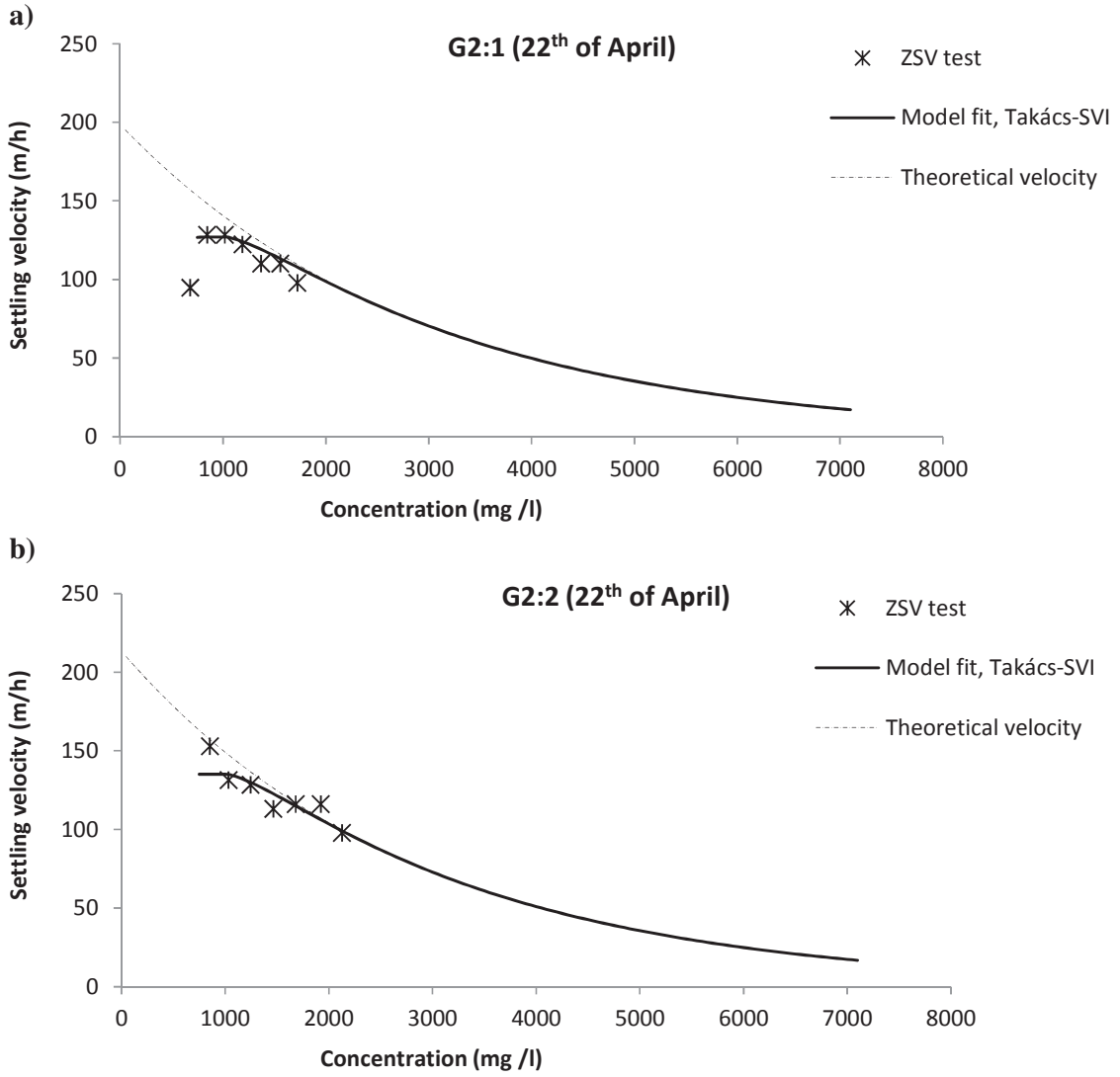


*Figure 5.25. Experimental ZSV data fitted to the Takács-SVI settling model The experiment was performed on the 22th of April with ML from **a)** the G2:1 HLAS line and **b)** the G2:2 HLAS line.*

The maximal practical settling velocity was somewhat higher than for the experiment on the 24th of March, but very similar between the two lines ($v_0'_{,G2:1}$ = 127 m/h; $v_0'_{,G2:2}$ = 135 m/h). SVI were also similar as were the maximum theoretical settling velocities which were lower than for the 24th of March (Table 5.2). It appeared as the studied settling parameters was not very SRT dependent, although there were uncertainties regarding the actual SRT at which the plants were operating at for the time of the ZSV tests (section 5.1.2).

In addition, a SVI index of 94 mL/g, which was recorded for the G2:1 line, is lower than the WEST default value ( = 100 mL/g) for the Takács-SVI model. Balmér (1984) reported even lower SVI (≈ 50 L/mg) for a HLAS at Rya WWTP in Gothenburg operated at an SRT ≈ 0.5 d, which was related to the very active biomass in that plant.

*Table 5.2. Operational data and derived model parameters for the Takács-SVI settling model based on ZSV tests. $f_{ns}$ was approximated from Equation 5.2.*

| **Date**<br>**HLAS line** | **24th of March**<br>**G2:1** | **22th of April**<br>**G2:1** | **22th of April**<br>**G2:2** |
|---|---|---|---|
| Control strategy | MLSS | ICA | MLSS |
| Target SRT (d) | ≈ 2.0 | 1.2 | ≈ 2.0 |
| MLSS | 2567 | 1719 | 2124 |
| Effluent SS | 24 | 50 | 44 |
| $v_0$ (m/d) | 200 | 195 | 210 |
| $v_0$' (m/d) | 104 | 127 | 135 |
| SVI (mL/g) | 133 | 94 | 100 |
| $X_{Lim}$ | ≈ 700 | ≈ 700 | ≈ 700 |
| $f_{ns}$ | $9.4 \cdot 10^{-3}$ | $2.9 \cdot 10^{-2}$ | $2.1 \cdot 10^{-2}$ |

Still, rather high effluent SS was recorded for the G2:1 line at that day (50 mg/L) according to daily flow proportional effluent samples (section 5.3). This figure was somewhat higher than for the G2:2 line, although this line also produced a somewhat elevated level (44 mg/L). Since a consistent difference between the two lines had been observed for a period of time (section 5.3), it was reasoned that other settling parameters could be of importance. It was believed that the main reason was due to a difference in the non settleable fraction of solids, $f_{ns}$, for the different mixed liquors. At the occasions for the ZSV tests, no experiments were done to determine this fractions. Instead, it was estimated from the ratio between effluent SS and MLSS according to Equation 5.1:

$$f_{ns} \approx SS_{eff}/MLSS \tag{5.1}$$

It is realised that Equation 5.1 is only valid at moderate SST loadings; if overloaded the supernatant will hold far more solids than what is theoretically achievable given a sufficient settler height and surface area. The fraction was somewhat higher for G2:1 than for G2:2.

There were however attempts to quantify the $f_{ns}$ experimentally for the two lines during the second wastewater characterisation campaign on the 18th of May. An amount of 1 L of non-diluted mixed liquor was allowed to settle for about 24 h in a 1000 mL standardised settling column for $SV_{30}$ tests. The fraction was calculated as the ratio between SS in the supernatant of the top 100 mL of the column and MLSS, according to Equation (5.2):

$$f_{ns} \approx SS_{super}/MLSS \tag{5.2}$$

Results are depicted in Table 5.3. Table 5.3. Operational data and experimentally derived values for the $f_{ns}$ fraction. It is seen that $f_{ns}$ is actually higher for the G2:2 line. An explantion could be that this line was operating at a lower SRT than G2:1 at the time, although it was supposed to operate at an SRT ≈ 2.0 d (see section 5.9.1).

*Table 5.3. Operational data and experimentally derived values for the $f_{ns}$ fraction, based on experiments on ML (zone 5) from the G2:1 and G2:2 lines on the 18th of May.*

| **Time**<br>**HLAS line** | **10:00**<br>**G2:1** | **14:00**<br>**G2:1** | **10:00**<br>**G2:2** | **14:00**<br>**G2:2** |
|---|---|---|---|---|
| Control strategy | ICA | ICA | MLSS | MLSS |
| Target SRT (d) | ≈ 2.0 | 1.2 | ≈ 2.0 | ≈ 2.0 |
| MLSS | 2435 | 2342 | 1536 | 1476 |
| Effluent SS | 60 | 46 | 41 | 39 |
| $f_{ns}$ | 0.023 | 0.018 | 0.026 | 0.032 |

## 5.7 Results of the calibration of the initial model

### 5.7.1 Calibration with regard to suspended solid levels

Since suspended solids levels in the reactor and waste flows for the first model simulations did not closely match those of laboratory analysis and online sensors, a few calibration measures for a better fit were undertaken. The ASM2d model component for suspended solids, $X_{TSS}$, is described as "total suspended solids". According to the model description, analytically measured SS is always smaller than $X_{TSS}$ since a fraction of $X_S$ will pass the filter paper for the analysis (Henze *et al.*, 2000a). Coupling analytical SS directly to the $X_{TSS}$ model component is a typical pitfall which will cause an underestimation of the MLSS in relation to influent COD, even when using the finer 0.45 µm membranes. Since the ASM models are based on COD, model fitting should be done for COD first prior to finding the correct TSS:COD relation (Rieger *et al.*, 2013). In this case, calibration of COD and TSS levels were performed interchangeably, partly due to the fact that there were continuous online sensor records of the sludge concentrations but only four analytical measurements per day of the ML and the WAS total COD levels.

At Sjölunda WWTP, analytical SS is typically measured with 1.6 µm filter papers, which eventually causes an even larger underestimation of the $X_{TSS}$ component compared to using 0.45 µm membranes. The ratio between $X_{TSS}$ and analytically measured $SS_{0.45}$ for a typical influent wastewater would be 0.67 g TSS/g SS according to the ASM2d model description (Henze *et al.*, 2000a). However, these relations could of course differ between different wastewater. At Sjölunda, primary clarifiers using ferric sulphate for pre-precipitation precedes the AS plant. Pre-precipitation and clarification affects the wastewater composition regarding the relation between particulate, colloidal and soluble COD (Henze & Harremoes, 1992).

In a large study using a SBR pilot with primary settled municipal wastewater, Torrijos *et al.* (1994) found that the true readily biodegradable COD fraction can be isolated by 0.1 µm filters. Colloidal and particulate material larger than that will be degradable much slower. Since slowly biodegradable matter should be associated with the particulate COD (section 3.3.2), the weight of colloids in the size range [0.1 - 1.6] µm should thus be associated with TSS. Attempts were made to quantify this weight through filtrations with 0.1 µm filters, but the analytical precision of the standard method, which implies weighting dry baked (105 $^{o}$C) membranes on a precision scale (SIS, 1981) was insufficient.

Instead, the ratio between analytical $SS_{1.6\mu m}$ and $X_{TSS}$ was approximated from the ratio between $COD_{filt,0.1}$:$COD_{filt,1.6}$, which was on average 0.85 g COD/g COD for two influent

wastewater samples of the wastewater characterisation campaign (10th and 11th of February), by assuming a constant COD:TSS ratio throughout the particulate size range. Consequently, the influent $SS_{1.6}$:$X_{TSS}$ ratio was also set to 0.85 g/g. The $SS_{1.6}$:$X_{TSS}$ was also determined for the effluent in the same way (0.83 g/g) and implemented in the effluent defractionation scheme in order to be able to compare the simulated effluent SS concentrations with real data. The ratio for $SS_{1.6}$:$X_{TSS}$ was assumed to be 1 g/g for the mixed liquor and settler underflow sludge for the model fitting. The reason was that the $COD_{filt,1.6}$:COD ratio was less than 2% for analysis on WAS samples used for the BMP tests. However, it should be noted that Levine *et al.* (1991) in an extensive study found that a considerable fraction of HLAS mixed liquor solids mass can be found in the size range < 1.6 µm. The principle for the distinction between particulate, colloidal and soluble organic matter using filtrations is schematically described in Figure 5.26. The figure also illustrates how the VFA and OUR methods relates to the determination of the different fractions.

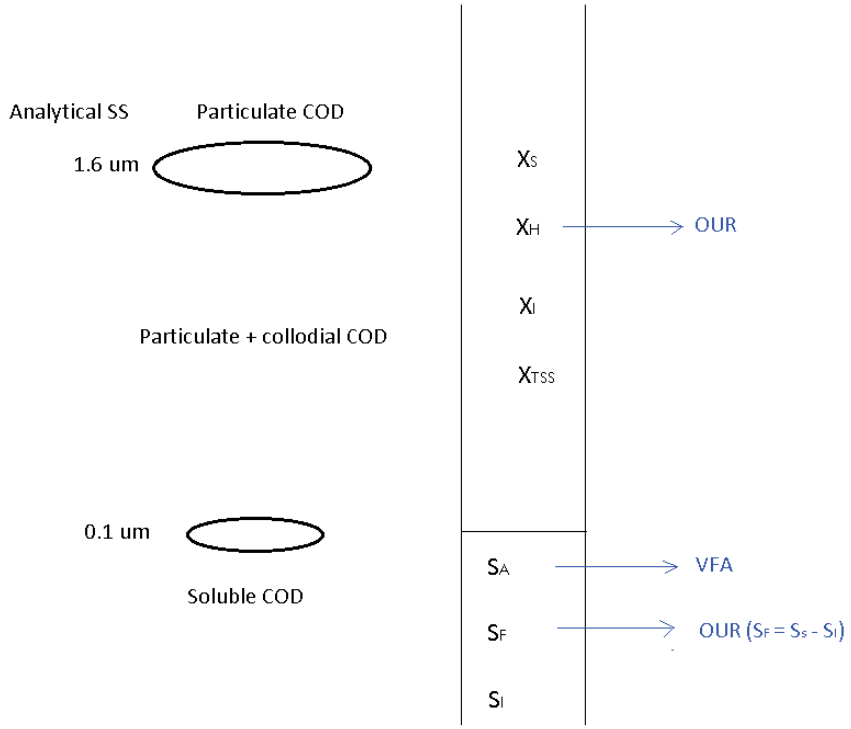


*Figure 5.26. The principle for distinction between particulate, colloidal and soluble COD fractions applied to the calibrated model. From analytical measurements of SS, $X_{TSS}$ was approximated based on the ratio between $COD_{filt,0.1}$ and $COD_{filt,1.6}$*

***Mass balancing***

Due to the less precise model SS prediction, two independent mass balances were set up. Analysing overlapping mass balances over the investigated process is an efficient approach for detecting systematic inconsistencies within the input data set. If these cannot be closed within an error margin of +/- [5 - 10]%, one should take measures to find the source of error (Rieger *et al.*, 2013). The general mass balance is typically written according to Equation 5.3:

$$\text{Accumulation} = \text{Input} - \text{output} + \text{Reaction} \quad (5.3)$$

With regard to the balancing variable investigated, Equation 5.3 can mathematically be expressed according to Equation 5.4:

$$\frac{\Delta M}{\tau} = \sum_{i=1}^{n} L_{In,i} - \sum_{i=1}^{m} L_{Out,i} + V \cdot r_v \quad (5.4)$$

for which;

$\Delta M$ = The change of mass stored within the system for the balancing period t.

$\tau$ = Balancing period

L = The mass load of the balanced variable in the influent and effluent respectively

V = Volume of the system

$r_v$ = Volumetric reaction rate

The first mass balance was set up around the SST according to Equation 5.5. Note that Equation 5.5 is written on the same form as Equation 5.4, but the reaction term has been cancelled since it can be presumed that suspended solids are neither formed nor hydrolysed into soluble material within the SST during the balancing period (Rieger *et al.,* 2013).

$$\frac{\Delta M}{\tau} = (Q_{In} + Q_{RS}) \cdot MLSS - (Q_{WAS} \cdot SS_{WAS} + Q_{eff} \cdot SS_{eff}) \quad (5.5)$$

Concentrations and flows for Equation 5.5 were accessed from the online sensors. All values were based on average records for 2 hours, since this was the resolution for the time proportional influent samples of the characterisation campaign.

The mass balance over the SST did not close satisfactory, since the accumulation term $\Delta M/\tau$ = 10.5 ton SS/d on average over the two day campaign, which was large in comparison to the input term $(Q_{In} + Q_{RS}) \cdot MLSS$ = 43.4 ton SS/d (the loading of suspended solids on the SST). It was found that this mass balance would precisely close within the +10% error margin for a decreased influent flow rate of 21%. However, it was realised that the inconsistency in mass balance could also be associated with errors in the suspended solids online sensors as well as for the return and WAS flows. Also, the balancing period $\tau$ was less than 2-3 times the SRT (≈ 2.0 d), which is the recommended period in order for the mass balance not to be dependent on temporarily accumulation of the balanced variable (Rieger *et al.,* 2013). For these reasons, it was decided to decrease the model input flow rate by 15% in comparison to the recorded input flow data, which was considered somewhat less radical than 21%. The motivation was a suspected inaccuracy in the influent flow sensor, which Persson (2015) investigated more closely through the comparison of flow rates to the HLAS lines of G1 and G2 at the time.

The system boundaries for the second mass balance for SS included the whole HLAS line with its SST, according to Equation 5.6

$$\frac{\Delta M}{\tau} = Q_{In} \cdot SS_{In} - (Q_{WAS} \cdot SS_{WAS} + Q_{eff} \cdot SS_{eff}) + V \cdot r_v \quad (5.6)$$

For this mass balance, the reaction term cannot be cancelled out since it represents the net production of solids in the reactor (production minus decay/degradation). This term could be estimated from the model or previous data, but that was not done in this case. Hence, this equation held two unknown terms (including the accumulation term). Assuming $\Delta M/\tau = 0$, the net production $V \cdot r_v$ was still calculated. Reducing the flow by 15% gave $V \cdot r_v = 0.11$ ton SS/day in comparison to 0.14 ton SS/day for a non-reduced flow. This accounted for 8% of the influent SS load for both cases.

Although there were only four grab samples performed per day of ML and settler underflow sludge, attempts were still made to evaluate the mass balance for total P, since this is a conservative process variable and hence often the most effective to use for detecting faults in the data set (Rieger, 2013). Equivalent mass balances as for SS were put up (Equations 5.7 and 5.8) for P-tot concentrations. Equation 5.7 illustrates the balance equation over the SST for P-tot:

$$\frac{\Delta M}{\tau} = (Q_{In} + Q_{RS}) \cdot P_{tot,ML} - (Q_{WAS} \cdot P_{tot,WAS} + Q_{eff} \cdot P_{tot,eff}) \quad (5.7)$$

This balance closed within +18% (inflow $P_{tot}$-loading to accumulation) for a reduced flow by 15% as compared to 27% for the original flow. The balance over the whole system, Equation 5.8, also closed better (+17%) also for a manipulated flow rate, than for the original rate of flow (+26%).

$$\frac{\Delta M}{\tau} = Q_{In} \cdot P_{tot,in} - (Q_{WAS} \cdot P_{tot,WAS} + Q_{eff} \cdot P_{tot,eff}) \quad (5.8)$$

Still, $P_{tot}$ mass balances did not close within the 10% margin, as recommended by Rieger (2013), even though the flow was reduced.

***Calibration of the SST model***

The only Takács-SVI model parameter determined experimentally during the wastewater characterisation campaign of the 10th and 11th of February was SVI (section 4.4.3). Consequently, the maximum theoretical and practical settling velocities, $v_0$ and $v_0$' as well as the fraction of non-settleable solids were initially set based on the results received from the complementary ZSV experiment of 24th March (section 5.6), which was before the aeration and SRT control strategies were changed for the G2:1 line (see section 4.4). However, the $v_0$ appeared somewhat high in relation to the calibrated results of previous models of the HLAS lines (Martinello, 2013; Klingstedt, 2015) and was thus slightly changed through model calibration, as was the practical settling velocity for a better model fitting. $X_{Lim}$, $X_T$ and $r_p$ were kept to model default values. Table 5.4 lists the calibrated parameters for the extended Takács-SVI secondary settler model for the initial calibrated model.

*5.4. Parameter values for the Takács-SVI settling model based on WEST default, the ZSV experiment of 24th of March and for the initial calibrated model.*

| Parameter | Default | Experimental | Calibrated | Unit |
|---|---|---|---|---|
| $v_0$ | 474 | 800* | 600 | m/d |
| $v_0'$ | 250 | 104 | 90 | m/d |
| $r_p$ | $2.86 \cdot 10^{-3}$ | - | $2.86 \cdot 10^{-3}$ | L/mg |
| $f_{ns}$ | $2.28 \cdot 10^{-3}$ | $9.0 \cdot 10^{-3}$ | $2.28 \cdot 10^{-3}$ | - |
| $X_{Lim}$ | 900 | ≈ 800 | 900 | mg/L |
| $X_T$ | 3000 | - | 3000 | mg/L |
| SVI | 100 | 133 | 123 | mg/L |

*For the experiment of 24th of March, $v_0$ was determined using the Vesilind settling model and not the Takács-SVI model.

***Suspended solids level fittings***

Figure 5.27 depicts the results of the model calibration of suspended solids levels. The figures illustrates rather good fittings. The variability in WAS SS is larger according to the sensor and lab values as compared to simulations.

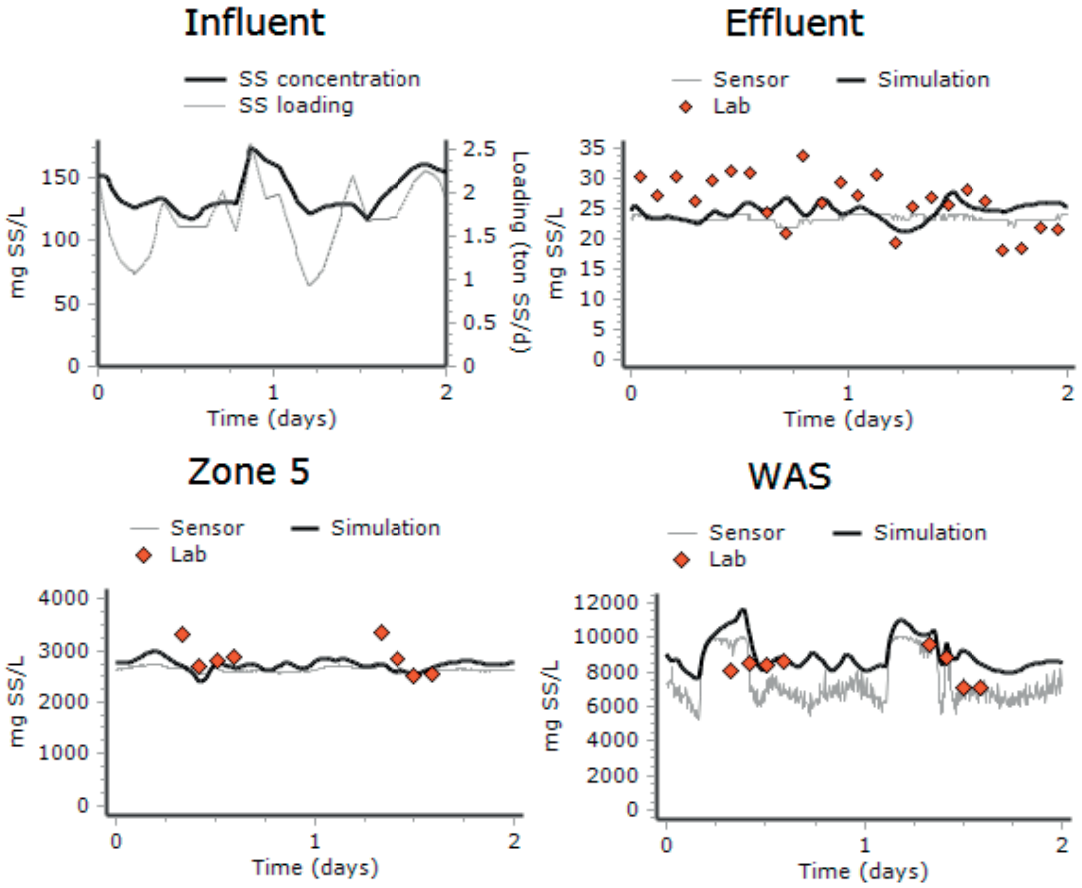


*Figure 5.27. Simulated suspend solids levels for the initial model of the G2:1 HLAS line, calibrated against data from the characterisation campaign of the 10th-11th February. The presented influent data is that for the model input, based on analytical SS concentrations of time proportional samples (every two hours) and online sensor flow rate records (5 min averages)*

### 5.7.2 Calibration with regard to COD levels

From the experimental results of three OUR tests (section 5.2.2) the easily biodegradable COD fraction, $S_S$, appeared small in comparison to analytical $COD_{filt,1.6}$. It was therefore decided that the input fractionation model should allocate part of the input $COD_{filt,1.6}$ to the particulate COD components based on the $COD_{filt,0.1}$:$COD_{filt,1.6}$ of two influent time proportional samples of the characterisation campaign (section 5.7.1). The variable $S_{COD}$ of the fractionation scheme was thus defined accordingly – the calibrated ratio between $S_{COD}$ and analytical input $COD_{filt,1.6}$ was finally set to 0.80 gCOD/gCOD. However, the experimentally determined $S_S$ to $S_F$ ratio ($f\_S_F$) resulted in a very high input of inert soluble COD, $S_I$. This resulted in an overestimation of the levels of soluble COD in the effluent as compared to analytical $COD_{filt,1.6}$ and $COD_{filt,0.1}$ levels. Consequently, $f\_S_F$ fraction was raised considerably as indicated by Table 5.5 (from 0.13 to 0.43).

The $COD_{filt,0.1}$:$COD_{filt,1.6}$ ratio in the effluent was on average 0.83 based on two 0.1 µm filtrations. Hence, analytical effluent $COD_s$ was calculated as $0.83 \cdot COD_{filt,1.6}$ and compared to simulated $COD_s$ levels, quantified as the sum of $S_A$, $S_F$ and $S_I$.

The experimental value of $f\_X_H$ was left non-calibrated. The $f\_X_S$ fraction was first found through model calibrations only, which is usual practise for ASM modelling if $X_H$ can be decided experimentally (Henze, 2000a). Its magnitude in relation to $X_I$, which was found by difference, had minor implications on reactor MLSS as well as for organic P and N. However, since it was later found that the fraction of $X_S$ seemed to affect the settling properties for the real plant, it was decided to give efforts to decide the $f\_X_I$ fraction analytically based on laboratory $BOD_7$ analysis. Roeleveled & van Loosdrecht (2002) found an empirical relation between the biodegradable part of analytical COD and total BOD, according to Equation 5.9:

$$bCOD = \frac{1}{(1-f_{BOD})} BOD_{tot} \quad (5.9)$$

bCOD = biodegradable COD

$BOD_{tot}$ = total BOD

$f_{BOD}$ = correction factor

$BOD_{tot}$ can be accessed through a long-term BOD analysis, after 20 days of incubation ($BOD_{20}$) 95 to 99% of the biodegradable COD will be oxidised. However, $BOD_{20}$ is not a reliable measurement. Instead, $BOD_{tot}$ can be accessed by determining BOD as a function of time based on multiple BOD measurements after 1-8 days of incubation (Roeleveld & van Loosdrecht, 2002). Since that was not possible for the present investigation, it was approximated that $BOD_{tot} = BOD_7$, as did Lysberg & Neth (2012) when determining the COD fraction of influent wastewater at Gryaab WWTP, Gothenburg, Sweden. The correction factor, $f_{BOD}$, is applied to account for the fact that some of the bCOD is degraded into an inert fraction during the BOD analysis, and hence bCOD> $BOD_{tot}$. Based on previous empirical observations, $f_{BOD}$ can be taken as 0.15 (Roeleveld & van Loosdrecht, 2002) and this value was consequently used also for the present investigation.

The particulate fraction of COD, $f\_X_I$, can be determined according to Equation 5.10:

$$f\_X_I = \frac{COD_X - bCOD_X}{COD_X} \quad (5.10)$$

for which:

$$COD_X = COD_{tot} - 0.80 \cdot COD_{filt,1.6} \quad (5.11)$$

$$bCOD_X = \frac{1}{1-f_{BOD}} BOD_{tot} \cdot \frac{COD_X}{COD_{tot}} \quad (5.12)$$

Using average values for analytically determined COD and BOD influent levels for the wastewater characterisation campaign, $f\_X_I$ was determined as 0.40 using the method of the Roeleveled & van Loosdrecht (2002). However, using this value for the model instead of the previously calibrated value (0.33) did not appear to affect the fitting with regard to COD, P, N and SS considerably. Therefore, it was decided not to recalibrate the model but to use $f\_X_I$ = 0.33. An experimental value was instead used for the final recalibrated model. Derived values for the model COD fractions are summarised in Table 5.5. Figure 5.29 illustrates the relative magnitude of the major model COD components in the influent in relation to total influent COD. Note again that $f\_X_I$ is not an input fraction in WEST model (section 4.5.1). The model input fraction $f\_X_S$ was hence calculated as

$$f\_X_S = 1 - f\_X_I - f\_X_H \quad (5.13)$$

where $f\_X_H$ was experimentally determined (section 4.3.1). There was some variation in $f\_X_I$ throughout the project period, as indicated from Figure 5.28.

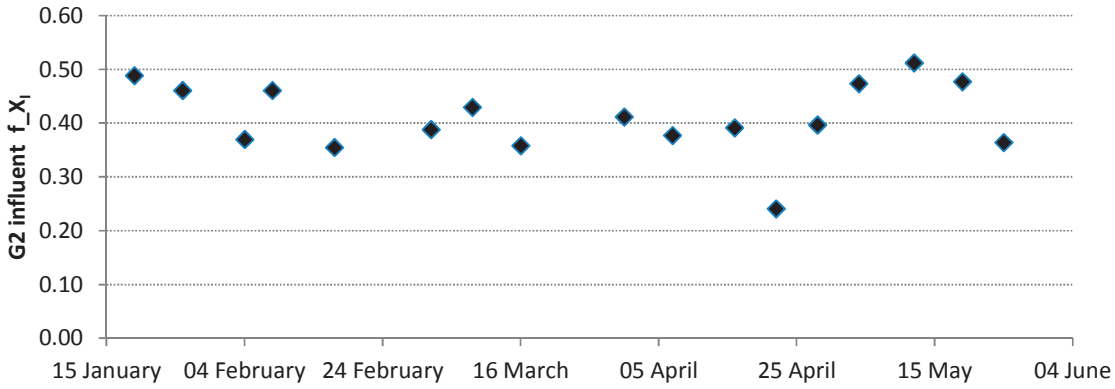


*Figure 5.28. Variation if the $f\_X_I$ fraction, estimated from influent $BOD_7$ and COD concentrations during the project period.*

*Table 5.5. Model COD fractions for major influent soluble and particulate COD components as determined through OUR experiments ($10^{th}$ - $11^{th}$ of February) and calibrations. $S_A$ was found through VFA analysis of influent samples and $S_I$ and $X_S$ through difference.*

| Fraction | Experimental | Calibrated |
|---|---|---|
| f_$S_F$ | 0.13 | 0.43 |
| f_$X_H$ | 0.16 | 0.16 |
| f_$X_I$ | 0.40 | 0.33 |
| f_$X_S$ | 0.44 | 0.51 |

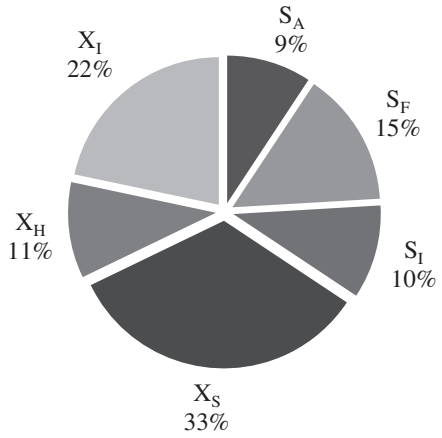


*Figure 5.29. Distribution of total influent COD between the major soluble and particulate model COD components. The remaining considered model COD components ($X_{AUT}$,$X_{PAO}$, $X_{PHA}$)are comparably very small.*

***Fitting of COD levels***

Figure 5.30 depicts the results of the model calibration of COD levels. As seen, both total and soluble COD levels corresponds well. VFA measurements were below the measurement interval (< 20mg/L) in the effluent and Simulations indicated that $S_A$ < 0.5 mg COD/L and $S_f$ < 1.0 mg COD/L. Hence, effluent $COD_s$ appeared to consist mainly of $S_I$.

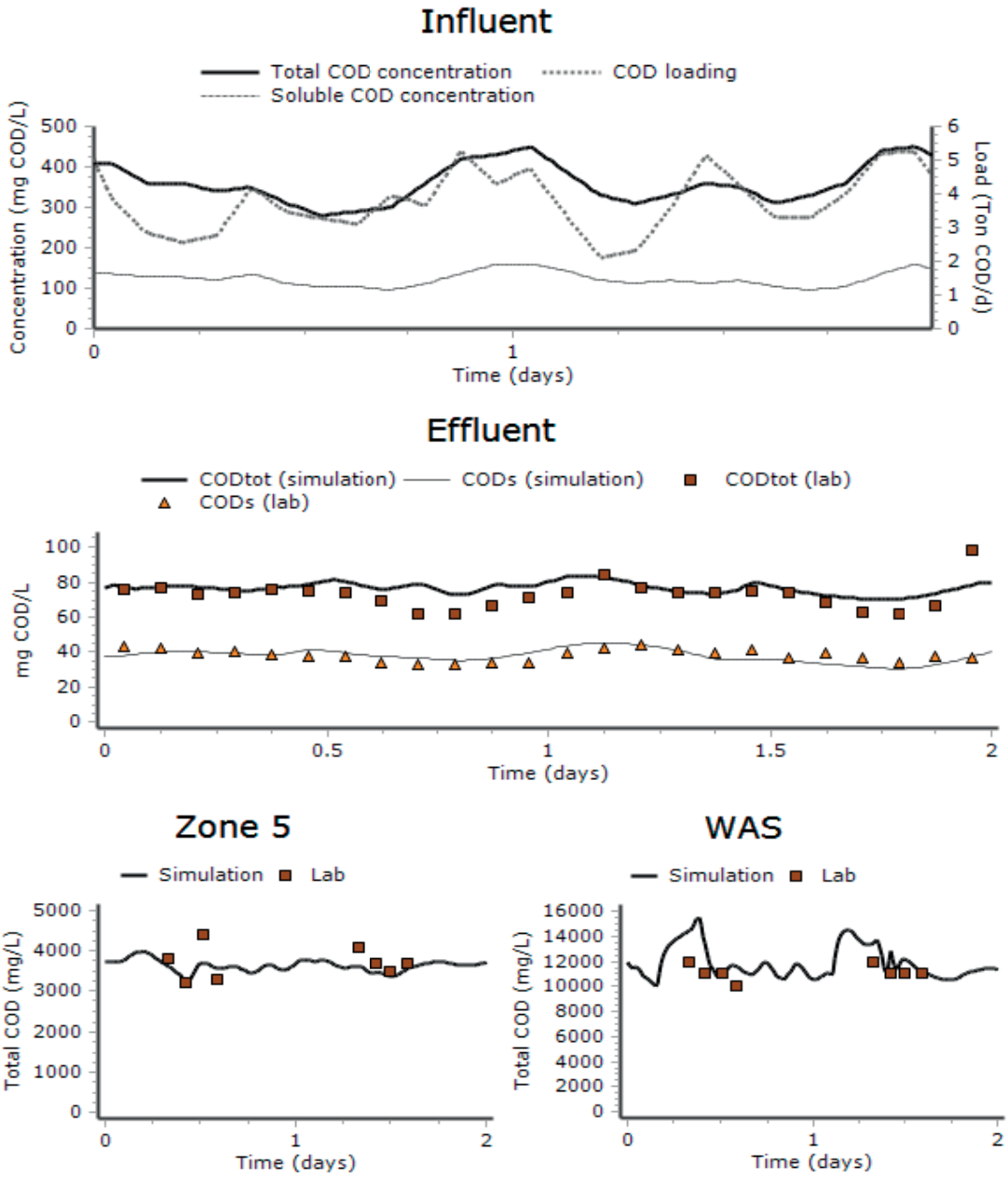


*Figure 5.30. Simulated COD levels for the initial model of the G2:1 HLAS line, calibrated against data from the characterisation campaign of the 10th-11th February.*

### 5.7.3 Calibration with regard to nitrogenous species

For the initial runs, total nitrogen levels were continuously lower than the analytical levels. The difference was approximately 2 mg throughout, which was approximately the level of model output nitrogen gas, $S_{N2}$. It was realised that the analytical N-tot method used possibly included dissolved dinitrogen. Consequently, a small experiment was conducted at the lab by the lab technicians, using the same analytical method on tap water to test the contribution of

nitrogenous gas. Since the experiment indicated a small contribution of $N_2$, the $S_{N2}$ component was coupled to output total nitrogen for the effluent defractionation model, according to Equation 5.14, which gave a better fit:

$$\mathrm{Ntot} = \mathrm{Org_N} + S_{NH} + S_{NO} + S_{N2} \tag{5.14}$$

Moreover, model output $NO_{2,3}$ levels, denoted $S_{NO}$, were infinitely small. From a model perspective, this seemed correct since a SRT = 2.0 days is too short for autotrophic nitrifying bacteria to be abundant in an AS system at the present temperature of 14 $^{o}$C (Salem, 2005). However, this did not fully correspond to the analytical levels. Although effluent nitrite levels were generally very small (< 0.02 mg/L), the average analytical nitrate levels were significantly larger (≈ 0.31 mg/L). It was realised that the influent possibly held some nitrifying bacteria, especially since there were nitrite and nitrate in the influent water. These species might have originated from the reject return flows of the downstream process, although measures had been taken to separate these from the influent water of the modelled HLAS line (G2:1). Consequently, the influent component $X_{AUT}$ was adjusted to a fixed value of 0.6 mg/L (default = 0.01 mg/L), which gave the best fit with regard to $NO_{2,3}$-N (Figure 5.31).

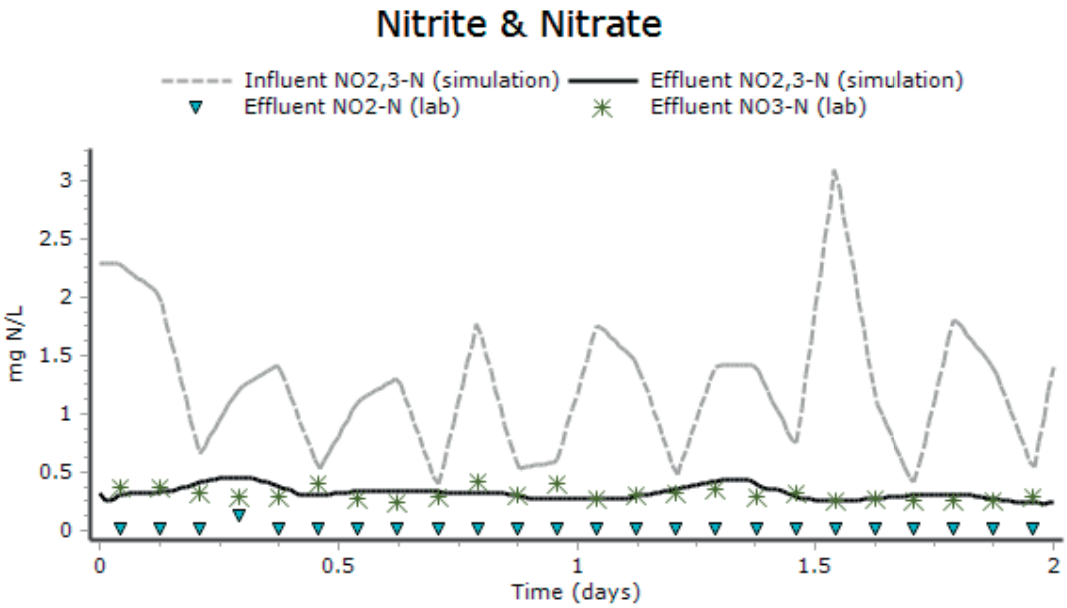


*Figure 5.31. Simulated $NO_2^-$* and *$NO_3^-$ levels ($S_{NO3}$, representing the sum of $NO_2^-$* and *$NO_3^-$ ) in the influent and effluent for the initial model of the G2:1 HLAS line, calibrated against data from the characterisation campaign of the 10$^{th}$ and 11$^{th}$ February.*

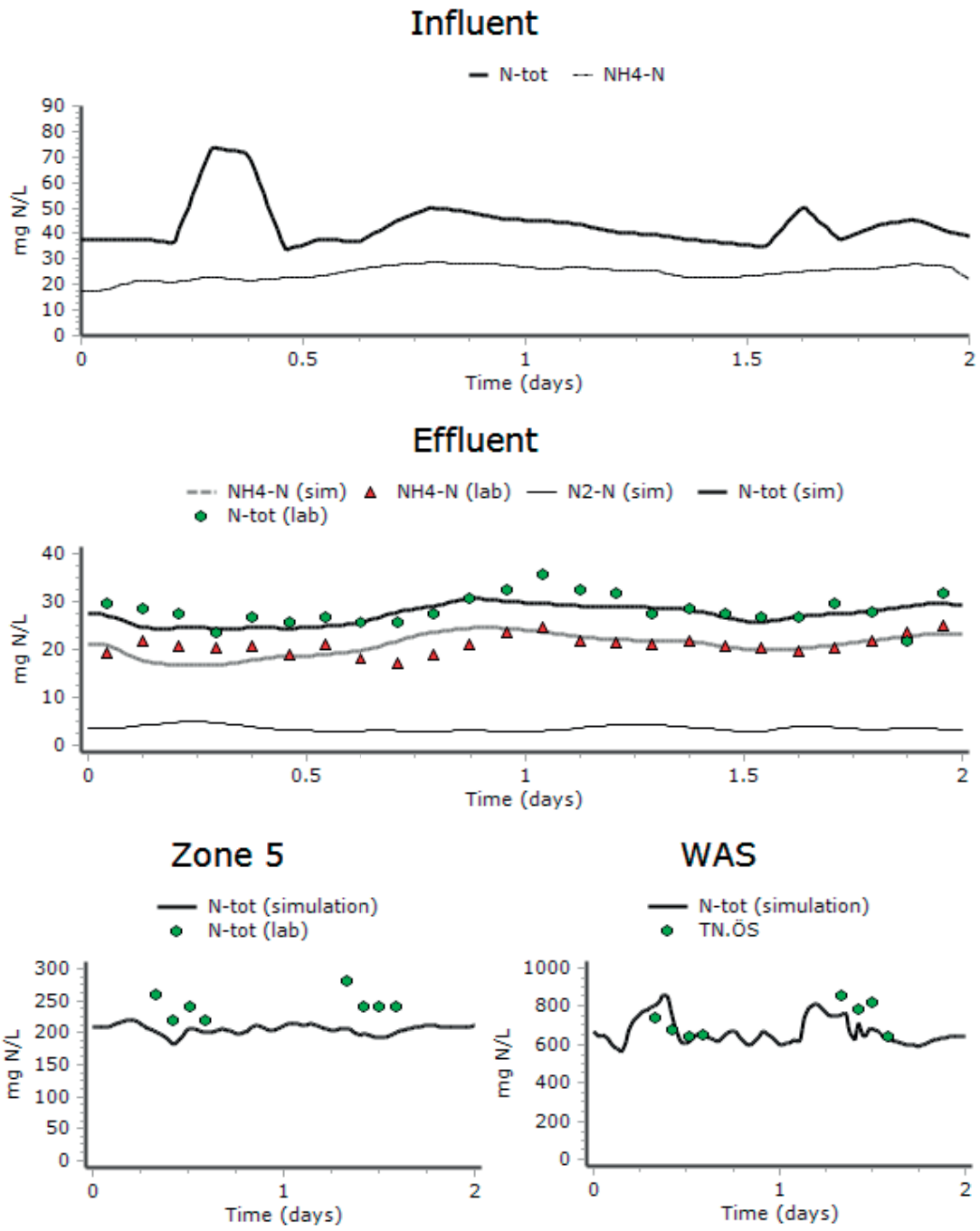


*Figure 5.32 Simulated ammonium and total nitrogen levels for the initial model of the G2:1 HLAS line, calibrated against data from the characterisation campaign of the 10th and 11th of February.*

### 5.7.4 Calibration with regard to phosphorus species

The use of metal hydroxides as coagulants for pre-precipitation in primary clarifiers might affect the AS system if residues of such species are present in the AS influent water, i.e. in the primary effluent (Henze & Harremoes, 1992; Henze *et al.*, 2000a). As $FeSO_4$ is added as an

agent for phosphorus precipitation in the primary clarifiers at Sjölunda, a complementary test was performed to check if any iron residues were present in the influent wastewater. The levels in the daily flow proportional AS influent sample of 16th of April 2015 amounted to: $Fe^{2+}$ = 2.96, $Fe^{3+}$ = 2.37, $Fe_{tot}$ = 5.33 g/m$^3$. In order to further fit the calibrated model, especially in regard to outflow phosphate levels, these experimental values were used to manipulate the model input component $X_{MeOH,}$ representing ferric hydroxide, $Fe(OH)_3$. Since 1 g of $Fe^{3+}$ yields 1.91 g of $Fe(OH)_3$, $X_{MeOH}$ was initially set to 4.53 g/m$^3$, but the calibrated to 5.0 g/m$^3$ to approximately account also for ferrous iron and to get a better model fitting. The possible presence of other phosphorus species, like $FePO_4$ which in the model corresponds to $X_{MeP}$ (Henze *et al.*, 2000a), was disregarded since the insolvable part of iron ($Fe_{insolvable}$ = $Fe_{tot}$ - $Fe^{2+}$-$Fe^{3+}$) was so small (0.02 g/m$^3$). Influent $X_{PAO,}$ representing polyphosphate accumulating microorganisms, were kept to default (0.01 mg/L), representing an infinitely small concentration. The calibrated results for model fit of phosphorus species are showed in Figure 5.33.

*5.6. Default, analytical (16th of April) and calibrated values for influent ferric model components.*

| Model component | Default | Experimental | Calibrated | Unit |
|---|---|---|---|---|
| $X_{MeOH}$ | 0.01 | 4.53 | 5.0 | mg $Fe(OH)_3$/L |
| $X_{MeP}$ | 0.01 | - | 0.01 | mg $FePO_4$/L |

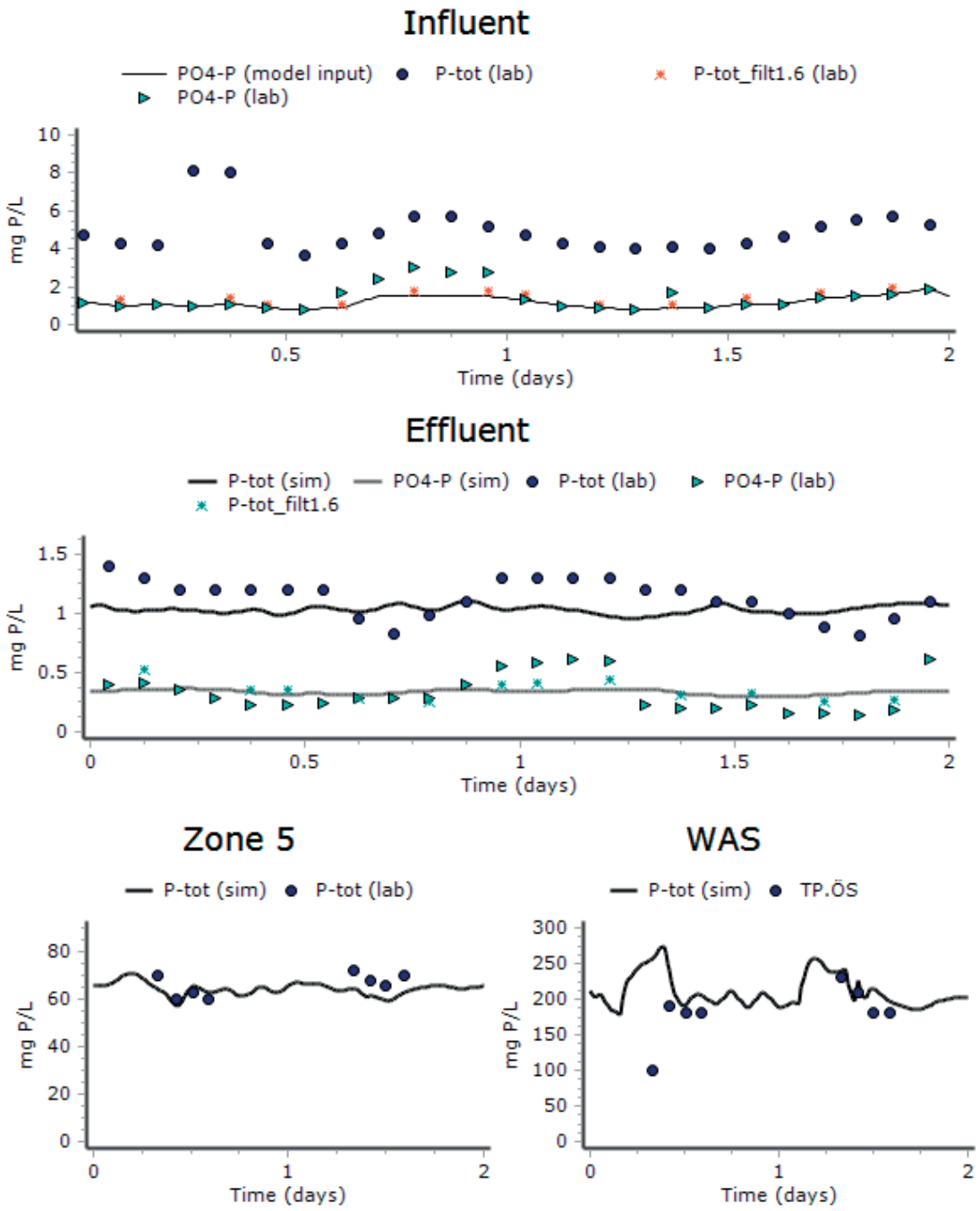


*Figure 5.33 Simulated levels for phosphorus species for the initial model of the G2:1 line, calibrated against data from the characterisation campaign of the 10th-11th February.*

### 5.7.5 Calibration with regard to dissolved oxygen and airflows

The aeration model of Persson (2015) was successful in fitting simulated DO levels and air-flows to real data from the characterisation of the 10th and 11th of February. However, it was necessary to change the empirical factors, A and B, for the aerator connected to the fifth zone

of the G2:1 line in order to get a close fit (Table 5.7). This suggests that there was some small discrepancy between the initial HLAS model presented herein and that of Persson (2015).

The model fittings for the airflows and DO levels are found in appendix (section 9.2.1). The very high air flows and DO levels at around 13.00 the first day is due to an upkeep procedure for the bubble disc diffusers performed each Tuesday at the WWTP, during which the diffusers are let to distribute air at full power. The upkeep procedure was not simulated in the model since it was considered not to have a substantial effect for the outcome of the simulation.

*Table 5.7. Calibrated empirical factors (A and B) for the aeration model. The initial parameter values were given from the calibrated aeration model of Persson (2015).*

| | A | | B | |
|---|---|---|---|---|
| | **Initial** | **Calibrated** | **Initial** | **Calibrated** |
| **Zone 3** | 6.6 | 6.6 | 2.6 | 2.6 |
| **Zone 4** | 5.0 | 5.0 | 4.5 | 4.5 |
| **Zone 5** | 7.0 | 6.0 | 6.2 | 5.2 |

## 5.8 Results of HLAS optimisation using the model

### 5.8.1 Sludge Production

Based on the simulations, sludge production (ton SS/d) appeared to be rather constant in the SRT interval of [1.2 - 2.0], which was the approximate interval studied during the full-scale tests. Below an SRT of 1 day, the mass flow of wasted solids (ton SS/d) decreases rapidly with decreasing SRT, as indicated by Figure 5.34a. This is partly due to a higher effluent solids concentration (section 5.3) but profoundly due to less production per input degradable substrate. This can be related to less hydrolysis and oxidation of substrate. Since all the simulations were run towards the same input data (from the characterisation of the $10^{th}$ and $11^{th}$ of February), the $BOD_7$ loading was of course the same for all simulations. This means that the sludge production, quantified as the mass flow of waste solids (mg SS/L), is analogous to the sludge yield in this case. An optimum is observed at SRT = 1.5 d, for which the simulated sludge production is 1.52 ton SS/d. This corresponds to a sludge yield of 0.67 ton $SS_{WAS}$/ton $BOD_7$ for the average input of 2.26 ton $BOD_7$/d that was observed during the characterisation campaign.

However, the hydraulic WAS flow increases substantially towards lower SRT (Figure 5.34), since this is the mechanism through which the ICA controller regulates the SRT. This sludge will however be much less dense in terms of solids concentrations (Figure 5.34), which is why sludge production is disproportional to waste sludge outtake. MLSS also decreases substantially at lower set-point SRT for an equal loading.

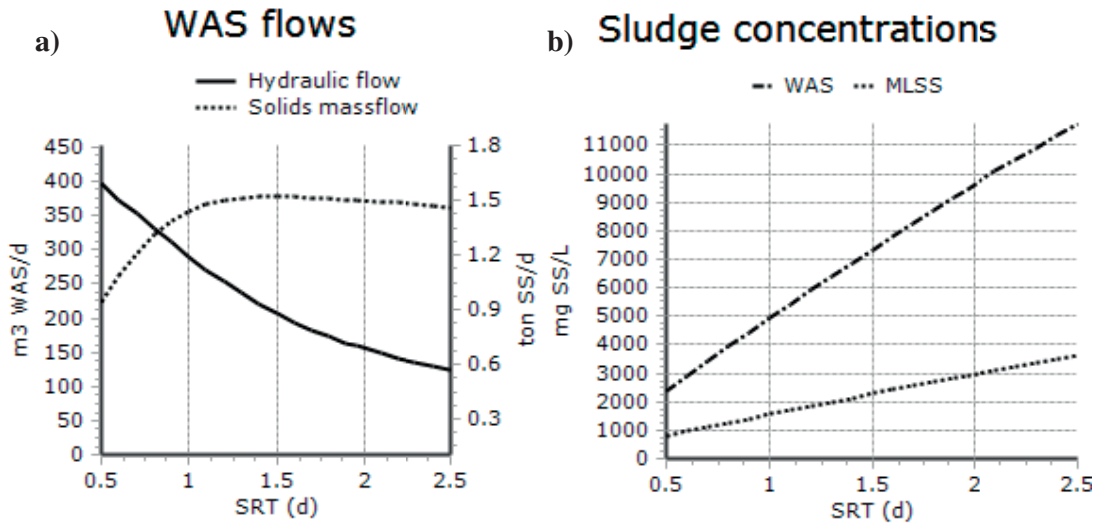


*Figure 5.34. a) WAS flows and b) sludge concentrations (right) at steady state for simulations at different controller set-point SRT. Activated sludge unit temperatures and DO set-point values were kept the same as for the characterisation campaign of the 10th and 11th of February (T = 14 °C; DO = [0.3;0.8;2.0] mg $O_2$/L for zones 3, 4 and 5.)*

In Figure 5.35a, it is seen that the inert fraction of particulate biomass decreases to total particulate COD towards lower SRT. The opposite holds for substrate particulate COD. Consequently, sludge biodegradability increases somewhat towards lower SRT, but there is no substantial effect (Figure 5.35b). The particulate fraction of biomass COD ($X_H$) slightly increases with decreased SRT for an SRT> 1.5 days, which is the SRT corresponding to maximum sludge yield.

Since the BMP was believed to be coupled to the degradability of the organic matter in the sludge, it was expected that minor adjustments in SRT would have very limited effect on sludge BMP. This was confirmed through the laboratory BMP tests performed for WAS at an target SRT of 1.2 and 2.0 days respectively (section 5.4), which showed no significant difference in BMP.

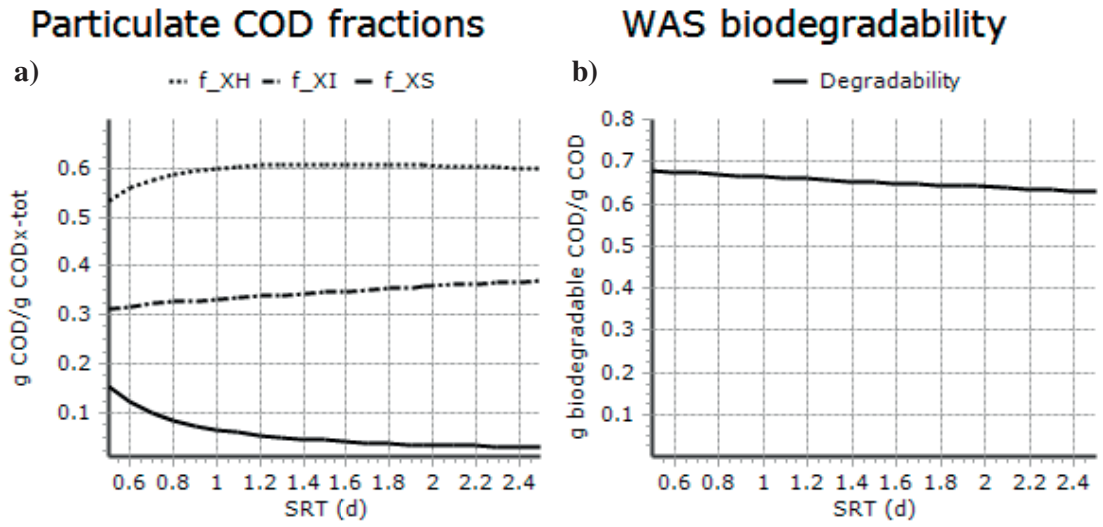


*Figure 5.35. a) Particulate COD fractions of the sludge. b) WAS biodegradability calculated as the ratio between inert and biodegradable COD model components,*

### 5.8.2 Effluent quality

For the initial simulations, effluent quality consistently improved in terms of suspended solids and COD levels with decreasing SRT. This was the opposite from what was observed in full-scale tests (section 4.4.1). Since settling velocity and SVI had proven to be less SRT dependent, attention was put towards the fraction of non-settleable solids, $f_{ns}$, which had proven to increase at operation at higher SRT (section 5.6). It was theorised that the fraction of non-settleable solids fraction was related to the fraction of particulate substrate in the reactor. It was believed that the non-hydrolysed substrate accounted for the small particles that did not settle.

Since f_$X_S$ was observed to increase exponentially towards lower SRT, a function was derived for the $f_{ns}$ fraction based on a curve fit for the f_$X_S$ relation. Initially, the $f_{ns}$(SRT) function was set to be proportional to the derived f_$X_s$ to SRT relation. However, strict proportionality appeared to underestimate the deterioration of effluent quality, since the simulated effluent SS level for SRT = 1.2 d then became much higher than that observed in full-scale tests. The $f_{ns}$(SRT) function was therefore set to grow somewhat faster towards lower SRT in order for $f_{ns}$ to correspond to observed levels at an SRT = 1.2 days and for SRT = 2.0, for which there were some full-scale records (section 5.6). The equation for the two term exponential f_$X_S$ curve fit and the constructed $f_{ns}$(SRT) function are given below (Equation 5.16 and Equation 5.17). Figure 5.36 depicts the $f_{ns}$ function.

$$f_{X_S(SRT)} = 0.63e^{-4.00SRT} + 0.086e^{-4.78SRT} \qquad 0.8 < SRT < 2.4\ days \tag{5.16}$$

$$f_{ns(SRT)} = 3.09e^{-4.00SRT} + 0.086e^{-4.78SRT} \qquad 0.8 < SRT < 2.4\ days \tag{5.17}$$

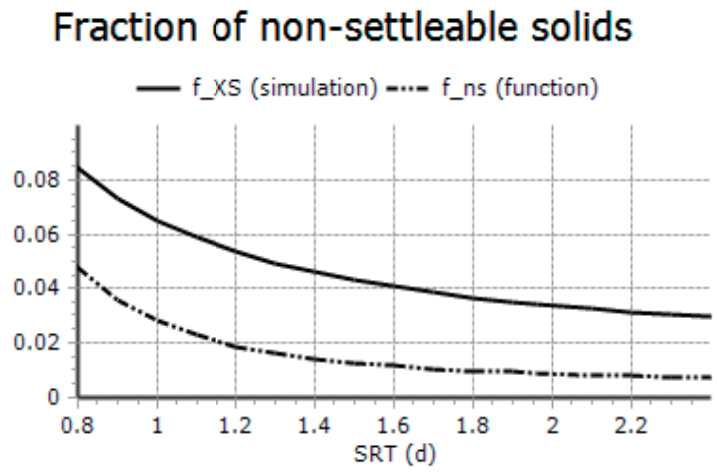


*Figure 5.36. Fraction of non-settleable solids derived as a function based on the fraction of particulate substrate to SRT relation. There is no reference to the validity for the $f_{ns}$(SRT) function outside the range of SRT = [1.2 - 2.0] based on real full-scale operation.*

The effluent model predictions presented in Figure 5.37 are rather uncertain. Especially due to the fact that there was a limited amount of settling tests performed for operation at different SRT (section 4.4.3). Especially, there is less confidence in the results outside the range of SRT = [1.2 - 2.0] days. It is seen that the removal efficiency is not very affected by the SRT, which corresponds to full-scale observations. However, the ASM-models have been criticized for predicting too high $COD_S$ removals at lower SRT, especially of the more slowly biodegradable, colloidal part (Nogaj *et al.,* 2015).

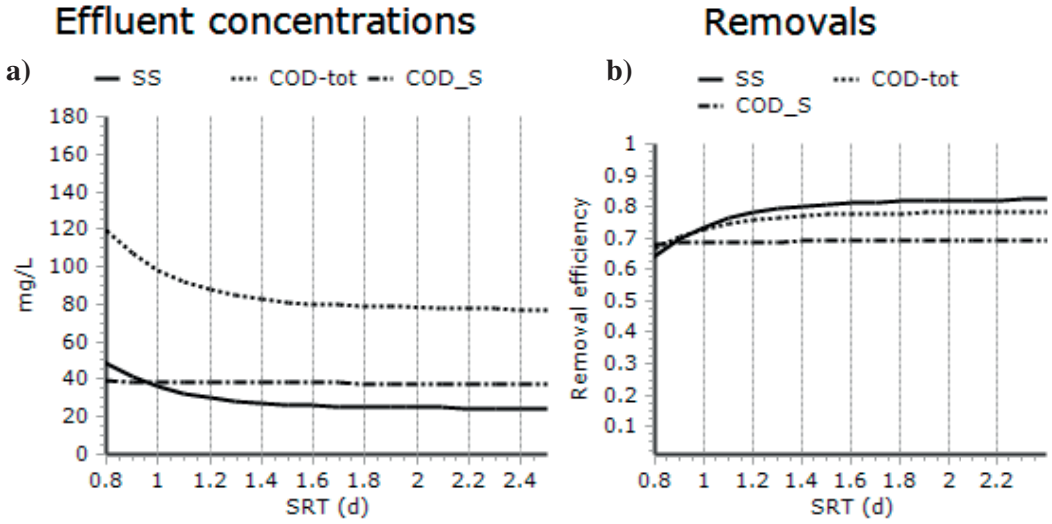


*Figure 5.37 a) Effluent COD and suspend solids levels as well as b) removal efficiencies. There is no reference to the validity for these values outside the range of SRT = [1.2 - 2.0] based on real full-scale operation. $COD_S$ denotes soluble COD (the sum of $S_A$, $S_F$ and $S_I$).*

Since particulate effluent COD levels increases towards lower SRT, the COD:N-tot ratio also increases. The $COD_S$:N-tot ratio is however unaffected, as was seen for the full scale tests (Figure 5.38).

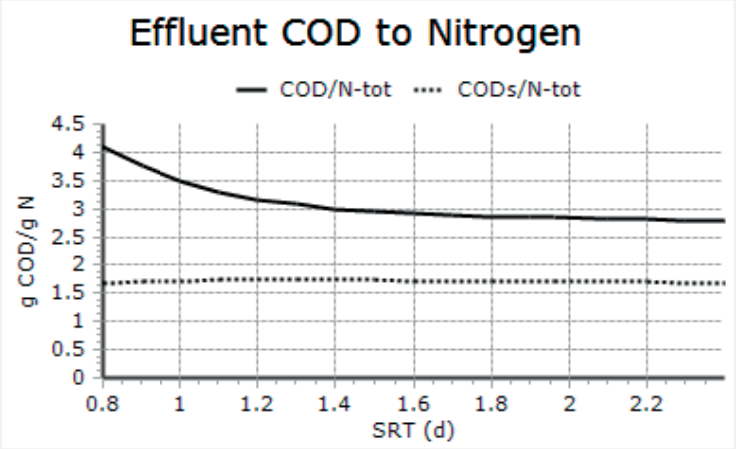


*Figure 5.38. Effluent COD to nitrogen levels at different simulated SRT.*

### 5.8.3 Energy balance: aeration demands

As seen from Figure 5.39, total aeration demands are only marginally affected for the SRT range studied in full-scale, [1.2 - 2.0] days. In opposite to what was expected, aeration needs per kg COD removed appears to increase towards lower SRT, despite the fact that endogenous respiration is expected to decrease. An explanation might be that the aeration model used predicts a decreasing oxygen transfer efficiency with decreasing SRT (section 4.5.1). However, the results of the aeration simulations must be received with caution, since it was found difficult to validate the applied aeration model (5.9.1).

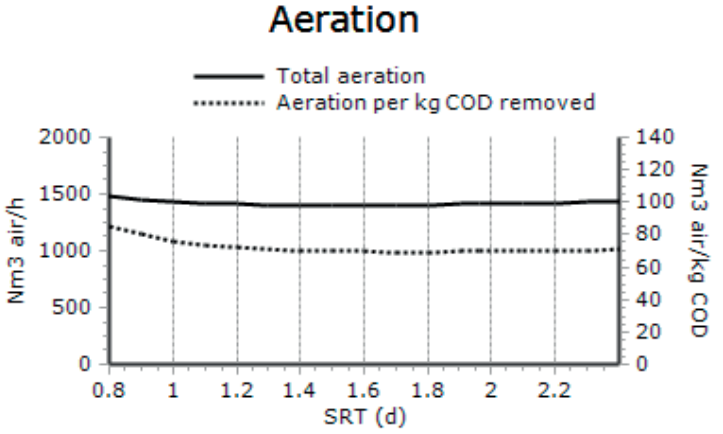


*Figure 5.39. Airflows and air used per unit of removed COD for the aerated basin as a function of SRT, using the present aeration settings of the full-scale plant.*

### 5.8.4 Optimised SRT control strategy implemented at the full-scale HLAS line

Based on the model simulations presented in section 5.8.1, 5.8.2 and 5.8.3, it was decided to operate the ICA controlled HLAS line (G2:1) at a set-point SRT = 1.6 d. The implications of

such operation compared to operation at SRT = 2.0 d are presented below (according to simulations):

The sludge yield would increase by 1.6% and biodegradability by 0.71% (g COD/g COD), which taken together means an increase in total methane production by 2.3% (assuming a constant SS/COD ratio for the sludge). At the same time, the required aeration would decrease by approximately 10 $Nm^3$/kg COD removed, which corresponds to a decrease by 0.71%.

From these results, it is realised that the potential gains in terms of plant energy balance, taking methane production and aeration demands in consideration, are very modest according to the simulations. In addition, operation at the lower SRT is likely to slightly deteriorate effluent quality. From the effluent model predictions presented, SS and total COD removal efficiency would decrease very little (≈ 1%), although the uncertainties are significant regarding the predicted effluent quality. At least, $COD_S$ removal efficiency and the $COD_S$:N-tot ratio are believed to be unaffected. Possibly, the $COD_{tot}$:N-tot ratio could increase slightly.

A consequence for operation at a lower SRT than at present is an increased hydraulic waste sludge flow rate which would increase by 23% according to the model predictions. In addition, the WAS suspended solids concentration would decrease by 17% (as would MLSS). This might lead to increased costs for sludge pumping and dewatering. For the present investigation, the magnitude of such costs was not determined. Thus, there are uncertainties whether operation at an SRT = 1.6 days actually improves the energy balance compared to operation at an SRT ≈ 2.0 days.

Since the optimised SRT control strategy was implemented towards the end of the full-scale test period (on the 30th of April), it was hard to evaluate its performance from experimental tests (the daily flow proportional effluent sample and foam observation campaign was ended on the 5th of May). Also, there was considerable upset with the controller shortly after the implementation of the new set-point SRT (section 5.1.2).

## 5.9 Results of model validation

Since no ZSV tests were performed for the two lines on the day of the second characterisation campaign (18th of May), the derived theoretical and practical settling velocities for the two lines from the ZSV tests of the 22th of March (Table 5.2) were used. SVI was calculated as a mean of four tests performed on the day of the campaign and used for the settling model in WEST. The $f_{ns}$ parameters for the settling model was derived from two tests on each line on the day of the campaign, as described in section 5.6. Using these values gave a close fit to laboratory data in terms of sludge and effluent SS levels (Figure 5.41, next page). No measures were undertaken to improve the fitting.

Note that the online sensors for SS measurements of the WAS are measuring a concentration of exactly 10 000 mg SS/L during most of the days at both lines. This is due to the fact that SS > 10 000 mg/L is outside the range of measuring for the sensors. This illustrates an issue with the ICA based SRT control system. It is also seen that the MLSS online sensor at G2:2 registers twice the MLSS compared to laboratory measurements and simulations. These issues explain the fact that neither of the lines were operating at the target SRT that day. Figure 5.40 illustrates the SRT of the two lines based on model simulations and online sensor records, the latter which should be considered misleading. In this case, simulations give a truer picture since the simulated SS concentrations appear to closely follow laboratory measurements. Since there is no SS sensor for the effluent G2:2, the observed SRT was calculated from the approximation that $SS_{eff,G2:1} \approx SS_{eff,G2:2}$ since the magnitude of $SS_{eff}$ has little effect on the SRT calculation (Equation 3.1, section 3.1). From the simulated results, it is clear that G2:2 was actually operated at a lower SRT than G2:1 on that day ($SRT_{G22,mean}$ = 0.65 d; $SRT_{G2:1,mean}$ = 1.1 d). Both HLAS lines were operated at much lower SRT than was intended (target SRT = 1.2 d for G2:1, and 2.0 d for G2:2). It is understood that if the sensor for WAS suspended solids gives a to low value to the calculator, the control system will not "realise" that more solids are wasted than indented and thus $SRT_{calculator} > SRT_{real}$.

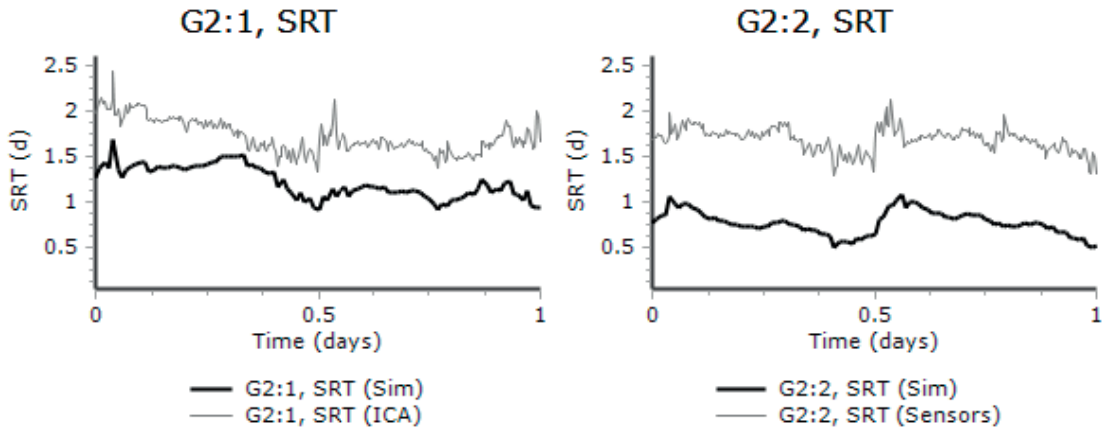


*Figure 5.40. Simulated and observed SRT based on online sensor measurements at the 18th of May.*

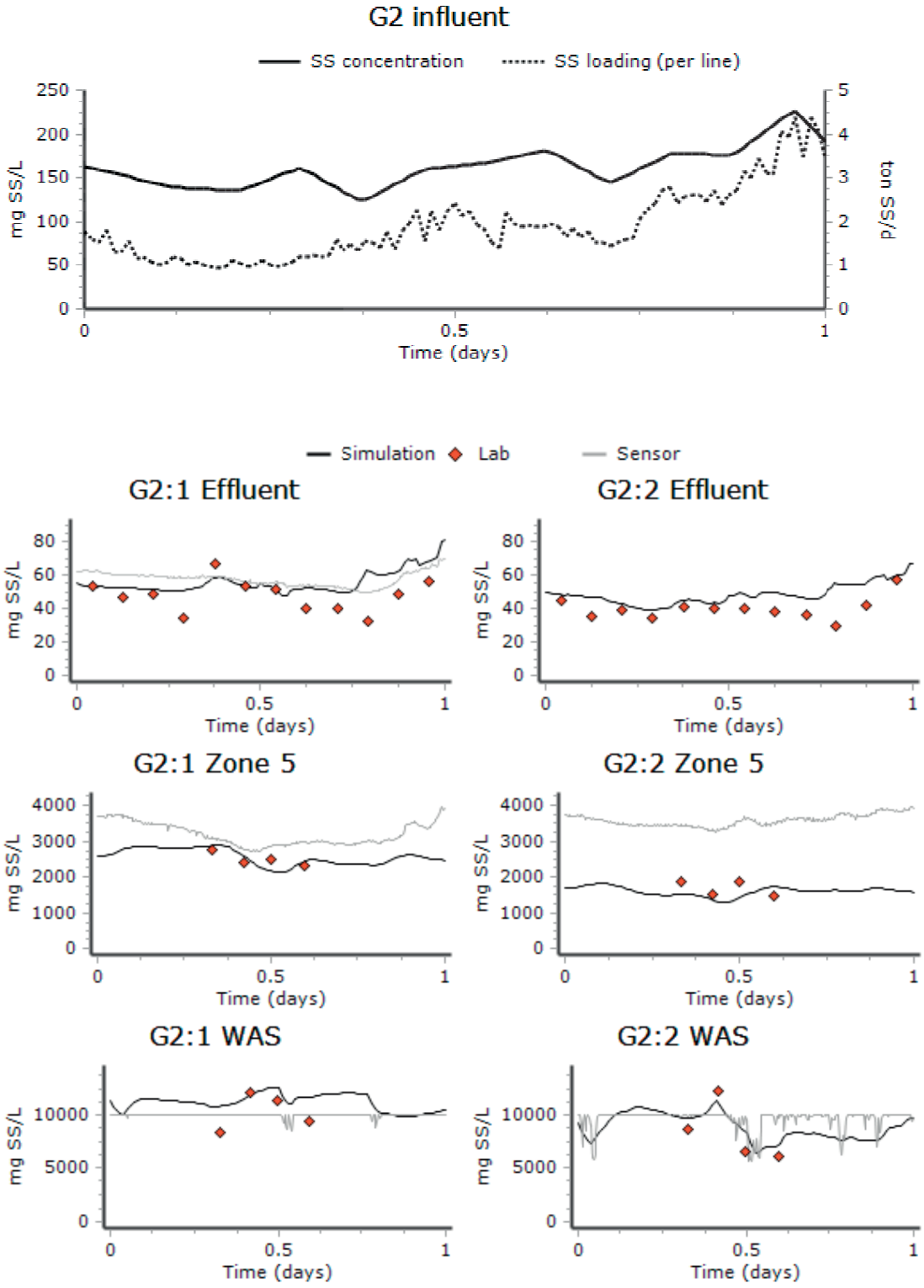


*Figure 5.41. Simulated and observed SS levels at G2:1 and G2:2 on the 18th of May, 2015.*

Figure 5.42 (next page) illustrates the simulated and analytical COD levels based on laboratory measurements. As for SS, a close fitting is achieved with the experimentally based settling parameters for the Takács-SVI model applied. Simulated $S_A$ and $S_F$ levels were low (< 4 mg COD/L) and analytical VFA was below the range o measurement in the effluent. The f_$S_f$ fraction was calibrated in order to better fit analytical $COD_s$ levels to simulated levels. The final calibrated value was 0.26, as compared to 0.15 as an average of two OUR tests performed that day (at 14-16 and 22-24, section 5.2.2, Table 5.1). The calibrated f_Sf value was considerably lower than for the 10$^{th}$ and 11$^{th}$ of February.

The $COD_{filt,0.1}$:$COD_{filt,1.6}$ ratio in the effluent was considerably lower than for the first characterisation campaign (section 5.7.2) for both of the lines, on average 0.65 for G2:1 and 0.78 for G2:2 based on three filtrations at each line. Due to the considerable variation between filtrations and the few number of 0.1 µm filtrations performed, it was decided to use a mean value for both lines based on the six filtrations in total. Analytical $COD_s$ was thus calculated as $0.72 \cdot COD_{filt,1.6}$ and compared to simulated $COD_s$ ($S_A$+ $S_F$ + $S_I$). Table 5.8 gives the $COD_{filt,0.1}$:$COD_{filt,1.6}$ ratios for the influent and effluent wastewaters,

Note also the increase in COD loading that was observed towards the end of the day, corresponding to the increased SS loading (Figure 5.41, previous page). This increase is to be associated with the rain event at that time of the day (note the increased influent flow rate).

*Table 5.8. $COD_{filt,0.1}$:$COD_{filt,1.6}$ ratios for the characterisation campaign of the 18$^{th}$ of May.*

| | **$COD_{filt,1.6}$:$COD_{filt,0.1}$** | | |
|---|---|---|---|
| **Time** | **G2 influent** | **G2:1 effluent** | **G2:2 effluent** |
| **06-08** | 0.71 | 0.55 | 0.58 |
| **14-16** | 0.88 | 0.65 | 0.86 |
| **22-24** | 0.84 | 0.74 | 0.89 |
| **Average** | 0.81 | 0.65 | 0.78 |
| **SD** | 0.09 | 0.09 | 0.17 |

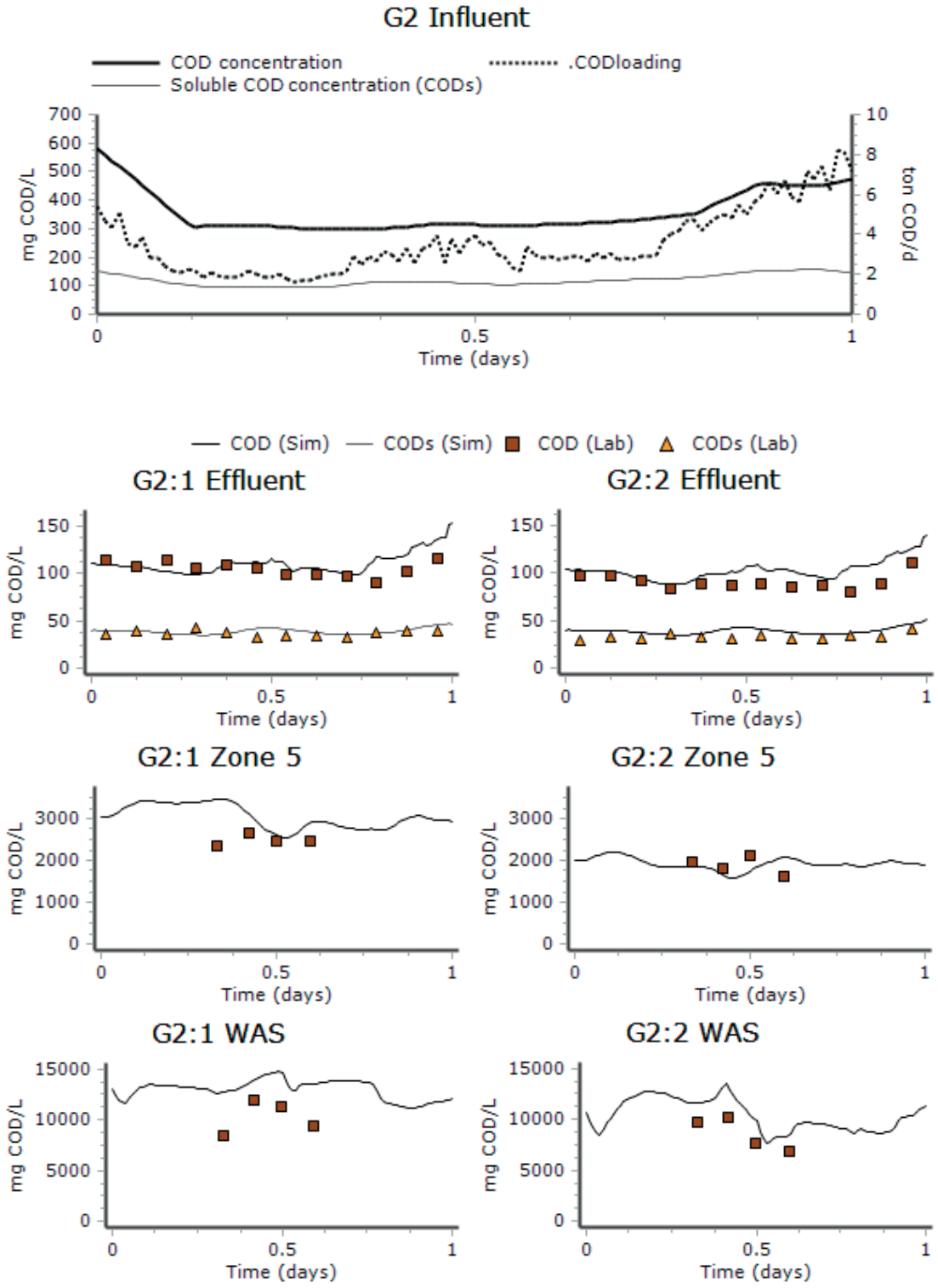


*Figure 5.42. Simulated and analytical COD levels on the 18th of May.*

Analytical effluent nitrate levels corresponded quite well to simulations, as depicted in Figure 5.43. Model input $X_{Aut}$ was kept at 0.6 mg/L, as for the initial calibrated model.

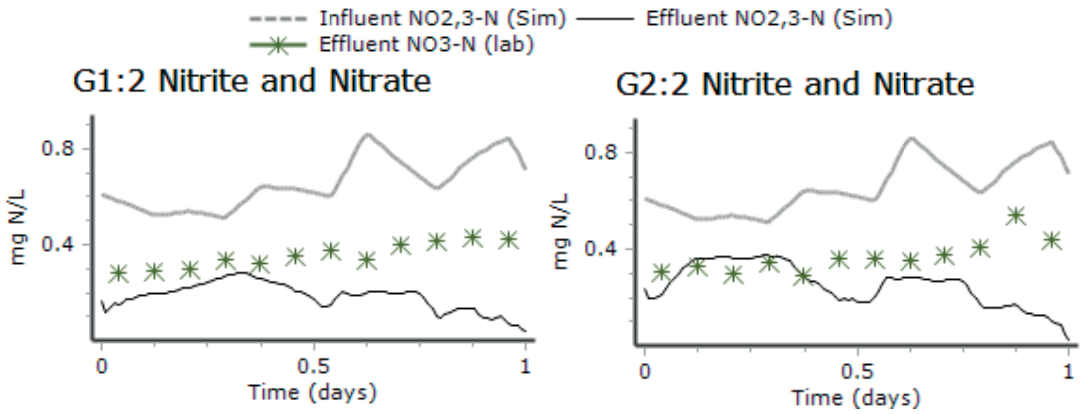


*Figure 5.43. Influent and effluent nitrate and nitrate levels for simulations and laboratory analysis on the 18th of May, 2015.*

Effluent total nitrogen and ammonium levels corresponded quite well to analytical values, at least for part of the day (Figure 5.44). Very poor fitting was achieved for the sludge samples. It should be noted that N-tot analysis could not be performed on the sampling day. Instead, samples were frozen on 100 mL plastic flasks and analysed one week after. If the composition of the sludge in terms of organic nitrogen is modelled right, sludge N-tot analysis should correspond to simulations if the sludge COD levels are satisfying. From Figure 5.42, it is seen that simulated COD levels were higher than analytical levels. Attempts were made to recalibrate the model by changing the $f\_X_I$ fraction a bit, since inert particulate organic matter holds less organic nitrogen per g COD than substrate particulate organic matter. For the validation, $f\_X_I$ was set to 0.50 based on the mean of two $BOD_7$ influent daily flow proportional analysis performed for the 12th ($f\_X_I = 0.51$) and 19th of May ($f\_X_I = 0.48$). No $BOD_7$ analysis could be performed for the 18th of May. However, changing $f\_X_I$ back to 0.34 as for the initial model calibration did not have any effect. Thus, it was set at 0.48 for the final validated model of the calibration of the 18th of May.

Total phosphorus levels for sludge samples were somewhat closer fitted to simulations than was total nitrogen levels, as indicated by Figure 5.45. Neither where total P analysis performed on the sampling day, but conserved with $H_2SO_4$ and kept refrigerated at ≈ 4 °C for one week prior to analysis. Filtrated samples (1.6 µm retention filter papers) were also conserved in the same manner prior to phosphate analysis. Phosphate levels were a bit low compared to simulations. Elaborations were made on increasing input $Fe(OH)_3$ (corresponding to model input $X_{MeOH}$) by 50% compared to the recorded value for the characterisation (on average 4.1 mg/L, based on three samples), but simulated were still higher than for laboratory analysis.

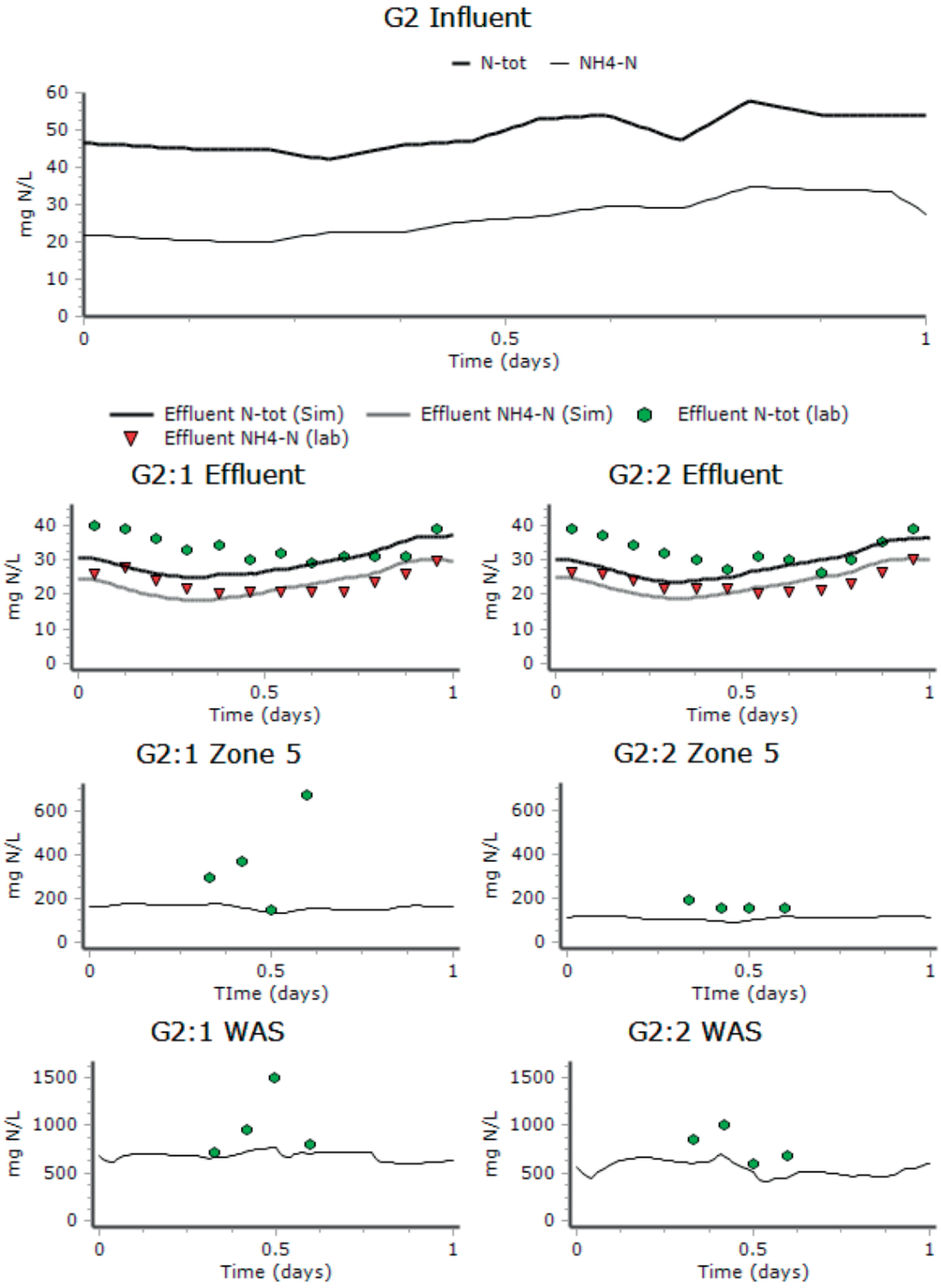


*Figure 5.44. Simulated and analytical values for total nitrogen and ammonium at the 18th of May, 2015.*

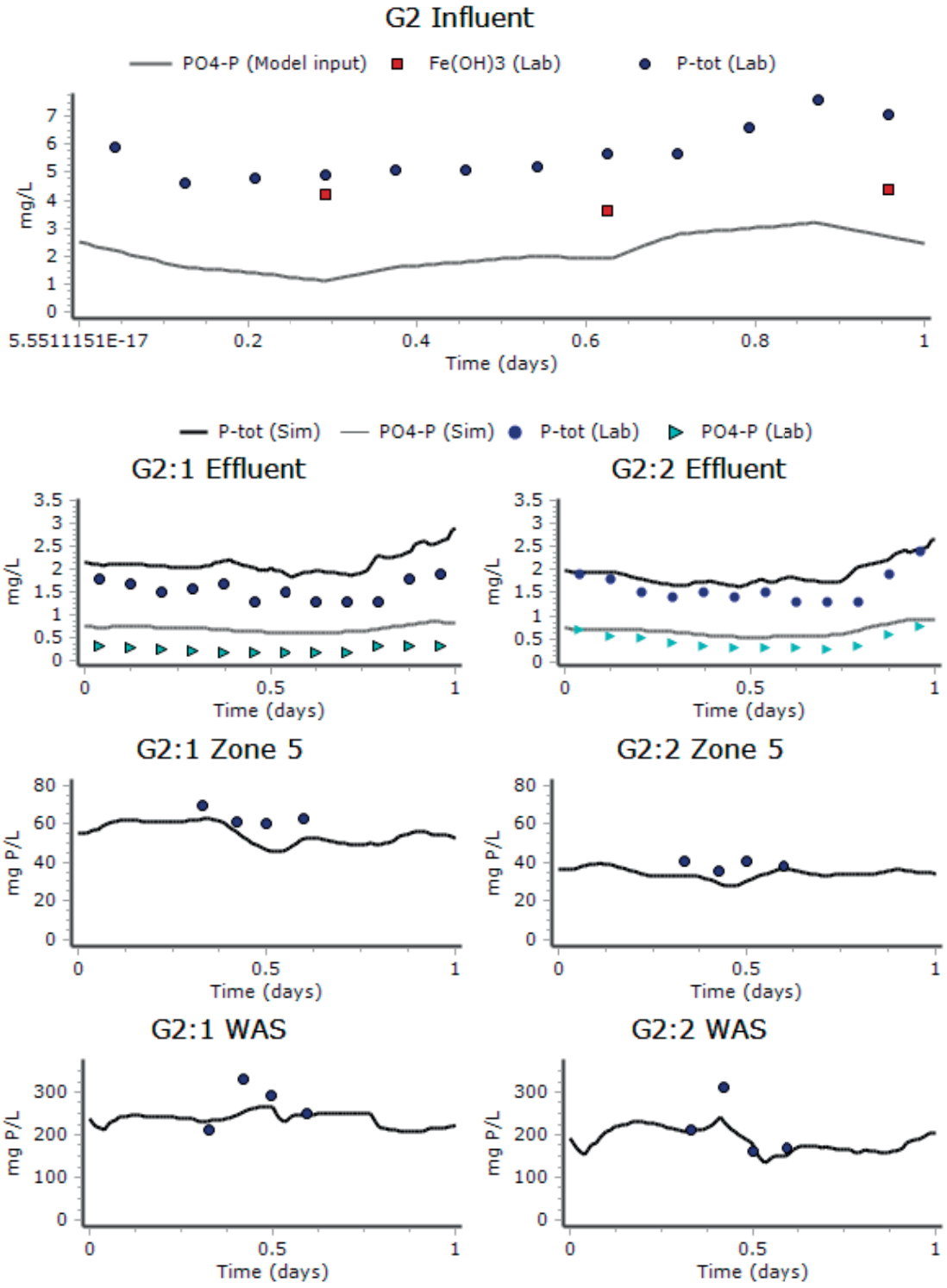


*Figure 5.45. Simulated and analytical values for total phosphorus and phosphate for the 18th of May, 2015.*

### 5.9.1 Validation of the aeration model

It was not possible to successfully validate the aeration model towards data from the characterisation of the 18th of 2015. Especially, the DO levels recorded for the full-scale plant did not correspond to simulated DO levels towards the end of the simulated day at which the organic loading increased significantly (due to a rain event). Airflows corresponded even less well. For the real plant, the increased loading induced substantially higher airflows in zone 3. For the simulations, the increase was instead seen in zone 4. This was true for both of the studied lines (G2:1 and G2:2). There was also a considerable discrepancy in total airflows (airflow in all the aerated zones taken together) as indicated by Table 5.9, especially for the G2:1 line. The aerator model parameters were not recalibrated, but some were updated in accordance with the changed air and water temperatures (Table 5.10). The model fittings for airflows and DO levels for the validation are to be found in Appendix (section 9.2.2).

*Table 5.9. Simulated and real total airflows (sum of airflows for the aerated zones) for the two studied HLAS lines for the 18th of May, 2015.*

| HLAS line | Simulated total airflow ($Nm^3/d$) | Real total airflow ($Nm^3/d$) | Difference (%) |
|---|---|---|---|
| **G2:1** | 77967 | 58003 | 26 |
| **G2:2** | 62826 | 59261 | 6 |

*Table 5.10. Changed parameters for the aeration model for simulations due to a higher temperature at the 18th of May, 2015.*

| Parameter | Description | Initial | Validation | Unit |
|---|---|---|---|---|
| **$Rho_{air}$** | Air density | 1272 | 1229 | $g/m^3$ |
| **$T_{air}$** | Temperature of the air | 3 | 14 | $^oC$ |
| **$T_{water}$** | Temperature of the water | 14 | 16 | $^oC$ |

# 6 Conclusions

I. In an approximate SRT interval of [1.0 - 2.0] days, effluent quality deteriorates with lower SRT with regard to COD and suspended solids levels. The effluent C:N ratio is increased at lower SRT, since the concentration of organic matter increases compared to ammonium. The difference in the level of organic matter in the effluent is mainly to be related to particles and not to solutes. The change in the composition of the mixed liquor results in different sludge settling properties at lower SRT. The fraction of non-settleable solids is the settling parameter mostly affected by the SRT. Settling velocity and compressibility of the sludge blanket is less affected by the SRT, at least down to an SRT = 1.0 d.

II. Operation at a lower set-point SRT appears to increase foaming issues at the plant. Especially, it is the very bright and less dense sludge that is produced during low SRT (≈ 1.2 d). Still, there appears to be other mechanisms related to the foaming that is of greater importance than the SRT.

III. The difference in WAS methane potential as well as sludge to substrate yield are very small in an operational interval of SRT = [1.2 - 2.0] days. Consequently, methane production cannot be significantly increased by lowering the SRT.

IV. Lowering the SRT results in an increased WAS flow rate and a less dense sludge in terms of solids concentration. Consequently, operation at lower SRT may potentially increase the energy use for sludge pumping energy and dewatering. Aeration energy use per unit mass of removed organic substrate is not likely to decrease at an SRT lower than at present operation (SRT ≈ 2.0 days).

V. An appropriate target SRT with regard to effluent quality, energy balance and foaming for the present plant is believed to be about 1.6 days according to model simulations. However, further full-scale observations are required to ensure this number and sludge dewaterability and pumping cost considered more closely.

VI. The evaluated ICA based SRT controller is unreliable and is not able to continuously fix the SRT to the set-point value. The reasons for the insufficient performance is mainly due to inaccurate online sensor readings but also due to an error in the programming of the controller. Neither the manual SRT control strategy is sufficient in fixing the SRT. Fixing the SRT will be even more accentuated for a futuristic higher plant loading. Therefore, it is motivated to implement an automated control system at all of the HLAS lines of Sjölunda WWTP, if the control system can be made reliable.

VII. It is possible to successfully model a HLAS operated at an SRT = [1.0 - 2.0] days with the ASM2d. A limitation is that it is hard to make effluent quality predictions for operation at i.e. different SRT, at least if used with the empirically based SST model of Takács *et al* (1991). The latter model does not recognise relative changes in distribution between particulate organic constituents in the mixed liquor at different modes of operation.

# 7 Recommendations and Future Work

Sjölunda WWTP needs to evaluate strategies for the removal of HLAS effluent COD in the future event of a higher organic load in order not to violate threshold limits for the recipient and to ensure that the C:N ratio is not too high for preceding nitrogen removal processes to function properly. Since it is the particulate fraction of effluent COD that increases at lower SRT, it might be possible remove that COD with micro-screens. Thus, one should test the effluent filterability and investigate if coagulants and flocculants are needed for that purpose. There are also ideas of introducing coagulants and flocculants in the SST at the HLAS plant, which should be further evaluated and tested.

To test the implications of a higher future load, one should elaborate with changed inflow distributions to the HLAS lines. For example, the ICA controlled line (G2:1) and the reference line (G2:2) could be subjected to a higher load compared to other HLAS lines. That way, it may be possible to test operation at low SRT at a maintained MLSS level since an increased loading would increase the biomass growth.

Efforts need to be made in minimising uncertainty in online sensor SS measurements. Alternatively, the difference between $u_{min}$ and $u_{max}$ for the regulated WAS flow rate could be set smaller in order to keep it within an interval which would have been chosen if regulated manually. Also, alternative control methods should be evaluated. For example, OUR in the aerobic basin could be related to the F/M ratio and thus to SRT. Hence, OUR may be used as a SRT control mechanism.

An alternative way to cope with a higher future load would be to aerate the presently anoxic part of the basin of the HLAS lines. Since the anoxic zones accounts for one fourth of the total basin volume, the plant could possibly be operated at the same aerobic SRT as today even if the load was to increase considerably. One aspect that has to be considered is whether the present SST can handle the increased loading and whether denitrification can be allocated completely to preceding processes.

Research should be performed in order to bring further clarity about the relation between the non-settleable fraction and the composition of organic constituents in the reactor. One should look into the effect of such mechanisms as adsorption and storage as well as the extraction of extra-cellular polymeric substances from heterotrophic biomass on effluent quality for operation at different SRT.

Characterisation campaigns and simulations should be performed for wet-weather flow in order to better understand the implications of such conditions.

# 8 References


Andersson B., Aspegren H., Parker D. S., Lutz M. P. (1994). High rate nitrifying trickling filters. *Water Science and Technology* **29**(10-11), 47-52.

Balmér P., Hallqvist S., Hernebring M. (1984). Ten years experience with a high-loaded activated sludge plant. *Water Science and Technology* 16(12), 649-660.

Boyle W. C., Craven A., Danley W., Rieth M. (1989). Oxygen Transfer Studies at the Madison Metropolitan Sewerage District Facilities. *Environmental Protection Agency: EPA/600/R-94/096*, Washington D.C., U.S.

Böhnke B., Diering B. (1986). Method of treating sewage in sewage treatment installations having an adsorption stage. *US Patent* (US4568462 A).

Catunda PFC., van Haandel AC. (1992). Activated sludge settling Part I: Experimental determination of activated sludge settleability. *Water SA* **18**(3), 165-172

Choubert J-M., Rieger L., Shaw A., Copp J., Spérandio M., Sörensen K., Rönner-Holm S., Morgenroth E., Melcer H., Gillot S. (2013). Rethinking wastewater characterisation methods for activated sludge systems – a position paper. *Water Science and Technology* **67**(11), 2365-2373.

Copp J.B. (2015). The COST simulation benchmark: description and simulator manual. *COST action* 624 & 682.
http://apps.ensic.inpl-nancy.fr/benchmarkWWTP/Pdf/Simulator_manual.pdf
(2015-05-28)

Corominas Ll., Rieger L., Takács I., Ekama G., Hauduc H., Vanrolleghem P. A., Oehmen A., Gernaey K. V., van Loosdrecht M. C. M., Comeau Y. (2010) New framework for standardized notation in wastewater treatment modelling. *Water Science and Technology* **61**(4), 841-857.

Daigger G.T., Roper R.E., Roper R.E. Jr (1985). The relationship between SVI and activated sludge settling characteristics. *Water Pollution Control Federation* **57**(8), 859-866.

DHI (2014). *MIKE by DHI - WEST 2014, SP2*. Build date: Sep 11 2014. DHI, Denmark.

Dold P.L., Ekama G.A., Marais G.v.R. (1980). A general model for the activated sludge process. *Progress in Water Technology* **12**(6), 44-77.

Ekama G.A., Dold P.L., Marais G.v.R. (1986). Procedures for determining influent COD fractions and the maximum specific growth rate of heterotrophs in activated sludge systems. *Water Science and Technology* **18**(6), 91-114.

Ekama G.A. (2010). The role and control of sludge age in biological nutrient removal activated sludge systems. *Water Science & Technology* **61**(7), 645-1652.

Garret M.T. Jr (1958). Hydraulic control of activated sludge growth rate. *Sewage and Industrial Wastes* **30**(3), 253-261.

Ge H., Batstone D. J., Keller J. (2013). Operating aerobic wastewater treatment at very short sludge ages enables treatment and energy recovery through anaerobic sludge digestion. *Water Research* **47**(17), 6546-6557.

Gustavsson D. J. I., Lindqvist P., Sandström D., Lumley D. (2013). (In Swedish): eWASTE – a data analysis tool for the water and wastewater works developed by the water and wastewater utilities. Poster at: *13th Nordic Wastewater Conference*, Malmö, Sweden, October 8-10, 2013.

Gustavsson D. J. I., Persson F., la Cour Jansen J. (2014). Manammox – mainstream anammox at Sjölunda WWTP. In: *Proceedings of 9th IWA World Water Congress and Exhibition*, Lisbon, Portugal, September 21-26, 2014.

Hagman M., la Cour Jansen J. (2007). Oxygen uptake rate measurements for application at wastewater treatment plants. *Vatten* **63**, 131-138.

Hanner N., Aspegren H., Nyberg U., Andersson B. (2003). Upgrading the Sjölunda WWTP according to a novel process concept. *Water Science and Technology* **47**(12), 1-7.

Hansen T. L., Schmidt J. E., Angelidaki I., Marca E., la Cour Jansen J., Mosbaek H, Christensen T. H. (2004). Method for determination of methane potentials of solid organic waste. *Waste Management* **24**, 393-400.

Hammer, M. J. – Hammer, M. J. Jr (2012). *Water and Wastewater Technology*, **7th ed**. Pearson Education, Inc (New Jersey).

Henze M., Gujer W., Mino T., van Loosdrecht M.C.M. (2000a). *Activated sludge models ASM1, ASM2, ASM2d and ASM3*. IWA publishing, London, England.

Henze M., Harremoës P., Jansen J.C., Arvin E. (2000b). *Wastewater treatment – biological and chemical processes*, **3rd ed**. Springer-Verlag, Berlin-Heidelberg, Germany.

Henze M., Harremoës P. (1992). Characterisation of Wastewater: The effect of chemical precipitation on the wastewater composition and its consequences for biological denitrification. *Chemical water and wastewater treatment II*, pp. 299-311, Springer-Verlag (Berlin/Heidelberg, Germany).

Kappeler J, Guyer W, (1992). Estimation of kinetic parameters of heterotrophic biomass under aerobic conditions and characterisation of wastewater for activated sludge modeling. *Water Science and Technology* **25**(6), 125-140.

Kartal B, Kuenen J.G., van Loosdrecht M.C.M. (2010). Sewage Treatment with Anammox. *Science* **328**, 702-703.

Kos, P. (1998). Short SRT (Solids Retention Time) nitrification process/flowsheet. *Water Science and Technology*, **38**(1), 23-29.

Levine D., Tchobanoglous G., Asano T. (1991). Size distribution of particulate contaminants in wastewater and their impact on treatability. *Water Research* **25**(8), 911-922.

Lund University (2012a). (In Swedish:) *Description of method for batch reactor methane potential measurements*. Department of Chemical Engineering, Lund University, Lund, Sweden.

Lund University (2015). (In Swedish:) *Description of methodology: VFA, Volatile Fatty Acids (GC-method)*. Version: 08-09-25. Department of Chemical Engineering, Lund University, Lund, Sweden. Accessed: 26th of June, 2015.

Lysberg M., Neth M. (2012). (In Swedish:) *Influent water characterisation - determination of COD fractions*. Gryaab Rapport 2012:14.

Martinello N. (2013). *Integrating experimental analyses and a dynamic model for enhancing the energy efficiency of a high-loaded activated sludge plant*. MSc thesis, Università degli Studi di Padova, Italy.

Miller M. W., Regmi P., Wett B., Murthy S., Bott C. B. (2014). On-line sensors for the control and optimization of an adsorption-style HRAS pilot study. In: *Proceedings of 9th IWA World Water Congress and Exhibition*, Lisbon, Portugal, September 21-26, 2014.

Nogaj T., Randall A., Jiminez J., Takács I., Bott C., Miller M., Murthy S., Wett B. (2015). Modeling of organic substrate transformation in the high-rate activated sludge process. *Water Science and Technology* **71**(7), 971-979.

Olsson G., Aspegren H., Nielsen M. (1998). Operation and control of wastewater treatment - a Scandinavian perspective over 20 years. *Water Science and Technology* **37**(12), 1-13.

Persson G. (2015). *High-loaded activated sludge - Effects of different aeration strategies*. MSc thesis, Lund University, Sweden.

Polizzi C. (2013). *Dynamic evaluation of a high-loaded activated sludge plant as pretreatment for deammonification in the mainstream*. MSc thesis, Università degli Studi di Padova, Italy.

Rieger L., Thomann M., Gujer W., Siegrist H. (2005). Quantifying the uncertainty of on-line sensors at WWTPs during field operation. *Water Research* **39**(20), 5162-5174.

Rieger L., Gillot S., Langergraber G., Ohtsuki T., Shaw A., Takács I., Winkler S. (2013). Guidelines for using activated sludge models. *Scientific and Technical Report Series* **22**.

Roeleveld P.J., van Loosdrecht M.C.M. (2002). Experience with guidelines for wastewater characterisation in the Netherlands. *Water Science and Technology* **45**(6), 77–87

Rosso, D., Iranpour, R. and Stenstrom, M.K., 2005. Fifteen Years of Offgas Transfer Efficiency Measurements on Fine-Pore Aerators: Key Role of Sludge Age and Normalised Air Flux. *Water Environmental Research* **77**(3), 266-273.

Rosso D., Stenstrom K. (2005). Comparative economic analysis of the impact of mean cell retention time and denitrification on aeration systems. *Water Research* **39**(16), 3773-3780.

Salem S., Berends D.J., Heijnen J.J., van Loosdrecht M.C.M. (2005). Bio augmentation of nitrification with return sludge. *Water Research* **37**(8), 1794-1804.

Shao Y.J., Crosse J., Keller E., Jenkins D (1992). High rate air activated sludge operation at the city of Los Angeles Hyperion Wastewater Treatment Plant. *Water Science and Technology* **25**(4-5), 75-87.

Siegrist H., Salzgeber D., Eugster J., Joss A. (2008). Anammox brings WWTP closer to energy autarky due to increased biogas production and reduced aeration energy for nitrogen removal. *Water Science and Technology* **57**(3), 383-388.

SIS (1981). *Determination of dry matter and ignition residue in water, sludge and sediment*. SS 028113, Swedish Standards Institute, Stockholm.

Smith R., Elger S., Mleziva S. (2013). *Implementation of Solids Retention Time (SRT) control in wastewater treatment*. Xylem analytics, internet source: http://www.xylemanalytics.co.uk/media/pdfs/W20-Implementation-of-Solids-Retention-Time-Control-in-Wastewater-Treatment.pdf Date of access: 9th of June, 2015

Strous M., Heijnen J. J., Kuenen J. G., Jetten M. S. M. (1998). The sequencing batch reactor as a powerful tool for the study of slowly growing anaerobic ammonium-oxidizing microorganisms. *Applied Microbiology and Biotechnology* **50**(5), 589–596.

Takács I., Patry G.G, Nolasco D. (1991). A dynamic model of the clarification-thickening process. *Water Research* **25**(10), 1263-1271.

Torrijos M., Cerro R.-M., Capdeville B., Zegal S., Payraudeau M., Lesouef A. (1994). Sequencing batch reactor: A tool for wastewater characterisation for the IAWPRC model. *Water Science and Technology* **29(**7), 81-90.

van Loosdrecht M.C.M., Henze M. Maintenance, endogenous respiration, lysis, decay and predation. *Water Science and Technology* **39**(1), 107-117.

Vanderhasselt A., Vanrolleghem P.A. (2000). Estimation of sludge sedimentation parameters from single batch settling curves. *Water Research* **34**(2), 395-406.

Wahlberg E., Keinath T.M. (1988). Development of settling flux curves using SVI. *Water Pollution Control Federation* **60**(12), 2095-2100.

Walker L. (1971). Hydraulically controlling solids retention time in the activated sludge process. *Water Pollution Control Federation* **43**(1), 30-39.

Wentzel M.C., Mbewe A., Ekama G.A (1995). Batch test measurement of readily biodegradable COD and active organism concentration in municipal wastewaters. *Water SA* 21(2), 117-124.

# 9 Appendix I - additional results of experiments and simulations

## 9.1 Results of the reference BMP test, at the 2th of March 2015

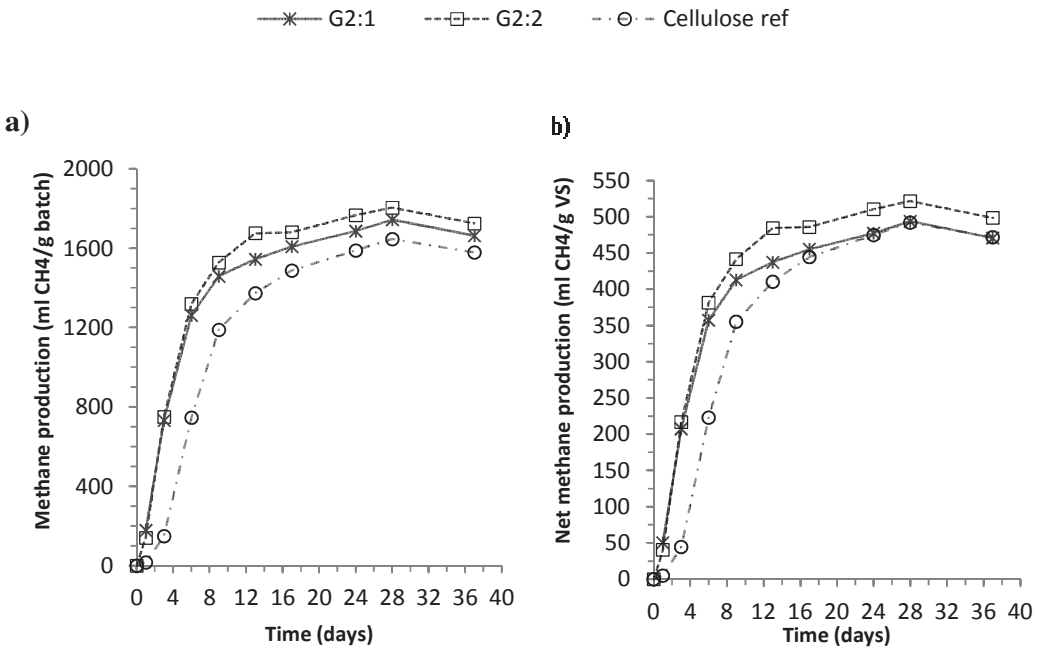


*Figure 9.1. a) Mean accumulated methane production in batch reactors for WAS from the two HLAS lines G2:1 and G2:2, collected at the 3rd of March 2015, as well as for the cellulose reference reactors and reactors containing only inoculum. b) Corresponding net accumulated methane production per gram of substrate (average inoculum methane production subtracted). The depicted results are for the mean production of triplicate batch reactors for each type of evaluated substrate, as well as for the reactors with inoculum only. However, production in Batch 1 for G2:1 series and Batch 1 for the cellulose series were not considered for the calculation of the average production since these appeared to be leaking.*

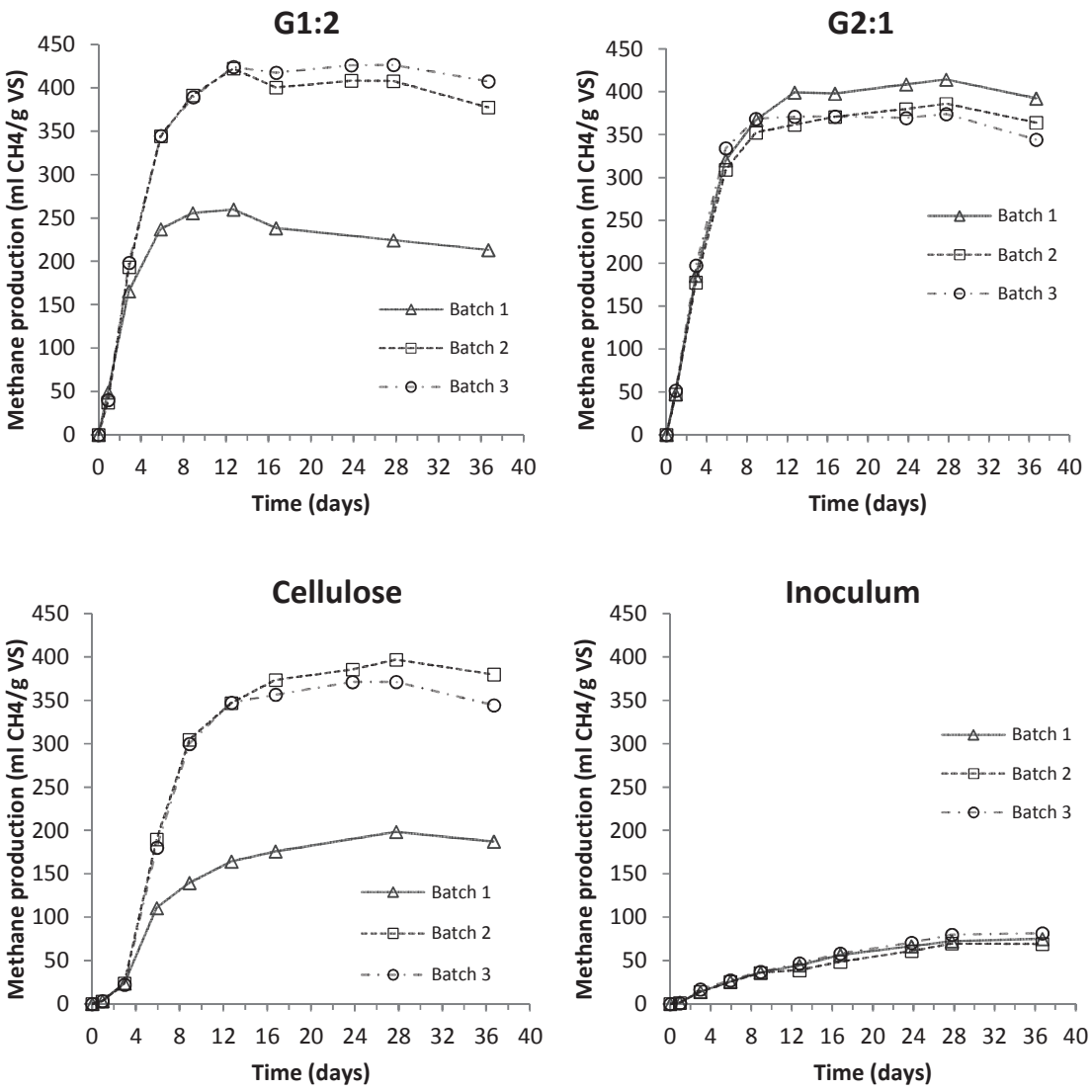


*Figure 9.2. Accumulated methane production per gram of substrate in individual triplicate batch reactors for each of the tested type of substrates, as well as for inoculum only. The results of Batch 1 for the G1:2 reactor series and Batch 1 for the cellulose reactors series appeared to be leaking as can be seen from the deviating production in these reactors.*

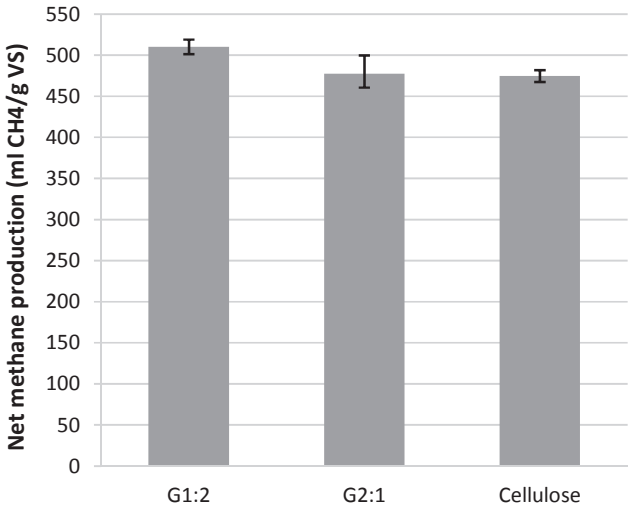


*Figure 9.3 The bars depict the net accumulated methane production, as mean production in triplicate batch reactors after 24 days of incubation. Error bars gives maximum and minimum accumulated methane production within triplicate reactors. Batch 1 for the G1:2 reactor series and Batch 1 for the cellulose reactors series were discarded and are thus not represented by the bars and error bars.*

## 9.2 Results of model calibrations with respect to airflows and DO.

### 9.2.1 Characterisation of G2:1, 10th and 11th of February 2015 (initial model)

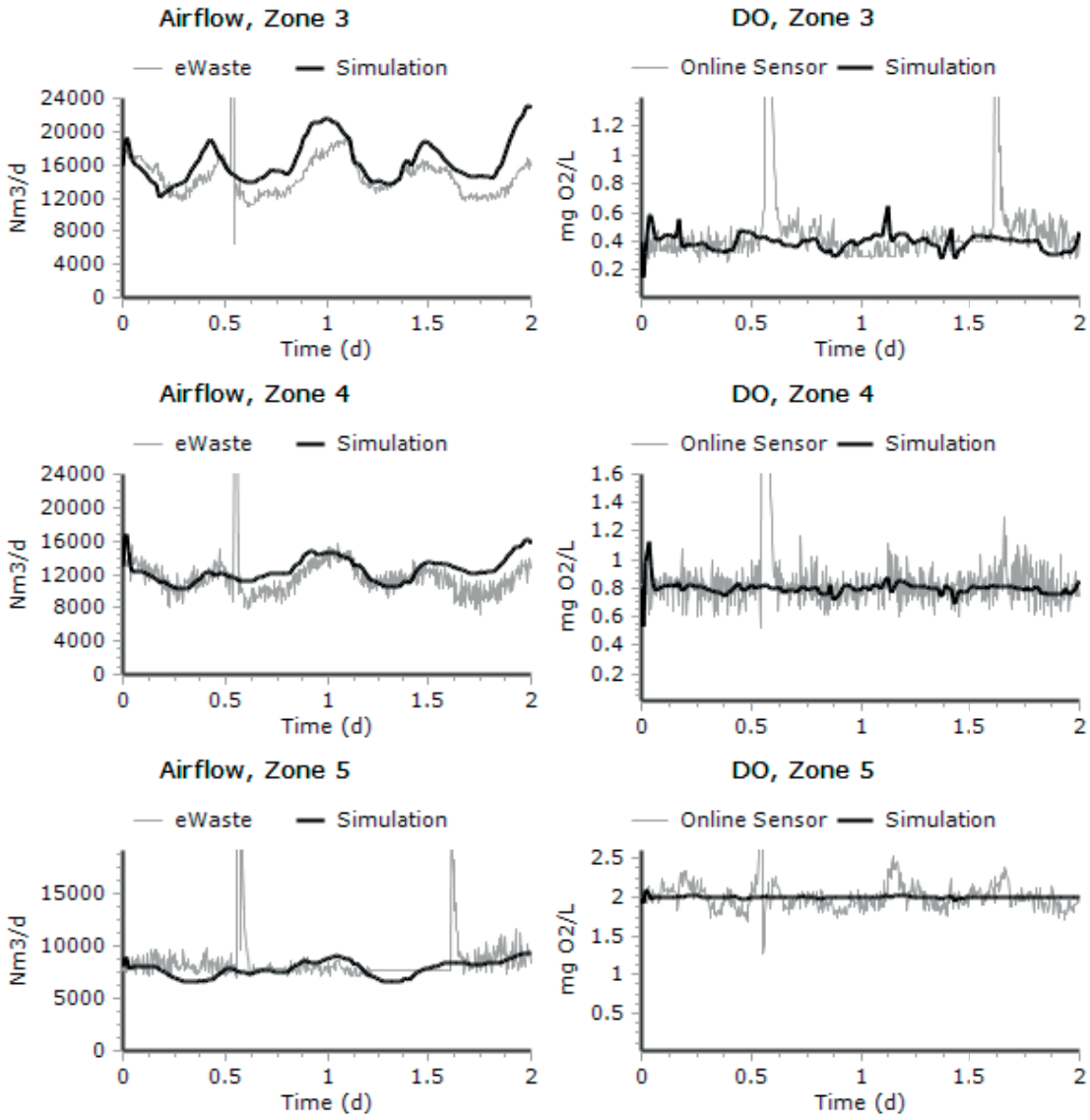


*Figure 9.4. Simulated and observed airflows and DO levels at G2:1 during the 10th and 11th of February 2015.*

### 9.2.2 Characterisation of G2:1 and G2:2, 18th of February, 2015 (validated model)

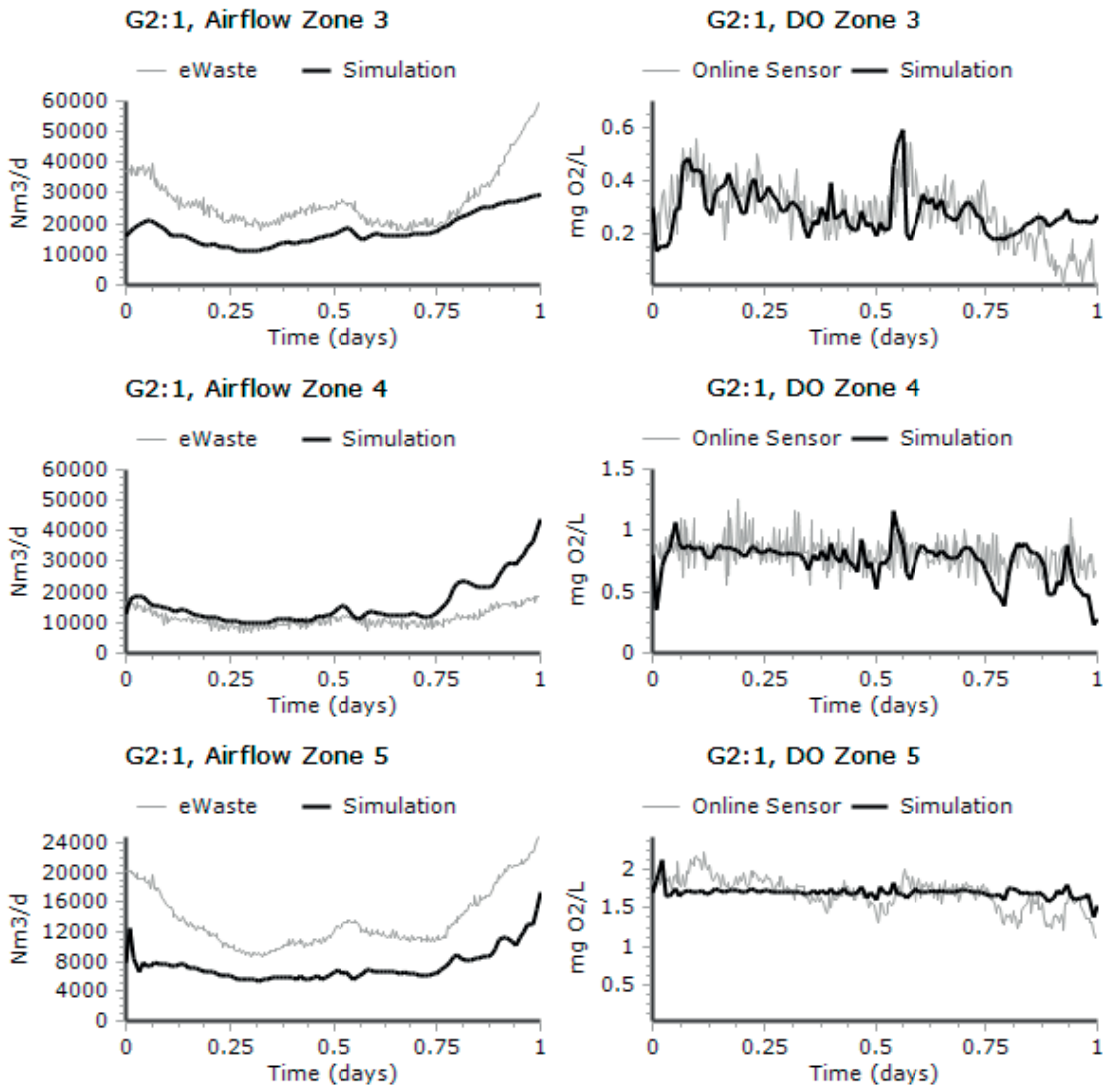


*Figure 9.5. Simulated and observed airflows and DO levels at G2:1 during the 10th and 11th of February 2015.*

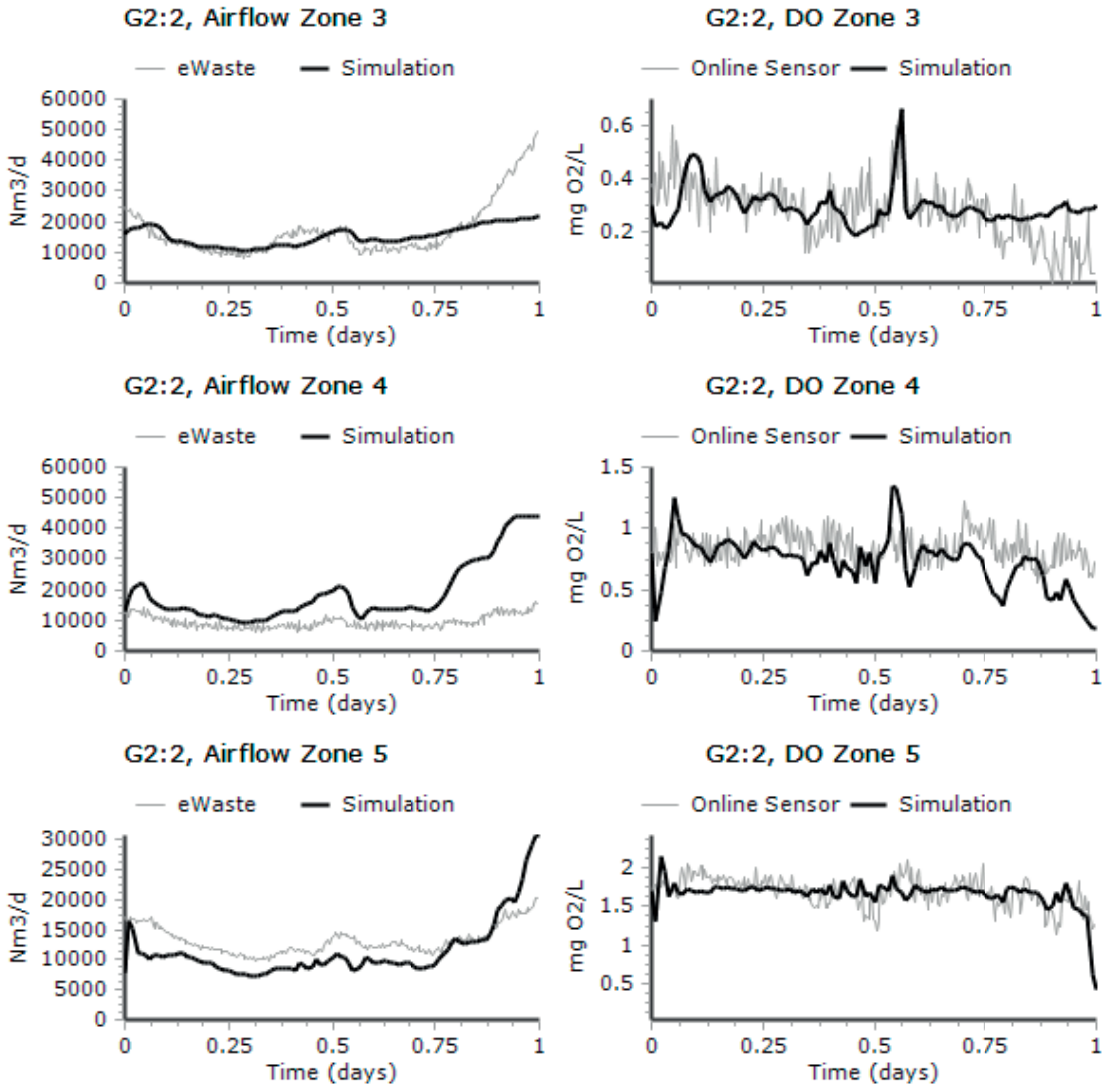


*Figure 9.6. Simulated and observed airflows and DO levels at G2:2 during the 10th and 11th of February 2015.*

# 10 Appendix II - Popular scientific article

# What do we mean by sludge age? And why should we control it?

**The Sjölunda wastewater treatment plant faces the challenge of tougher demands for the quality of the water leaving the plant and entering the Öresund strait between Denmark and Sweden. At the same time, the population of Malmö with neighbourhood is growing rapidly, which means an increase in the loading on the plant. The residence time for the active microbes, the "sludge", in the first biological treatment step has important implications for the treatment efficiency and also for the energy balance at the plant. Consequently, the "sludge age" must be determined and precisely controlled.**

Even though the technique is just about 100 years old, the activated sludge treatment process is to be found at the very majority of modern plants. The original purpose of this technique was for removal of organic matter in the wastewater, which in the case of the Sjölunda plant originates from industries as well as from households. The removal is facilitated by respiring microorganisms which feed on the sewage in an aerated basin. These microorganisms grow rapidly and agglomerate into a sludge which is eventually removed through gravity settling.

It has been found that the average time for which the active microorganisms stay in the system, or equivalently the sludge age, has many implications on the performance of an activated sludge plant. For sludge ages larger than one day, the degradable part of the soluble matter is always taken care of by the microbes, at least at Sjölunda. However, particulate matter needs to be digested prior to being taken up by the cells. The sludge age relates to the amount of microbes in relation to the amount of food in the basin. If the cells are few in relation to the amount of incoming food, the food will simply not be digested and instead float through the system and out of the plant.

However, a long sludge age requires a larger plant if a sufficient volume of wastewater is to be treated each day. Large basins require lot of space and are costly to build and to operate. In addition, a much too long sludge age increases the aeration demand in relation to the removed amount of food and may decrease the potential for production of biomethane from wasted sludge.

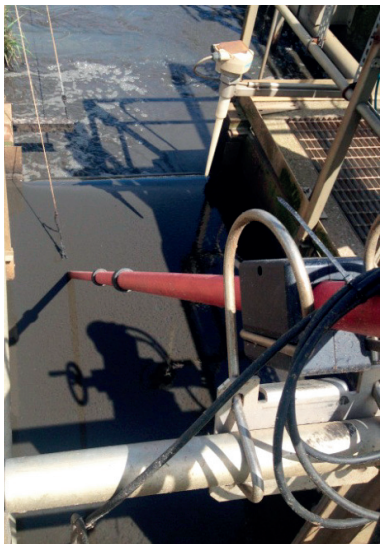

During the spring of 2015, an automatic sludge age controller based on optical online sensors (picture to the right) was evaluated at Sjölunda WWTP. A computer model was constructed for the plant which was used to simulate the outcome of operation at different sludge ages. With the aid of several experiments and full-scale tests it was found that the current sludge age, which is about 2 days, is rather appropriate for sustaining effluent water quality with a reasonable energy balance. But when the loading on the system increases in the future, the sludge age may have to decrease. Then, an automatic controller may be essential in order to provide a stable process so that the sludge age and the quality of effluent water are newer allowed to become to low. That is one measure for assuring the marine environment of Öresund!